

Characterization of protein import channel-forming proteins in chloroplasts

Dissertation der Fakultät für Biologie

der

Ludwig-Maximilians-Universität München

vorgelegt von

Erika Kovács-Bogdán

aus Budapest, Ungarn

München, den 09.05.2011

Erstgutachter: Prof. Dr. Jürgen Soll
Zweitgutachter: Prof. Dr. Michael Schleicher

Tag der mündlichen Prüfung: 08. Juli 2011

Abstract

Most chloroplast proteins are encoded for in the nucleus and have to be transported into the organelle after translation in the cytoplasm. The TOC and TIC machineries (Translocon at the Outer/Innner envelope membrane of Chloroplasts) mediate the import of these proteins across the chloroplast membranes. The major aim of this work was to characterize two TIC translocon components: Tic110, the main protein translocation channel in the inner envelope, and Tic20, which was proposed to also form a protein import channel.

After a detailed study of Tic110, a topological model could be established, demonstrating that the protein is inserted into the membrane with two hydrophobic and four amphipathic helices, placing residues both to the intermembrane space and to the stromal side. The presence of highly conserved cysteine residues and experiments demonstrating that Tic110 possess a redox active disulfide bridge, which could be reduced by stromal thioredoxins *in vitro*, indicated that Tic110 might be a possible target for thioredoxin regulation. To explore which cysteines are involved in disulfide bridge formation, mutations were generated for conserved cysteines in Tic110. As a result, Cys⁴⁹² and Cys⁸⁹⁰ were identified as possible candidates. To define the functional role of disulfide bridge(s), components of the TIC motor complex were overexpressed and purified and their interaction was analysed with Tic110 via different approaches.

The second part of this work focuses on the channel activity of Tic20. Although both Tic110 and Tic20 are clearly important for plant viability and preprotein translocation, there were neither electrophysiological nor biochemical data supporting that Tic20 can form a channel. After inserting the heterologously overexpressed and purified protein into liposomes, swelling assays and electrophysiological measurements provided the first experimental evidence for the channel activity of Tic20, being a cation selective channel with a pore size of about 8-14 Å. Therefore, it was concluded that the TIC translocon consists of at least two distinct translocation channels: Firstly, Tic110 forms the main translocation pore and therefore facilitates import of most of the chloroplast-targeted preproteins. Secondly, Tic20 might be specifically required for the translocation of some possibly essential proteins.

To gain further insight into the structure and function of both proteins, preliminary tests were performed for crystallization in lipidic phases. The large sample of grown crystals observed under different conditions will presumably enable to crystallize these proteins and resolve their crystal structures in the future.

Zusammenfassung

Die meisten chloroplastidären Proteine werden im Zellkern kodiert und nach der Translation an cytosolischen Ribosomen in die Chloroplasten transportiert. Die TOC und TIC Komplexe (Translocon at the Outer/Innner envelope membrane of Chloroplasts) katalysieren den Transport dieser Proteine durch die Chloroplastenhüllmembranen. Der Hauptziel dieser Arbeit war die Charakterisierung von zwei Komponenten des TIC Komplexes: Tic110, der Hauptimportkanal in der inneren Hüllmembran und Tic20, ebenfalls als Proteinimportkanal vorhergesagt.

Die Topologie von Tic110 wurde nach ausführlichen Studien etabliert. Diesem Model zufolge inseriert Tic110 in der inneren Hüllmembran mit zwei hydrophoben und vier amphipathischen Transmembrandomänen, besitzt folglich Domänen in dem Intermembranraum und auf der stromalen Seite. Hochkonservierte Cysteine in der Sequenz und Oxidationsversuche beweisen, dass Tic110 über eine (oder mehrere) redoxsensitive Disulfidbrücken verfügt. Die Reduktion dieser Disulfidbrücken durch Thioredoxine *in vitro* weist darauf hin, dass Tic110 von Thioredoxinen reguliert werden könnte. Um zu untersuchen, welche Cysteine an der Disulfidbrücke beteiligt sind, wurden Mutationen in der Tic110-Sequenz erstellt. Als mögliche Kandidaten für die Oxidation ergaben sich Cys⁴⁹² und Cys⁸⁹⁰. Um die Funktion der Redoxzustände zu bestimmen, wurden Komponenten des TIC Motorkomplexes überexprimiert, aufgereinigt und deren Interaktion mit Tic110 in unterschiedlichen Verfahren untersucht.

Im zweiten Teil dieser Arbeit wurde die Kanalaktivität von Tic20 untersucht. Obwohl Tic110 und Tic20 beide essentiell für die Lebensfähigkeit der Pflanzen und Proteintranslokation sind, gab es weder elektrophysiologische noch biochemische Daten, die zeigen dass Tic20 einen Kanal bildet. Überexprimiertes Tic20 wurde aufgereinigt und in Liposomen rekonstituiert. Anschließende Liposomen-Schwellversuche und elektrophysiologische Messungen haben die ersten Hinweise darauf gegeben, dass Tic20 einen kationenselektiven Kanal mit einer Porengröße von 8-14 Å bildet. Demzufolge gibt es wahrscheinlich zwei unterschiedliche TIC Komplexe: Tic110 bildet den Hauptkanal und importiert die meisten chloroplastidären Proteine. Tic20 könnte für die Translokation eines kleinen aber vermutlich essentiellen Satzes an Proteinen verantwortlich sein.

Um mehr Information über die Struktur und Funktion von Tic110 und Tic20 zu erhalten, wurden erste Kristallisationsversuche in Lipidphasen durchgeführt. Die vielen beobachteten Kristalle deuten darauf hin, dass bald Kristallstrukturen aufgeklärt werden könnten.

Table of contents

Abstract	3
Zusammenfassung	4
Table of contents.....	6
Abbreviations.....	9
1. Introduction.....	11
1.1. Protein import into chloroplasts	11
1.2. The TIC complex	14
1.2.1. Channel-forming components	14
1.2.2. Import motor complex(es)	17
1.2.3. Redox regulation.....	23
1.3. Aims of this work.....	27
2. Materials	28
2.1. Chemicals	28
2.2. Enzymes, kits and other proteins	28
2.3. Strains, vectors and oligonucleotides	29
2.4. Molecular weight markers and DNA standards.....	30
2.4.1. Antibodies.....	31
2.4.2. Columns and column materials	31
2.4.3. Plant material.....	31
3. Methods.....	32
3.1. Molecular biological methods.....	32
3.1.1. General molecular biological methods	32
3.1.2. <i>In vitro</i> transcription and translation	32
3.2. Biochemical methods.....	32
3.2.1. General biochemical methods	32
3.2.2. Isolation of intact chloroplasts from <i>Pisum sativum</i>	33
3.2.3. Preparation of inner and outer envelope vesicles from <i>Pisum sativum</i>	33
3.2.4. Isolation of stroma from <i>Pisum sativum</i>	33

3.2.5.	Two-dimensional blue native (BN) / SDS-PAGE	33
3.2.6.	Immunoblotting	34
3.2.7.	Protein identification by mass spectrometry (MS)	34
3.2.8.	Protein expression and purification	34
3.2.9.	Influence of oxidizing/reducing conditions on Tic110.....	36
3.2.10.	PEGylation assay	37
3.2.11.	Limited proteolysis assays with thermolysin.....	37
3.2.12.	Liposome preparation	38
3.2.13.	Flotation assay	38
3.2.14.	Cross-linking	38
3.2.15.	Swelling assay	39
3.2.16.	Electrophysiological measurements	39
3.2.17.	Protein crystallization	42
4.	Results	44
4.1.	Tic110.....	44
4.1.1.	Purification	44
4.1.2.	Complex formation.....	44
4.1.3.	Insertion into liposomes.....	46
4.1.4.	Crystallization.....	47
4.1.5.	Oxidation states	49
4.1.6.	Cysteines involved in disulfide bridge formation.....	52
4.1.7.	Effect on the channel activity and import rates	54
4.1.8.	Effect on the interaction with the motor complex	55
4.1.9.	Effect on the interaction with preproteins	62
4.2.	Tic20.....	64
4.2.1.	Purification	64
4.2.2.	Insertion into liposomes.....	65
4.2.3.	Complex formation in proteoliposomes	67
4.2.4.	Orientation in proteoliposomes	68
4.2.5.	Channel activity	70
4.2.6.	Crystallization.....	75
5.	Discussion	77

5.1.	Topology and structure of Tic110	77
5.2.	Redox characterization of Tic110	78
5.2.1.	Oxidation states	78
5.2.2.	Cysteines involved in disulfide bridge formation.....	79
5.2.3.	Roles of the oxidation states	80
5.2.4.	Oligomerization state of Hsp93	82
5.3.	Channel-forming components of the TIC complex	83
5.	References.....	87
	Acknowledgements.....	97
	Curriculum Vitae	98

Abbreviations

2D	Two dimensional
AAA	ATPases associated with a variety of cellular activities
ADP	Adenosine diphosphate
AMS	4-acetamido-4'-maleimidylstilbene-2,2'-disulfonic acid
AP	Alkaline phosphatase
<i>At</i>	<i>Arabidopsis thaliana</i>
ATP	Adenosine-5'-triphosphate
BCIP	5-bromo-4-chloro-3-indolyl phosphate
BN	Blue native
CD	Circular dichroism
CLIC	Chloride intracellular channel
Clp	Caseinolytic protease
Cys	Cysteine
DDM	<i>n</i> -dodecyl- β -D-maltoside
Dsb	Disulfide bond formation
DTT	Dithiothreitol
ECL	Enhanced chemiluminescence
Ero	Endoplasmic reticulum oxidation
Erv	Essential for respiration and vegetative growth
ESRF	European Synchrotron Radiation Facility
FNR	Ferredoxin-NADP ⁺ oxidoreductase
FTR	Ferredoxin-dependent Trx reductase
GSSG	Oxidized glutathion
GTP	Guanosine-5'-triphosphate
Hip	Hsp70 interacting protein
Hop	Hsp70 and Hsp90 organizing protein
Hsp	Heat shock protein
IAA	Iodoacetamide
IE	Inner envelope membrane
IMS	Intermembrane space
LC-MS/MS	Liquid chromatography with mass spectrometry
LS	<i>n</i> -lauroylsarcosine
M	Methionine

ME	β-mercaptoethanol
Mia	Mitochondrial IMS import and assembly
mSSU	mature part of SSU
NADP ⁺	Nicotinamide adenine dinucleotide phosphate
NBT	Nitro blue tetrazolium chloride
NTR	NADP ⁺ -dependent Trx reductase
OD	Optical density
OE	Outer envelope membrane
OE33	Oxygen-evolving complex 33 kDa subunit
PAGE	Polyacrylamide gel electrophoresis
PC	L-α-phosphatidylcholine
PEG-Mal	Metoxypolyethylenglycol-maleimide
PIC	Permease in chloroplasts
PMSF	Phenylmethylsulfonyl fluoride
pOE33	Preprotein of OE33
<i>Ps</i>	<i>Pisum sativum</i>
pSSU	Preprotein of SSU
PVDF	Polyvinylidene fluoride
RT	Room temperature
SDS	Sodium dodecyl sulfate
-SH	Sulfhydryl
SPP	Stromal processing peptidase
SSU	Small subunit of ribulose-1,5-bisphosphate carboxylase oxygenase
Sti	Stress inducible protein
TCA	Trichloroacetic acid
TCEP	Tris(2-carboxyethyl) phosphine
TIC	Translocon at the inner envelope membrane of chloroplasts
TIM	Translocase of the inner mitochondrial membrane
TOC	Translocon at the outer envelope membrane of chloroplasts
TOM	Translocase of the outer mitochondrial membrane
TP	Transit peptide
TPR	Tetratricopeptide repeat
Trx	Thioredoxin

1. Introduction

1.1. Protein import into chloroplasts

Chloroplasts derived from an endosymbiotic event involving a cyanobacteria-related organism. A heterotrophic cell already containing mitochondria took up the ancestor of chloroplasts - and all plastid types - about 1.6-1.5 billion years ago, giving rise to a eukaryotic cell being capable of photoautotrophic life style (Martin and Herrmann, 1998; Cavalier-Smith, 2000; Hedges *et al.*, 2004; Gould *et al.*, 2008; Gross and Bhattacharya, 2009). As the result of a massive gene transfer during evolution, only 50-200 plastid proteins are still encoded for in the plastid genome, whereas about 3000 genes were transferred to the host cell nucleus (Martin *et al.*, 2002; Leister, 2003; Timmis *et al.*, 2004; Bock and Timmis, 2008). Therefore, the chloroplasts had to develop a system to re-import the necessary proteins from the cytosol back into the organelle and to sort them to the correct sub-compartments.

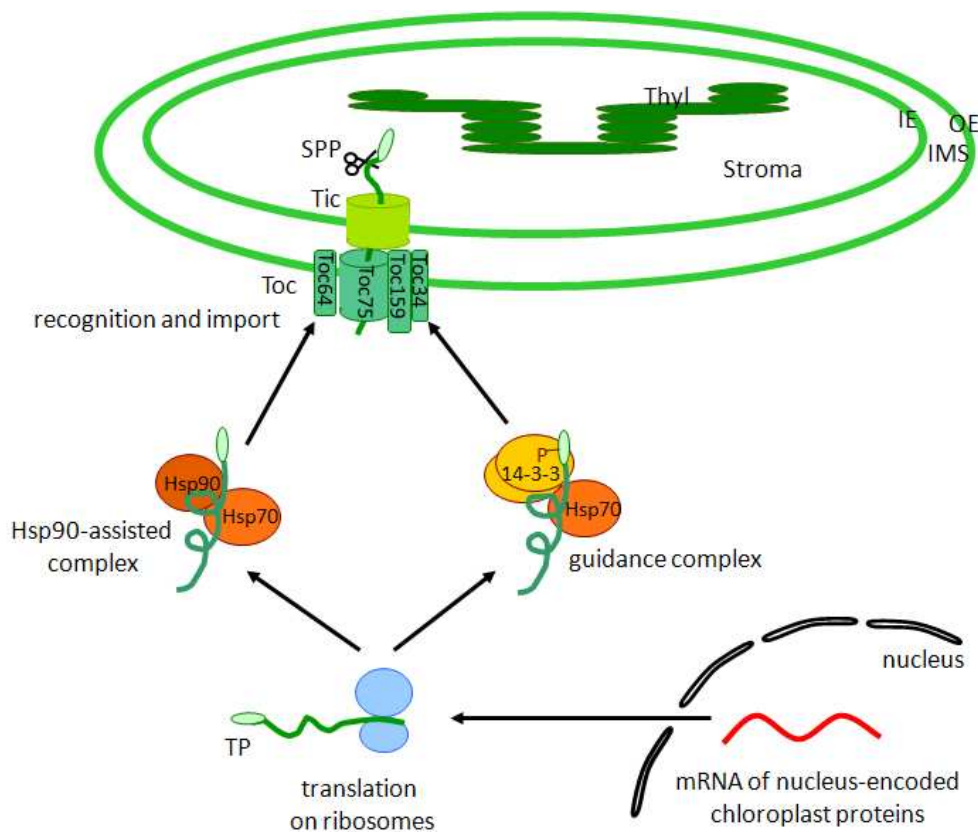


Figure 1. General import pathway

Figure was taken from Kovács-Bogdán *et al.* (2010). Nucleus-encoded chloroplast proteins are translated on cytoplasmic ribosomes and guided in an import-competent state with the help of molecular chaperones (Hsp90, Hsp70, 14-3-3) to the chloroplast surface. The import into the chloroplasts is catalysed by the TOC/TIC (Translocon at the Outer/Inner envelope membrane of Chloroplasts) complexes. After entering the stroma, stromal processing peptidase (SPP) cleaves the transit peptide (TP). OE/IE: outer/inner chloroplast envelope membrane; IMS: intermembrane space; Thyl: thylakoids.

Most of the chloroplast preproteins engage the so-called “general import pathway” (Figure 1). After translation on cytoplasmic ribosomes, preproteins bear an N-terminal transit peptide, responsible for specific targeting (Bruce, 2000; Lee *et al.*, 2008). They are kept in an import-competent state with the help of so far two identified chaperone-assisted complexes (Schwenkert *et al.*, 2011): One is the so-called “guidance complex”, which consists of Hsp70 chaperones, 14-3-3 proteins and possibly other unidentified components (May and Soll, 2000). Some preproteins can associate stronger with 14-3-3 proteins when certain Ser and Thr residues in the transit peptide are phosphorylated. A small kinase family in *Arabidopsis thaliana* was identified to be responsible for this phosphorylation (Waagemann and Soll, 1996; Martin *et al.*, 2006). The second cytosolic complex contains Hsp90 and Hsp70 chaperones associated with the preprotein (Waagemann and Soll, 1996; Qbadou *et al.*, 2006) and with two recently described co-chaperones: FKBP73 and an Hsp70/Hsp90 organizing protein (Fellerer *et al.*, in press).

On the chloroplast surface preproteins are recognized by specific receptors of the TOC complex (Translocon at the Outer envelope membrane of Chloroplasts), which catalyses the translocation across the outer envelope membrane (Figure 1) (for more details see Schwenkert *et al.*, 2011; Schleiff and Becker, 2011 and references therein). Toc34 and Toc159 serve as receptors for the preprotein, regulated by GTP binding and phosphorylation (Kessler *et al.*, 1994; Sveshnikova *et al.*, 2000; Schleiff *et al.*, 2002). Furthermore, Toc159 was described also as a GTP-driven motor that threads the preproteins into the Toc-channel (Schleiff *et al.*, 2003a). A third Toc component, Toc64 is a docking site for Hsp90-complexed preproteins (Sohrt and Soll, 2000; Qbadou *et al.*, 2006). After recognition by the receptors, the preprotein is transported across the outer envelope membrane via the Toc75 channel (Hinnah *et al.*, 2002). The fifth Toc subunit, Toc12 associates in the intermembrane space with Toc64, Tic22 and an Hsp70 chaperone, thereby forming the so-called intermembrane space complex that is thought to facilitate the efficient and direct translocation of preproteins between the two translocon complexes (Becker *et al.*, 2004; Ruprecht *et al.*, 2010). However, a recent study (Chiu *et al.*, 2010) demonstrated that the closest homolog of Toc12 in *Arabidopsis*, DnaJ-J8, localizes to the stroma. Furthermore, *dnaJ-J8* knock out mutants did not show defects in protein import, questioning the role of Toc12 in the import process.

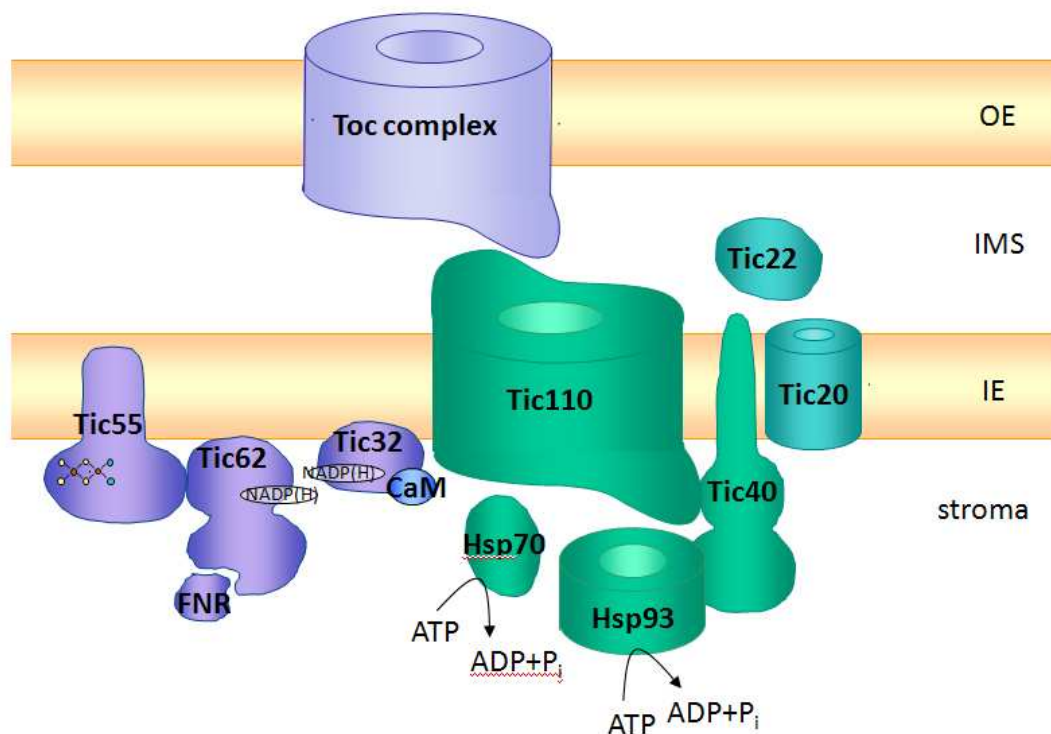


Figure 2. Translocon at the inner envelope membrane of chloroplasts (TIC)

Figure was adapted from Kovács-Bogdán *et al.* (2010). Tic110 and Tic20 are proposed to form a channel in the inner envelope membrane (IE) of chloroplasts. The Tic110 main import channel is associated with Tic40 and the stromal chaperones Hsp93 and Hsp70 forming the “motor complex(es)” (coloured in green). Hsp93 is depicted here as a hexameric ring. The only identified TIC component located in the intermembrane space (IMS) is Tic22. Tic62, Tic55 and Tic32 represent the redox regulon (coloured in purple). The Rieske-type iron-sulphur centre of Tic55 is symbolized. CaM: calmodulin; FNR: ferredoxin-NADP⁺ oxidoreductase. OE: outer envelope membrane.

The TIC complex (Translocon at the Innner envelope membrane of Chloroplasts) is responsible for preprotein translocation across the inner envelope (IE) (for review see Jarvis, 2008; Kovács-Bogdán *et al.*, 2010). Seven TIC components have been identified so far: Tic110, Tic62, Tic55, Tic40, Tic32, Tic22 and Tic20 (Figure 2). Tic22 is the only soluble TIC subunit in the intermembrane space, being part of the intermembrane space complex (see above). Two proteins, Tic110 and Tic20, presumably form protein translocation channel(s). Tic40, together with the stromal chaperones Hsp93 and Hsp70, is believed to provide the driving force (dependent on ATP hydrolysis) for the import as “motor complex(es)”. After the preprotein reached the stroma through the channel with the help of the motor complex, the transit peptide is cleaved off by the stromal processing peptidase. Tic62, Tic55 and Tic32 (the so-called “redox regulon”) enable redox regulation of the import via their redox-sensitive groups. In the following sections a more detailed overview presents our current knowledge about the TIC channel forming components, import motor(s) and about the redox regulation of the TIC complex.

1.2. The TIC complex

1.2.1. Channel-forming components

1.2.1.1. *Tic110*

The most abundant component of the TIC translocon is Tic110 (Block *et al.*, 1983; Schnell *et al.*, 1994; Lübeck *et al.*, 1996). It was cross-linked together with the imported preprotein in a complex also containing TOC components and molecular chaperones such as Cpn60, Hsp93 and Hsp70 (Kessler and Blobel, 1996; Jackson *et al.*, 1998; Inaba *et al.*, 2003; Su and Li, 2010; Shi and Theg, 2010).

The extreme N-terminus of Tic110 contains two hydrophobic transmembrane α -helices, which are responsible for the insertion of the protein into the IE (Lübeck *et al.*, 1996; Lübeck *et al.*, 1997). The localization of the hydrophilic rest of the protein was debated: According to one hypothesis this part is soluble, localized in the stroma, and is therefore responsible for chaperone recruitment (Jackson *et al.*, 1998; Inaba *et al.*, 2003). In contrast, proteolytical treatment of IE with trypsin resulted in partial degradation of the protein indicating that it is located in the intermembrane space (Lübeck *et al.*, 1996). Further analysis revealed that Tic110 even without its N-terminus is able to insert into liposomes and forms a cation-selective channel with an inner pore diameter of 15-31 Å, similar to the full-length protein (Heins *et al.*, 2002; Balsera *et al.*, 2009a).

Tic110 is not present in any prokaryotic organisms including cyanobacteria, thus it is of eukaryotic origin (Reumann and Keegstra, 1999; Kalanon and McFadden, 2008). In *Arabidopsis thaliana*, Tic110 is encoded by a single-copy gene. It is expressed in flowers, leaf, stem and root tissues indicating a role in all types of plastids (Dávila-Aponte *et al.*, 2003; Inaba *et al.*, 2005). Homozygous T-DNA insertion lines are embryo lethal (Inaba *et al.*, 2005), establishing that the Tic110 gene product is essential for growth. Reduction of the expression of *AtTic110* results in a pale green phenotype, defect in plant growth and strongly reduced amounts of thylakoid membranes and starch granules in chloroplasts. Furthermore, Inaba *et al.* (2005) reported a reduced content of nuclear encoded chloroplastic proteins indicating a defect in protein import.

Tic110 is imported into the chloroplast via the general import pathway. Following import into the stroma and processing to its mature size, it forms a soluble intermediate, which is inserted into the membrane. This re-insertion requires its N-terminal region (Lübeck *et al.*, 1996; Lübeck *et al.*, 1997), catalyzed by ATP and involves Hsp93 (Vojta *et al.*, 2007).

Due to its high abundance, the involvement in the import process, the channel activity, import defects in the heterozygous mutants and the lethal phenotype of homozygous mutant plants, Tic110 most probably forms the main protein import channel. Furthermore, it mediates the recruitment of chaperones at the stromal site providing the driving force for translocation and folding of preproteins. Moreover, it contacts the TOC complex and the incoming transit peptide on the intermembrane space side to facilitate the translocation process. However, at the beginning of this work, there was no topological model or structure of Tic110 available, which would further support these functions.

1.2.1.2. Tic20

Tic20 was detected in a cross-link with the TOC complex after *in vitro* import experiments in pea (Kouranov *et al.*, 1998). In a more recent study, Tic20 was found in a complex containing also a preprotein *en route* into the plastid after mild solubilization of pea and *Arabidopsis* chloroplasts (Kikuchi *et al.*, 2009), also suggesting its involvement in protein import.

According to *in silico* analysis, it is inserted into the IE via four α -helical transmembrane domains exposing its N- and C-termini to the stromal side (Kouranov *et al.*, 1998 and TMHMM Server). Additionally, recent CD-spectroscopical analysis and cysteine labelling assays supported its predicted secondary structure and topology (Benz, 2009; Kovács-Bogdán *et al.*, submitted). Similar N_{in}-C_{in} topology was also demonstrated for a highly divergent member of the Tic20 protein family from *Toxoplasma gondii* using a C-terminal GFP-fusion (van Dooren *et al.*, 2008). These parasites contain a special type of plastids (called apicoplasts) surrounded by four membranes as a result of secondary endosymbiosis. Moreover, some structural relation was observed between Tic20 and the mitochondrial inner membrane translocon components Tim17 and Tim23 (Kalanon and McFadden, 2008). These Tim proteins also have four transmembrane domains and form protein import channels in the inner mitochondrial membrane. Distant sequence similarity was also reported between Tic20 and two prokaryotic branched-chain amino acid transporters (Reumann and Keegstra, 1999), however, a recent study (Kasmati *et al.*, 2011) could not find any phylogenetical connection between Tic20 and the mentioned transporters.

The *Arabidopsis thaliana* genome encodes four Tic20 homologs: *AtTic20-I*, *-II*, *-IV* and *-V* (Kalanon and McFadden, 2008; Kasmati *et al.*, 2011). *AtTic20-I* shows the closest homology to *Pisum sativum* Tic20 (*PsTic20*). It is present in all plant tissues, and its expression is highest during rapid leaf growth (Chen *et al.*, 2002). It is much less abundant on the protein level in chloroplasts than Tic110 (Kovács-Bogdán *et al.*, submitted). *attic20-I* antisense plants

exhibit a severe pale phenotype, growth defects and deficiency in plastid function, such as smaller plastids, reduced thylakoids, decreased content of plastidic proteins, and altered import rates of preproteins (Chen *et al.*, 2002; Hirabayashi *et al.*, 2011). Knockouts of *attic20-I* are albino even in the youngest parts of the seedlings (Teng *et al.*, 2006; Kasmati *et al.*, 2011). The presence of another closely related *Tic20* homolog (*AtTic20-IV*) may prevent *attic20-I* plants from lethality, since *AtTic20-IV* is upregulated in the mutants (Teng *et al.*, 2006; Hirabayashi *et al.*, 2011). However, additional overexpression of *AtTic20-IV* can only compensate the observed defects to a very low extent indicating that *AtTic20-IV* cannot fully substitute for the function of *AtTic20-I* (Hirabayashi *et al.*, 2011; Kasmati *et al.*, 2011). Two more distantly related homologs are also present in *Arabidopsis* (*AtTic20-II* and *AtTic20-V*). A recent study by Kasmati *et al.* (2011) demonstrated that this separate group of *Tic20*-proteins also bear an N-terminal transit peptide and after import into chloroplasts they are inserted into the IE. Interestingly, *Tic20* is important for protein import and viability also in *Toxoplasma gondii* (van Dooren *et al.*, 2008).

Based on structural similarity to channel-forming proteins, cross-links to imported preprotein and protein import defects detectable in the knock down mutants, it was hypothesized that *Tic20* forms a protein translocation channel in the IE membrane (Kouranov *et al.*, 1998; Reumann and Keegstra, 1999; Kikuchi *et al.*, 2009). Furthermore, a cross-link of a minor fraction of *Tic110* to *Tic20* in a TOC-TIC supercomplex (Kouranov *et al.*, 1998) indicates an association of the two proteins. Therefore, it was proposed that the two proteins possibly cooperate in channel formation. However, there was no cross-link detected between the two proteins in the absence of the TOC complex, making a direct or permanent interaction unlikely. Recently, *Tic20* was demonstrated to be a component of a one megadalton complex detected on BN-PAGE, separately from *Tic110* after mild solubilization of IE and chloroplasts, supporting the idea that the two proteins do not associate (Kikuchi *et al.*, 2009; Benz, 2009; Kovács-Bogdán *et al.*, submitted). However, at the beginning of this work, the expected channel activity of *Tic20* had not been demonstrated experimentally.

Additionally, a very recent study (Hirabayashi *et al.*, 2011) suggested *AtTic20-IV* as an import channel working side by side with *AtTic20-I*. However, detailed characterization of *AtTic20-IV* (e.g. topology) and experimental evidence for channel activity are still missing.

1.2.1.3. *PIC1/Tic21*

Another potential TIC subunit, *PIC1/Tic21* was also proposed as a putative import channel (Teng *et al.*, 2006). Reminiscent of *Tic20*, it is an integral IE protein with four transmembrane

helices. According to the authors, *attic21* null mutants show a severe pale phenotype and accumulate preproteins in the cytosol suggesting defect in protein import. In contrast, the same protein was also characterized as an iron permease (Duy *et al.*, 2007; Duy *et al.*, 2011): The *atpic1* mutant plants are small and chlorotic as a result of impaired chloroplast development, but protein import into chloroplasts was described to be still functional. Furthermore, phytoferritin accumulated in the mutant chloroplasts. PIC1 and its cyanobacterial homolog, *sll1656* could complement the growth of iron-uptake deficient yeast mutants indicating a role in iron homeostasis and not in protein import.

Taken together, there are several candidates described so far that could constitute the protein import channel in the IE. However, it is not clear yet whether they function independently of each other or they are part of different TIC complexes. They might act in different stages of development, in different tissues and cell types, or be responsible for various preprotein substrates, thereby increasing the complexity and specificity of the import process.

1.2.2. Import motor complex(es)

Early import studies already demonstrated that the energy for protein translocation through the IE is provided by ATP hydrolysis, which is required for the function of an ATPase at the stromal side (Schindler *et al.*, 1987; Flüge and Hinz, 1986). Since then, cross-linking experiments and mutant analyses ascertained the role of several chaperones and co-chaperones involving in the late import process.

1.2.2.1. Cpn60

The first protein identified playing a possible role in the import process in an ATP-dependent manner was Cpn60, a cyanobacterial GroEL homolog and stromal chaperonin. It was found in a complex together with Tic110 after co-immunoprecipitation during *in vitro* import experiments (Kessler and Blobel, 1996). This interaction was abolished in the presence of ATP. Furthermore, the Rieske iron-sulphur protein of the cytochrome *b₆f* complex was described in a complex with Cpn60 after import experiments in chloroplasts pre-treated with valinomycin and nigericin (Madueno *et al.*, 1993). The two ionophores inhibited the insertion of the protein into the thylakoid membrane, therefore the majority of the protein remained in the stroma, bound by Cpn60 and Hsp70 (see below) to prevent premature folding and aggregation. However, this suggests a role after the translocation event and not during the import process. Notably, there are no recent studies demonstrating the role of Cpn60 in protein import.

1.2.2.2. *Hsp93 (ClpC)*

Another ATPase proposed to be involved in the import process is Hsp93: several cross-linking and co-immunoprecipitation experiments revealed a close proximity of Hsp93 to Tic110, supporting a role in protein import into chloroplasts (Akita *et al.*, 1997; Nielsen *et al.*, 1997; Chou *et al.*, 2003).

Hsp93 is a member of the HSP100 molecular chaperone family. These proteins possess unfolding capacity dependent on ATP hydrolysis. They form either hexameric rings (in the presence of nucleotides such as ATP or ADP) or migrate as smaller proteins (in the absence of nucleotides) (Schirmer *et al.*, 1996). Hsp93 has two distinct ATPase domains (AAA modules) and can be found in Gram-positive bacteria, cyanobacteria and plants. Hsp93 does not only associate with the import apparatus in plants, but also to the Clp protease complex, originated from the cyanobacterial ancestor (Shanklin *et al.*, 1995; Halperin *et al.*, 2001; Peltier *et al.*, 2004; Stanne *et al.*, 2007). The Clp protease consists of a proteolytic subunit (ClpP) and an ATPase subunit (Hsp93/ClpC), the latter being responsible for substrate recognition, unfolding and translocation into the proteolytic chamber.

In *Arabidopsis thaliana*, there are two nuclear encoded Hsp93 genes present: *AtHsp93-III* and *AtHsp93-V* (also called *ClpC2* and *ClpC1*, respectively). They are highly identical on the amino acid sequence level (91%) but the expression of *AtHsp93-V* is several-fold higher than that of *AtHsp93-III* (Kovacheva *et al.*, 2005). The *hsp93-III* knock out plants show no phenotype, while *hsp93-V* plants are paler and retarded in growth in comparison to the wild type. Their chloroplasts develop less thylakoid membranes, contain a decreased amount of photosystem I and II proteins and have reduced protein import efficiency (Constan *et al.*, 2004; Sjögren *et al.*, 2004; Kovacheva *et al.*, 2005). The double knock out mutant is lethal, indicating that at least partially they are able to functionally substitute for each other in the single mutants (Kovacheva *et al.*, 2007).

Taken together, due to the association of Hsp93 with the TIC complex and the protein import defects in Hsp93 loss-of-function mutants, this chaperone is believed to be a member of the TIC motor complex.

1.2.2.3. *Tic40*

Tic40 was described as a co-chaperone, which can trigger the ATP-hydrolysis of Hsp93 (Chou *et al.*, 2003; Chou *et al.*, 2006). Cross-linking experiments, yeast two-hybrid and bimolecular fluorescence complementation assays revealed also a close proximity and

interaction between Tic110 and Tic40 (Stahl *et al.*, 1999; Chou *et al.*, 2003; Bédard *et al.*, 2007).

Tic40 consists of an N-terminal transmembrane domain, anchoring the protein into the IE, and a large hydrophilic C-terminal domain facing the stromal side (Stahl *et al.*, 1999). The C-terminus was reported to contain a degenerated tetratricopeptide repeat (TPR) and a Sti1 (Hip/Hop-like) domain (Chou *et al.*, 2003). TPR domains are defined by the presence of two antiparallel-helices with a total length of 34 amino acids, usually present in several copies and they are known to mediate protein-protein interactions (Blatch and Lassle, 1999). Sti1 domains are characteristic of Hip/Hop co-chaperones (Hsp70 interacting protein/Hsp70 and Hsp90 organizing protein). In contrast to earlier studies, recent sequence analysis predicted two Sti1 domains (Stress inducible protein) instead, located in tandem at the C-terminus of the protein (Balsera *et al.*, 2009b). The alleged TPR-like domain of Tic40 is involved in the binding to Tic110, which is favoured in the presence of precursor proteins (Chou *et al.*, 2006). The second Sti1 domain of Tic40 mediates the interaction with Hsp93 (Chou *et al.*, 2003; Chou *et al.*, 2006). *In vitro* experiments revealed that this interaction is stronger in the presence of ATP and non-hydrolyzable ATP than in the presence of ADP, indicating that Tic40 stimulates the ATPase activity of Hsp93.

In *Arabidopsis*, null mutants of *attic40* display a pale green phenotype, slower growth and less grana stacks in the thylakoids than wild type plants (Chou *et al.*, 2003). A reduced import rate into chloroplasts isolated from mutant plants caused decreased amount of nuclear encoded proteins in the chloroplasts, whereas the binding of precursor proteins was not affected. During *in vitro* import experiments the amount of PIC1/Tic21, Tic40 and Tic110 soluble import intermediates increased in the stroma in *attic40* null mutant chloroplasts (Chiu and Li, 2008). The authors concluded that Tic40 is involved in the re-insertion of these proteins (and itself) into the envelope. However, another study (Firlej-Kwoka *et al.*, 2008) described that the PIC1/Tic21 import intermediate is already strongly membrane bound (not extractable even with urea), which may indicate that Tic40 is responsible for the insertion of the intermediate as well. Different Tic40 constructs lacking either the transmembrane, the alleged TPR-like or the second Sti1 domain were not able to complement the *attic40* phenotype, indicating that the full-length protein is necessary for proper activity (Bédard *et al.*, 2007). Interestingly, the phenotype of *attic40* knock-outs could be complemented with a construct, in which the second Sti1 domain was substituted by the corresponding domain of human Hip, supporting a role for Tic40 as a co-chaperone.

Intriguingly, a similar phenotype was described for the heterozygous *attic110*, homozygous *athsp93-V* and *attic40* mutants and all three double mutant combinations of these genes, without additive interactions (epistasis) (Kovacheva *et al.*, 2005). Additionally, the interaction pattern with precursor and mature proteins during import experiments is highly similar for Tic110, Hsp93 and Tic40 (Chou *et al.*, 2003). The *in vitro* and *in vivo* data (cross-linking, co-immunoprecipitation, import studies and mutant phenotypes) thus strongly suggest that these three components might act together in facilitating protein import into chloroplasts.

1.2.2.4. Hsp70

Hsp70 proteins are the members of a large protein family present in different cellular sub-compartments and involved in a variety of cellular processes (Sung *et al.*, 2001). In plants four subgroups of Hsp70 proteins are found in distinct compartments: in the cytosol, endoplasmic reticulum, plastids and mitochondria. Their roles include protein folding, modulation of protein activity, regulation of protein degradation and prevention of irreversible protein aggregation. Furthermore, Hsp70 motors drive protein translocation into the endoplasmic reticulum and into mitochondria (Johnson and van Waes, 1999; De Los *et al.*, 2006). Therefore, several studies aimed to find the linkage between Hsp70 and the translocation process in chloroplasts.

Early studies indicated the presence of Hsp70 in the intermembrane space, forming the intermembrane space complex with Toc12 and Tic22 (Schnell *et al.*, 1994; Becker *et al.*, 2004). However, the coding gene for this Hsp70 has never been identified. Furthermore, the detailed study of chloroplast Hsp70 proteins could not identify any chloroplast isoforms, which are sensitive to trypsin proteolysis (indicating the localization to the intermembrane space) (Ratnayake *et al.*, 2008), and the localization of Toc12 is also debated (Chiu *et al.*, 2010). On the contrary, *in vitro* studies importing titin fused to OE33 transit peptide supported the existence of an intermembrane space chaperone system providing the driving force for the initial step of translocation (Ruprecht *et al.*, 2010).

Recently, *Physcomitrella patens* Hsp70-2 (PpHsp70-2) was co-immunoprecipitated with the precursor protein in a complex containing also Hsp93 and Tic40, indicating that Hsp70 was associated with the TIC complex (Shi and Theg, 2010). Since *pphsp70-2* knock out mutants were lethal, the authors used a rescuing plasmid containing a mutated *PpHsp70-2* coding for a functionally impaired Hsp70 protein. Import into these chloroplasts after heat shock displayed a reduced transport capacity in comparison to the control plants, strongly suggesting that PpHsp70-2 is involved in protein import into chloroplasts. Furthermore, the authors generated

knock out mutants for the nucleotide exchange factors of Hsp70, *PpCGE1* and *PpCGE2*, which are the homologs of prokaryotic GrpE co-chaperones. Double mutants of the two genes were lethal, whereas *ppcge1* knock out and *ppcge2* knock down double mutants were viable, however displayed slow growth rate, less and smaller chloroplasts and severe defects in protein import into chloroplasts. The latter phenotype clearly indicates a role in protein import of these co-chaperones. Furthermore, an elevated level of PpHsp70-2 in these mutants could suggest the compensation effect of Hsp70.

In *Arabidopsis*, there are two Hsp70 isoforms present in chloroplasts: *cpHsp70-1* and *cpHsp70-2* (or *cpHsp70-6* and *-7*, respectively) (Ratnayake *et al.*, 2008), which are both imported into the stroma (Su and Li, 2008). Knock out mutants of *cphsp70-1* exhibit growth retardation, impaired root growth and thermosensitive seeds. In contrast, *cphsp70-2* mutants show no phenotype. Furthermore, deletion of both genes causes lethality. A more recent study demonstrated that *cphsp70-1* and *cphsp70-2* mutants display a defect in protein import into chloroplasts, however this observation was dependent on the age of the used plants (Su and Li, 2010). After cross-linking during *in vitro* import experiments, co-immunoprecipitation with a cpHsp70 antibody resulted in a complex containing Hsp70, the preprotein, Tic110, Tic40, Hsp93 and TOC components. The authors furthermore demonstrated that cpHsp70 is important for the import of both photosynthetic and non-photosynthetic proteins. Additionally, Hsp70 was present in the TOC/TIC supercomplex also in the absence of the preprotein. Applying different amounts of ATP during import experiments indicated that cpHsp70 acts as a driving force for translocation across the membrane (similarly to Hsp93).

The studies described above clearly demonstrate that there are two ATPases involved in the late translocation process across the chloroplast envelope membranes: Hsp93 (a member of the HSP100 protein family) and Hsp70. To unveil whether these chaperones work together or in parallel during the import process, double mutants were generated. *cphsp70-1 hsp93-V* has more reduced chlorophyll amount and import efficiency in comparison to the single mutants, whereas *cphsp70-1 tic40* double mutants are lethal (Su and Li, 2010). These observations support the hypothesis that Hsp93/Tic40 and Hsp70 have overlapping functions. Since no epistasis was observed (as in the case of Hsp93 and Tic40) these complexes might work in parallel associated with Tic110 (Figure 3 B). However, a common function could not be unequivocally ruled out (Figure 3 A). Moreover, Tic40 might interact also with Hsp70 and thus two different complexes could be formed, both containing Tic40 (Figure 3 C).

Additionally, similarly to *Physcomitrella patens*, GrpE homolog co-chaperones might also act in seed plants helping the action of Hsp70.

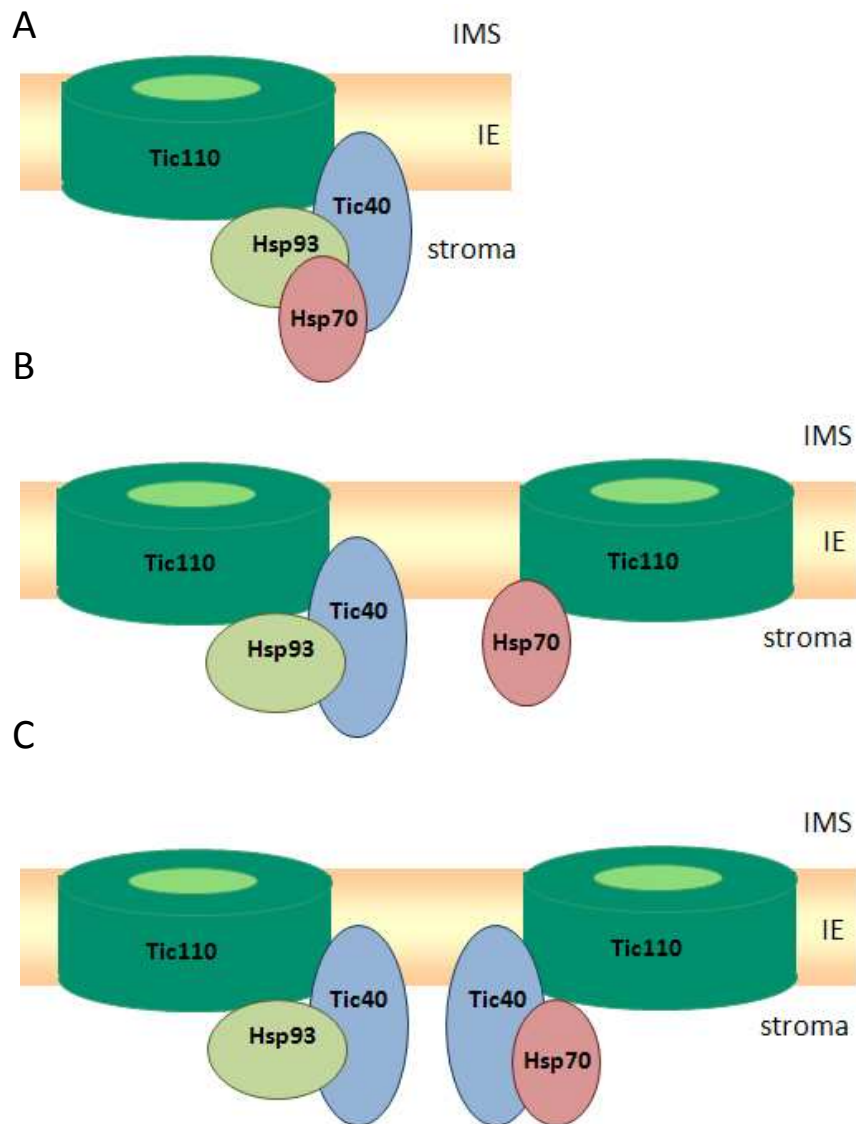


Figure 3. Possible assembly of the TIC motor complex(es)

Figure was depicted based on Su and Li (2010). Translocation through the Tic110 channel can be facilitated by one (A) or two (B,C) motor complexes. Tic40, Hsp93 and Hsp70 are working either together in one complex (A), or functioning parallel. In the latter case, Hsp93 is associated with Tic40, whereas Hsp70 might form the motor complex in the absence (B) or presence (C) of Tic40. IE: inner envelope membrane; IMS: intermembrane space.

Since a wide spectrum of preproteins has to be imported into plastids, two motor complexes may work more efficiently to fulfill all the requirements. However, both complexes were demonstrated to import photosynthetic and non-photosynthetic preproteins (Kovacheva *et al.*, 2005; Su and Li, 2010). Affinity to proteins of different hydrophobicity or a function in certain developmental stages or tissues might explain a different role for two complexes.

1.2.3. Redox regulation

Chloroplasts constantly have to adapt to the developmental and environmental conditions of the plant. Changing demands require adaptation of the protein complement and therefore protein import needs to be tightly regulated. This seems to occur at the stage of the TOC complex via phosphorylation, GTP-hydrolysis and thiol regulation and at the TIC complex via the stromal redox status, thioredoxins and calcium/calmodulin signalling (for more details see also Schwenkert *et al.*, 2011).

1.2.3.1. Regulation via the metabolic redox state

Three proteins in the TIC translocon (components of the redox regulon) have domains, which strongly suggest the involvement in redox regulation. They contain either NADP(H)-binding sites (Tic62 and Tic32) or a Rieske-type iron-sulphur centre (Tic55) (Figure 2).

Tic62 was initially described to form a complex together with Tic110 and Tic55 (Küchler *et al.*, 2002). The NADP(H) binding site in its N-terminal domain acts as a dehydrogenase in the presence of NADPH and not of NADH (Stengel *et al.*, 2008). In addition, the localization of Tic62 was shown to be dependent on the chloroplastic $\text{NADP}^+/\text{NADPH}$ ratio (Stengel *et al.*, 2008; Benz *et al.*, 2009). In an oxidized environment (high $\text{NADP}^+/\text{NADPH}$ ratio) Tic62 is mostly membrane-bound (attached to the IE or to thylakoids) and associates stronger with the TIC complex. Under reduced conditions (low $\text{NADP}^+/\text{NADPH}$ ratio) the amount of Tic62 relatively increases in the stroma. The C-terminus of Tic62 contains several Pro/Ser-rich repeats, which were demonstrated to specifically bind to ferredoxin-NADP⁺ oxidoreductase (FNR) (Küchler *et al.*, 2002; Alte *et al.*, 2010). FNR catalyses the last step of photosynthetic electron transport in chloroplasts, delivering electrons from reduced ferredoxin to NADP^+ . The thylakoid bound Tic62 tethers FNR in high molecular weight complexes dynamically to the thylakoids, dependent on the stromal pH and light (Benz *et al.*, 2009; Benz *et al.*, 2011). Via FNR, Tic62 could thus represent a link between photosynthesis and protein import into chloroplasts.

Tic32 was initially identified as interaction partner of the N-terminus of Tic110 (Hörmann *et al.*, 2004). This protein, similarly to Tic62, belongs to the (extended) family of short-chain dehydrogenases, and was characterized as enzymatically active dehydrogenase in the presence of NADPH (Chigri *et al.*, 2006). It dissociates from the TIC complex under reduced conditions (low $\text{NADP}^+/\text{NADPH}$ ratio), but is presumably still membrane bound (in contrast to Tic62), whereas under oxidized conditions (higher $\text{NADP}^+/\text{NADPH}$ ratio) it is connected to the TIC complex.

Tic55 contains a Rieske-type iron-sulphur centre and a mononuclear iron-binding site (Caliebe *et al.*, 1997), therefore being a member of the small family of non-heme oxygenases. Rieske-type proteins often function in electron transfer chains, such as cytochromes in the thylakoid membrane of chloroplasts or in the respiratory chain in the mitochondrial inner membrane. This, together with its close proximity to Tic62, suggests a role of Tic55 in redox regulation of protein import and raises the intriguing possibility of an electron transfer chain being present at the IE involving Tic62, Tic32 and Tic55.

The possible connection between the metabolic redox state and import efficiency was analysed by different studies: Hirohashi *et al.* (2001) demonstrated that the import efficiency of some precursors differs under dark/light conditions (when the photosynthetic activity and thereby the redox environment via the changed $\text{NADP}^+/\text{NADPH}$ ratio varies). Additionally, the increase of the $\text{NADP}^+/\text{NADPH}$ ratio in the stroma favours the import efficiency of a subgroup of proteins (Stengel *et al.*, 2009). Tic62 might be the linkage between the metabolic redox state and the TIC translocon, possibly with the involvement of the whole redox regulon.

1.2.3.2. Regulation via thioredoxins

Apart from regulation of protein import by the $\text{NADP}^+/\text{NADPH}$ ratio, another redox system, the thioredoxins (Trxs), might also be involved in import redox regulation. Trxs are small proteins with a disulfide-oxidoreductase function (Schürmann and Jacquot, 2000; Hisabori *et al.*, 2007; Schürmann and Buchanan, 2008). By oxidation of their conserved cysteine (Cys) residues they can reversibly reduce different types of proteins and thereby modulate their activity and/or conformation. In *Arabidopsis*, there are six sub-groups of Trxs: *f*, *m*, *x* and *y* are located to plastids, *o* to mitochondria and *h* to cytosol and other cellular compartments. Trx *f*, *o* and *h* have eukaryotic origin, whereas *m*, *x* and *y* are prokaryotic. Trx *f* and *m* had originally been described as activators of the Calvin-Benson cycle enzymes fructose 1,6-bisphosphatase and NADP-malate dehydrogenase, respectively. Trx *x* and *y* primarily play a role not in regulation of enzyme activity, but in stress response. The increasing amount of identified Trx targets (e. g. components of the Calvin-Benson cycle, pentose phosphate cycle, the ATP synthase, light-harvesting antenna complex II, enzymes involved in lipid and starch biosynthesis, nitrogen and hydrogen metabolism, etc.) shows a central regulatory role of Trxs in chloroplasts (Figure 4).

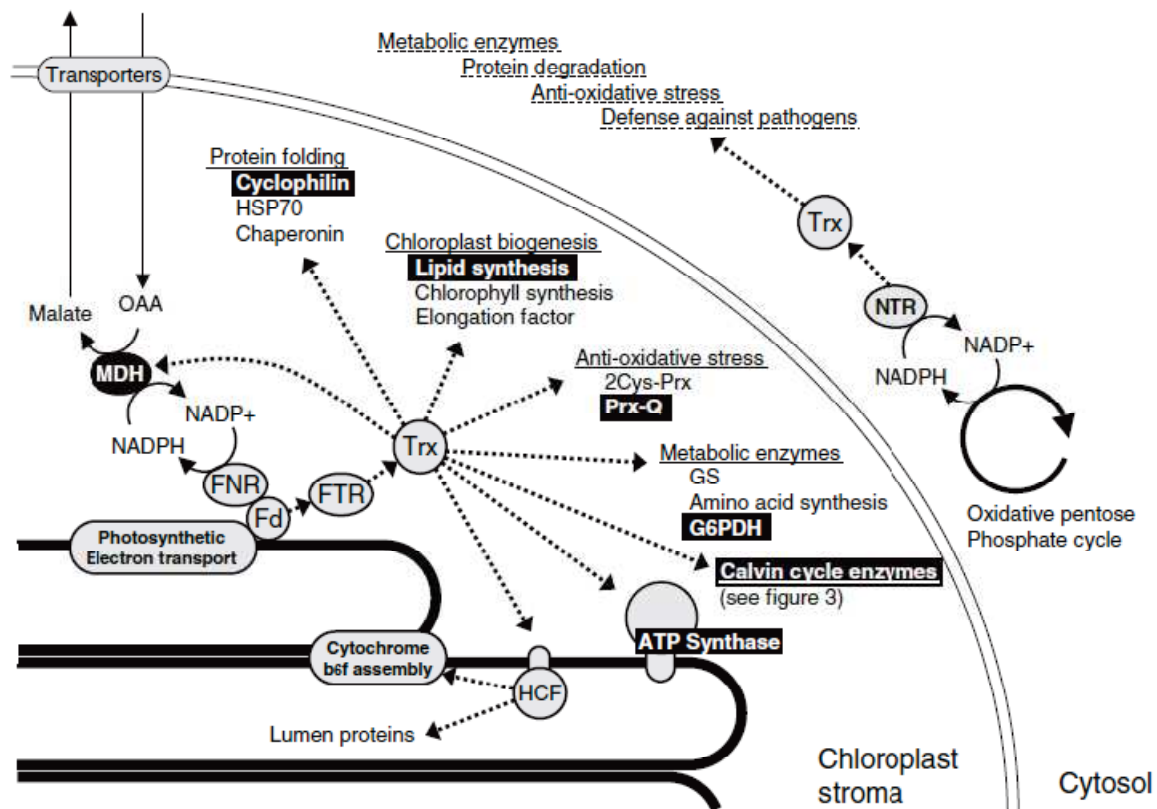


Figure 4. Thioredoxin network of chloroplasts and the cytosol

Figure was taken from Hisabori *et al.* (2007). Thioredoxins (Trx) are reduced by NADP⁺-dependent Trx reductase (NTR) in the cytosol and by ferredoxin-dependent Trx reductase (FTR) in plastids. FTR is reduced by ferredoxin (Fd), which also reduces ferredoxin-NADP⁺ oxidoreductase (FNR). The presented groups of targets were identified by proteome analysis, whereas black shaded-targets are already experimentally verified. MDH: malate dehydrogenase; OAA: oxalacetate; Prx: peroxiredoxin; GS: glutamine synthase; G6PDH: glucose-6-phosphate dehydrogenase; HCF: “high chlorophyll fluorescence”.

Trxs are reduced in the cytosol via NADP⁺-dependent Trx reductase (NTR) and in plastids via ferredoxin-dependent Trx reductase (FTR) (Figure 4). FTR is reduced by ferredoxin, which is directly reduced by photosystem I, therefore establishing a link between Trx regulation and photosynthesis (and thus light). Therefore, Trxs are reduced during the day and oxidized at night via oxygen or other oxidants. The oxidized form of Trx is also enzymatically active, one described target is glucose-6-phosphate dehydrogenase, an enzyme of the oxidative pentose phosphate pathway.

Trxs contain a highly conserved motif (WCGPC) in their active site, in which two Cys play a crucial role in reducing and oxidizing substrate proteins (Figure 5 A). The reduction occurs in two steps: the sulfhydryl (-SH) group of the N-terminal Cys attacks the disulfide bridge of the target, and establishes a covalent intermediate between the substrate and Trx. In the second step, the -SH group of the C-terminal Cys builds an intramolecular disulfide bridge, thereby releasing the reduced substrate. This mechanism allows a tool for identifying Trx targets:

mutation in the C-terminal Cys (to serine or alanine) prevents the dissociation of the intermediate complex, hence substrates can only be released via reduction e.g. with DTT (Figure 5 B) (Motohashi *et al.*, 2001).

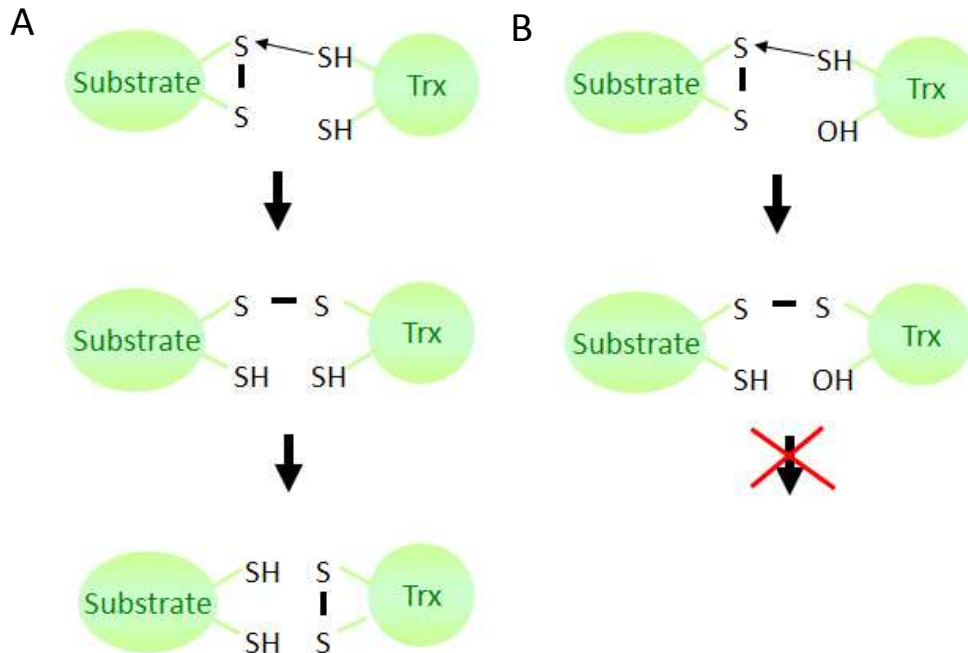


Figure 5. Reaction mechanism of the reductase activity of thioredoxins

A) Reduced thioredoxin (Trx) binds covalently to the oxidized substrate protein via a disulfide bridge. The other conserved sulfhydryl group (-SH) attacks the bond, therefore the substrate will be released in a reduced form and Trx will be oxidized. B) Mutation in the second (C-terminal) cysteine to serine (hydroxyl group, -OH) arrests the second, releasing step, therefore a stable intermediate will remain after the reaction containing Trx and its substrate.

Expanding the list of Trx targets, the involvement of Trxs in protein import into chloroplasts has also been suggested: Bartsch *et al.* (2008) found Tic55 together with PAO and Ptc52 (two other members of the non-heme *oxygenases* family) as Trx targets in the IE. However, the denaturing solubilization of envelopes (in 3% SDS) during their experiments questions the physiological significance of these results. Furthermore, the presence of highly conserved Cys residues in other TIC components, such as Tic20, Tic22 and Tic110, also suggests regulation via disulfide bridges (Balsera *et al.*, 2009b and Sections 4.1.5, 4.1.6). Hsp93 in cyanobacteria was identified as a Trx target by Ni-affinity chromatography followed by 2D SDS-PAGE under non-reducing/reducing conditions (Mata-Cabana *et al.*, 2007). In *Arabidopsis*, there are two conserved Cys in Hsp93, positioned sufficiently close to each other - after a homology modelling using ClpB structure as a template - to form a disulfide bridge, therefore *Arabidopsis* Hsp93 could be also a possible target for Trx regulation (Balsera *et al.*, 2009b). However, all of these indications have to be experimentally verified.

1.3. Aims of this work

This work consists of the structural and functional characterization of two chloroplast IE proteins, Tic110 and Tic20.

In the first part, three aims were defined to further characterize Tic110: Firstly, to demonstrate the insertion of Tic110 into the membrane, which study is part of the topological characterization of the protein (aiming to clear the role of the N-terminal hydrophilic part). Secondly, the detection of different oxidation states of Tic110 represented a main focus of the study: to analyse the possible roles of the oxidation states of Tic110 (e.g. altered import and channel activity, modified binding to the Tic40/Hsp93 motor complex and to preproteins) together with the identification of Cys residues involved in disulfide bridge formation. Thirdly, to find a suitable method for the crystallization of Tic110, since earlier attempts failed to crystallize the protein.

In the second part, two projects were set up in order to characterize Tic20: Firstly, since there were several indications that Tic20 forms a channel without any experimental evidence, the main goal was to demonstrate and characterize the channel activity of Tic20 *in vitro* in proteoliposomes, and thereby get implications about protein import channels functioning in the TIC translocon. Last but not least, after finding a sufficient tool for membrane protein crystallization, the aim of this work was to establish crystallization conditions, which would lead to the resolved structure of Tic20.

2. Materials

2.1. Chemicals

All used chemicals were purchased in high purity from Sigma-Aldrich (Steinheim, Germany), Fluka (Buchs, CH), Roth (Karlsruhe, Germany), Roche (Penzberg, Germany), Merck (Darmstadt, Germany), AppliChem (Darmstadt, Germany) or Serva (Heidelberg, Germany).

Special chemicals were purchased as follows: Radiolabeled amino acids ([³⁵S]Met) were obtained from DuPont-NEN (Dreieich, Germany), *n*-dodecyl- β -D-maltoside (DDM), sodium dodecyl sulphate (SDS) and Triton X-100 from Roth, digitonin from Calbiochem/Merck, *n*-lauroylsarcosine (LS), L- α -phosphatidylcholine (PC, Type-IV-S), Tris(2-carboxyethyl) phosphine (TCEP), iodoacetamide (IAA) from Sigma, bilayer lipids from IonoVation (Osnabrück, Germany), 4-acetamido-4'-maleimidylstilbene-2,2'-disulfonic acid (AMS) from Invitrogen (Eugene, Oregon, USA), Bio-Beads SM-2 Adsorbent from Bio-Rad Laboratories (Hercules, CA, USA), metoxypolyethylenglycol-maleimide 5000 Da (PEG-Mal) from Laysan Bio (Arab, AL, USA), 9-monoolein from Nu-Check-Prep (Elysian, MN, USA).

2.2. Enzymes, kits and other proteins

Restriction enzymes for cloning, RNA- and DNA-polymerases, T4-DNA ligases and RNase were obtained from Roche, MBI Fermentas (St. Leon-Rot, Germany), New England Biolabs (Frankfurt a. M., Germany), Qiagen (Hilden, Germany), Eppendorf (Hamburg, Germany), Diagonal (Münster, Germany), GeneCraft (Köln, Germany), Finnzymes (Espoo, Finnland) and GE Healthcare (Münich, Germany).

“Plasmid Midi Kit” and “Nucleospin Extract II Kit” from Macherey and Nagel (Düren, Germany) were used for DNA purification and purification of DNA fragments from agarose gels, respectively. *In vitro* translation was performed with the “Flexi Rabbit Reticulocyte Lysate System” from Promega (Madison, USA). Crystallization kits (MemStart, MemSys, MemGold I and II) were obtained from Molecular Dimensions (Suffolk, UK), bicelle kit containing CHAPS, CHAPSO, DMPG and DMPC from Affymetrix (Santa Clara, CA, USA).

Thrombin protease was applied from GE Healthcare, Trx *E. coli* from Sigma, complete EDTA-free protease inhibitor cocktail tablets from Roche. Trx *f* and *m* from spinach were a kind gift from Prof. Bob B. Buchanan (University of California, USA).

2.3. Strains, vectors and oligonucleotides

E. coli TOP10 (Invitrogen, Darmstadt, Germany) and BL21 (DE3) (Novagen/Merck, Darmstadt, Germany) strains were used for cloning and heterologous expression of proteins, respectively.

Table 1. Primers used in this work

Introduced mutation sites are shaded.

Primer name	Primer sequence	Application
dNTic110 C445S fw	GGCATTCTTCAAATTTGTCTGACGAGCTG	site directed mutagenesis in dNTic110
dNTic110 C445S rev	ACAAATTTTGAAGGAATGCCGCTTGCTATC	site directed mutagenesis in dNTic110
dNTic110 C492S fw	GAAGCTGCGTGTAATGCTCTCTGTACCTCAAC	site directed mutagenesis in dNTic110
dNTic110 C492S rev	AGAGCATTACACGCAGCTTCAACAAAGCAG	site directed mutagenesis in dNTic110
dNTic110 C470S fw	CGCCAAAAGCTTCAGCAATCTGTTGCTGATG	site directed mutagenesis in dNTic110
dNTic110 C470S rev	ATTGCTGAAGCTTTTGGCGATAAATTTCTTC	site directed mutagenesis in dNTic110
dNTic110 C506S fw	GGCAGCTCATGCAGAAATCTCTGGCAATTTG	site directed mutagenesis in dNTic110
dNTic110 C506S rev	AGATTTCTGCATGAGCTGCCTCAACCGTCTG	site directed mutagenesis in dNTic110
dNTic110 C674S fw	CAAGACATTTTGGACTTACTCTCTAACCGGTG	site directed mutagenesis in dNTic110
dNTic110 C674S rev	AGTAAGTCAAAAATGTCTTGTAAGATCAG	site directed mutagenesis in dNTic110
dNdCTic110 fw	GATCCCATGGCTAGCTGGAGCC	dNdCTic110/pET21d (<i>NcoI</i>)
dNdCTic110 rev	GATCCTCGAGGCTGTCTAAATCAACATTGG	dNdCTic110/pET21d (<i>XhoI</i>)
NtTic110 fw	GATCCATGGAGCTCACTGGATTGCAAC	NtTic110/pET21d (<i>NcoI</i>)
NtTic110 rev	GATCCTCGAGCTGTTCTGCATCACCTTC	NtTic110/pET21d (<i>XhoI</i>)
Hsp93 fw	GATCCATATGTCAAAGGCAGTTTCTTCACGG	Hsp93/pET14b (<i>XhoI</i>)
Hsp93 rev	GATCCTCGAGCTATATAGAAAGAGCCTCTGGTAAC	Hsp93/pET14b (<i>NdeI</i>)

pET21d, pET14b (Novagen/Merck) vectors were used for cloning. Oligonucleotide primers were ordered in standard desalted quality from either Operon (Cologne, Germany) or Metabion (Martinsried, Germany) (Table 1). Used clones are listed in Table 2.

Table 2. Clones used in this work

Inserted references show if the clone was already published. *At.*: *Arabidopsis thaliana*; TP: transit peptide. *Trx *f* C49S clone in pET3c/d was kind gift from Prof. Peter Schürmann (University of Neuchâtel, Switzerland).

Construct name	Insert	Organism	Vector	Notes
dNTic110	N-terminally truncated mature Tic110, aa. 85-996	pea	pET21d	overexpression (Balsera <i>et al.</i> , 2009a)
dNTic110 Cys mutants	N-terminally truncated mature Tic110 with pointmutations	pea	pET21d	overexpression
dNdCTic110	N- and C-terminally truncated mature Tic110, aa. 85-803	pea	pET21d	overexpression
NtTic110	N-terminal part of mature Tic110 aa. 25-258	<i>At.</i>	pET21d	overexpression
tpSSU-NtTic110-mSSU	TP of SSU Tic110, aa. 38-269 mature SSU	tobacco pea tobacco	pET21d	overexpression (present in the group)
Trx <i>f</i> C49S	mature Trx <i>f</i> with pointmutation	spinach	pET15b (with TEV digestion site)	overexpression (present in the group*)
Hsp93	mature Hsp93	pea	pET14b	overexpression
Tic40sol	soluble part of Tic40, aa. 120-436	pea	pPROEX	overexpression (present in the group)
Tic20	mature part of Tic20, aa. 59-274	<i>At.</i>	pCOLDII	overexpression (present in the group)
pSSU	preprotein of SSU	TP: soybean mature: pea	pSP65	<i>in vitro</i> transcription/translation (Lubben and Keegstra, 1986)
pOE33	preprotein of OE33	pea	pSP64	<i>in vitro</i> transcription/translation (Cline <i>et al.</i> , 1993)

2.4. Molecular weight markers and DNA standards

*Pst*I restricted λ -Phage DNA (MBI Fermentas) was used as a molecular size marker for agarose-gel electrophoresis.

For SDS-PAGE the “MW-SDS-70L” and “MW-SDS-200” markers from Sigma-Aldrich (Steinheim, Germany) and for BN-PAGE the “HMW Native Marker Kit” from GE Healthcare (München, Germany) were used.

2.4.1. Antibodies

Primary antibodies directed against Tic110 (*Pisum sativum*), Tic62 (C-terminus from *Pisum sativum*) and Tic20 (*Pisum sativum* and *Arabidopsis thaliana*) were already available in the laboratory. Secondary antibodies, coupled to alkaline phosphatase or horseradish peroxidase, against rabbit were purchased from Sigma-Aldrich.

2.4.2. Columns and column materials

HisTrap HP 1 ml and 5 ml, Superdex 200 (10/300 GL) and Superose 6 (10/300 GL) columns and Ni Sepharose Fast Flow column material were supplied by GE Healthcare (München, Germany). Protein concentration columns (Amicon Ultra 10K and 4K) were purchased from Millipore (Billerica, MA, USA).

2.4.3. Plant material

Peas (*Pisum sativum*) var. “Arvica” were ordered from Bayerische Futtersaatbau (Ismaning, Germany).

3. Methods

3.1. Molecular biological methods

3.1.1. General molecular biological methods

General molecular biological methods like growing conditions of bacteria, preparation of transformation-competent bacteria, DNA precipitation, determination of DNA concentration and bacterial transformation were performed as described by Sambrook *et al.* (1989) with slight modifications. Preparation of plasmid DNA, restrictions, ligations and agarose gel electrophoresis were carried out as in Sambrook *et al.* (1989) with modifications according to the manufacturer's recommendations of the corresponding enzymes. Polymerase chain reactions (PCR) were performed according to Saiki *et al.* (1988) under the conditions recommended by manufacturer of the DNA polymerase containing kit (Phusion, Finnzymes, Espoo, Finland). For site directed mutagenesis, clones containing the wild type insert of interest were amplified by PCR using two specific primers, one containing the mutation (Table 1). The PCR reaction mix was transformed in TOP10 cells and colonies were tested for plasmids containing the mutation.

3.1.2. *In vitro* transcription and translation

Transcription of linearized plasmids was carried out as previously described (Firlej-Kwoka *et al.*, 2008). Translation was carried out using the Flexi Rabbit Reticulocyte Lysate System (Promega) following the manufacturers protocol in presence of [³⁵S]-methionine for radioactive labelling. Signals were detected by exposure on X-ray films (Kodak Biomax MR, PerkinElmer, Rodgau, Germany) after polyacrylamide SDS-PAGE electrophoresis.

3.2. Biochemical methods

3.2.1. General biochemical methods

SDS-PAGE was performed according to Laemmli (1970).

Gels were stained either by Coomassie Brilliant Blue R250 (Sambrook *et al.*, 1989) or silver-stained according to Blum *et al.* (1987) with modifications.

Determination of protein concentration was performed with the Bio-Rad Protein Essay Kit (Bio-Rad, München, Germany).

3.2.2. Isolation of intact chloroplasts from *Pisum sativum*

For isolation of intact chloroplasts (Schindler *et al.*, 1987), pea seedlings were grown for 9-11 days on vermiculit, under 12/12 hours dark/light cycle. Plants were taken from the dark except where illumination ($100 \mu\text{mol photons m}^{-2} \text{ s}^{-1}$) is indicated. All procedures were carried out at 4°C. About 200 g of pea leaves were ground in a kitchen blender in approximately 300 ml isolation medium (330 mM sorbitol, 20 mM MOPS, 13 mM Tris, 3 mM MgCl_2 , 0.1% (w/v) BSA) and filtered through four layers of mull and one layer of gauze (30 μm pore size). The filtrate was centrifuged for 1 min at 1,500 g and the pellet was gently resuspended in about 1 ml wash medium (330 mM sorbitol, 50 mM HEPES/KOH (pH 7.6), 3 mM MgCl_2). Intact chloroplasts were reisolated via a discontinuous Percoll gradient of 40% and 80% (in 330 mM sorbitol, 50 mM HEPES/KOH (pH 7.6)) and centrifuged for 5 min at 3,000 g in a swing out rotor. Intact chloroplasts were taken from the 40%/80% interface, washed two times, and resuspended in a suitable volume of wash medium. Samples of chloroplasts (5 μl) were resolved in 5 ml of 80% acetone and chlorophyll concentration was estimated by measuring the optical density at three wavelengths (663, 645 and 750 nm) against the solvent (Arnon, 1949).

3.2.3. Preparation of inner and outer envelope vesicles from *Pisum sativum*

For isolation of IE and OE vesicles from pea, chloroplasts were isolated from ~ 20 trays of pea seedlings grown on sand, as it is described in 3.2.2. Further isolation of IE and OE vesicles was performed according to the modification (Waegemann *et al.*, 1992) of the previously described method (Keegstra and Youssif, 1986).

3.2.4. Isolation of stroma from *Pisum sativum*

Freshly isolated pea chloroplasts were incubated in 5 mM Tris-HCl (pH 8.0) for 20 min on ice. Stroma was separated from the membrane fraction by centrifugation (50,000 g, 30 min, 4°C).

3.2.5. Two-dimensional blue native (BN) / SDS-PAGE

BN-PAGE was performed essentially as described by Schagger and von Jagow (1991) and K  chler *et al.* (2002) with minor modifications. Tic20-proteoliposomes (30 μg protein) were solubilized in 50 mM Bis-Tris/HCl (pH 7.0), 750 mM 6-aminocaproic acid and 5% digitonin. After incubation at room temperature (RT) for 15 min, samples were centrifuged at 256,000 g for 10 min at 4°C. The supernatant was supplemented with 0.1 volume of a Coomassie Blue G solution (5% Coomassie Brilliant Blue G-250, 750 mM 6-aminocaproic acid) and loaded

on a polyacrylamide gradient gel. Following the first dimension, lanes were incubated sequentially in 1% SDS, 1 mM β -mercaptoethanol (ME), in 1% SDS without ME and in SDS-PAGE running buffer (25 mM Tris, 192 mM glycine and 0.1% SDS) at RT for 15 min each and then horizontally subjected to a second dimension SDS-PAGE.

3.2.6. Immunoblotting

For antibody detection, proteins were electro-blotted onto polyvinylidene fluoride (PVDF; Immobilon-P; Zefa, Harthausen) or nitrocellulose membrane (Protran; Whatman, Dassel) using a semi-dry Western blotting system (Hoefer TE 77; GE Healthcare, Freiburg, Germany). Labelling with protein-specific primary antibodies was carried out by standard techniques, and bound antibodies were visualized either with alkaline phosphatase (AP)-conjugated secondary antibodies (goat anti-rabbit IgG (whole molecule)-AP conjugated; Sigma) or using a chemiluminescence detection system (Enhanced Chemiluminescence, ECL) in combination with a horseradish peroxidase-conjugated secondary antibody (goat anti-rabbit (whole molecule)-peroxidase conjugated; Sigma). Detection of AP signals was performed in a buffer containing 66 μ l nitro blue tetrazolium chloride (NBT, 50 mg/ml in 70% N,N-dimethylformamide) and 132 μ l 5-bromo-4-chloro-3-indolyl phosphate (BCIP, 12.5 mg/ml in 100% N,N-dimethylformamide) in 10 ml 100 mM Tris-HCl (pH 9.5), 100 mM NaCl, 5 mM $MgCl_2$ buffer. Peroxidase-conjugated antibody signals were visualized by ECL detection. For this, solution 1 (100 mM Tris-HCl (pH 8.5), 1% (w/v) luminol, 0.44% (w/v) coumaric acid) and solution 2 (100 mM Tris-HCl (pH 8.5), 0.018% (v/v) H_2O_2) were mixed in a 1:1 ratio and added to the blot membrane (1-2 ml per small gel). After incubation for 1 min at RT (in the dark) the solution was removed and the luminescence was detected by exposure on Kodak Biomax MR films.

3.2.7. Protein identification by mass spectrometry (MS)

Coomassie- stained protein spots were cut from SDS-PAGE gels and send for identification to the “Zentrallabor für Proteinanalytik” (ZfP, Adolf-Butenandt-Institut, LMU München). Tryptic peptides were detected either by Peptide Mass Fingerprint (MALDI, Matrix Assisted Laser Desorption/Ionization) or LC-MS/MS (Liquid Chromatography with MS) runs. Protein identification was then accomplished with a Mascot software assisted database search.

3.2.8. Protein expression and purification

dNTic110 was overexpressed and purified as described previously (Balsera *et al.*, 2009a). Overexpression was performed using BL21 (DE3) at 27°C in LB medium till OD_{600} of 0.5.

After induction with 0.2 mM IPTG, temperature was shifted to 12°C for overnight. Cells were stored at -20°C until use. Cell lysis was performed in 20 mM Tris-HCl (pH 8.0), 300 mM NaCl, 10% glycerol, 1 mM phenylmethylsulfonyl fluoride (PMSF), 5 mM ME and protease inhibitor cocktail tablet by a French pressure cell press (Heinemann, Schwäbisch Gmünd, Germany), followed by centrifugation (40,000 g, 30 min, 4°C). The supernatant was purified using HisTrap HP column (1 or 5 ml) with an ÄKTA Purifier system (GE Healthcare, München, Germany). For wash and elution 20 mM Tris-HCl (pH 8.0), 300 mM NaCl with increasing concentrations of imidazole was used. Aliquots with high purity were collected and concentrated on an Amicon column for gel filtration (20 mM Tris-HCl (pH 8.0), 150 mM NaCl) on a Superdex 200 column to remove aggregates and remaining contaminants.

dNTic110 Cys mutants and **dNdCTic110** were overexpressed and purified similarly to dNTic110.

Trx f C49S was overexpressed in BL21 (DE3) in LB Medium at 37°C for 5 h after induction with 1 mM IPTG at OD 0.5. Cell lysis was performed in a buffer containing 20 mM Tris-HCl (pH 8.0), 150 mM NaCl, 0.5 mM DTT, 1 mM PMSF with French pressure cell press. After centrifugation (30,000 g, 30 min, 4°C) the supernatant was purified using Ni Sepharose with increasing concentrations of imidazole in the same buffer.

Hsp93 was overexpressed in BL21 (DE3) cells at 27°C overnight after the induction with 0.5 mM IPTG at OD 0.5. Cells were lysed in 20 mM Tris-HCl (pH 8.0), 150 mM NaCl, 1 mM PMSF, 1 mM ME and 5 mM MgCl₂ with M-110L Microfluidizer Processor (Microfluidics, Newton, MA, USA) and pelleted (40,000 g, 30 min, 4°C). The supernatant was purified with HisTrap HP columns applied in an ÄKTA Purifier system, using 20 mM Tris-HCl (pH 8.0), 150 mM NaCl with increasing imidazole concentrations for wash and elution. High purity elutions were collected and subjected to gel filtration on a Superose 6 column to eliminate remaining contaminations (20 mM Tris-HCl (pH 8.0), 150 mM NaCl). Calibration of the Superose 6 column was performed using thermolysin (660 kDa), ferritin (440 kDa) and aldolase (232 kDa) according to the supplier's instructions. To remove the His tag, purified protein was cleaved overnight by thrombin at 4°C (500 µg protein/1 unit protease).

Tic40sol was overexpressed similarly to Trx f C49S, and purified as Hsp93 except that the lysis buffer did not contain MgCl₂ and gel filtration was not needed to achieve homogeneity.

Tic20 was overexpressed and purified as described in Benz (2009) and Kovács-Bogdán *et al.* (submitted). Transformed BL21 (DE3) cells grown at 37°C in M9ZB medium to an OD₆₀₀ of

0.4 and then the temperature was shifted to 15°C for 30 min and induced with 1 mM IPTG. After induction, cells were further grown at 15°C overnight. The harvested cells were resuspended in 50 mM Tris-HCl (pH 8.0), 150 mM NaCl and 5 mM DTT, lysed (M-110L Microfluidizer Processor), pelleted (20,000 g, 4°C, 20 min) and solubilized in the presence of 1% LS for 1 h at 4°C. Purification was carried out in the presence of 0.3% LS using Ni Sepharose. For crystallization, samples were further purified using a Superdex 200 column equilibrated with 20 mM Tris-HCl (pH 8.0), 150 mM NaCl, 0.3 % LS.

NtTic110 and **tpSSU-NtTic110-mSSU** were overexpressed in BL21 (DE3) cells at 37°C for 3 h after induction at OD 0.5 with 0.5 mM IPTG, and pelleted. Purification was performed similarly to Tic20 except that in all buffers 300 mM NaCl was present.

3.2.9. Influence of oxidizing/reducing conditions on Tic110

dNTic110, dNTic110 Cys mutants and dNdCTic110 (0.1-0.2 mg/ml protein) were incubated with 50 µM CuCl₂, indicated concentrations of GSSG or 10 mM DTT for 30-60 min at 20°C. Precipitation with trichloroacetic acid (TCA) was performed (5% final concentration), followed by a wash with 100% acetone. The air-dried pellet was dissolved in freshly prepared 10 mM AMS, 100 mM Tris-HCl (pH 7.0) and 2 mM EDTA and incubated for 30-60 min in the dark at RT. Proteins were separated by non-reducing SDS-PAGE (8.5%) and Coomassie- or silver-stained.

To investigate the reversibility of the redox reaction, oxidized samples were dialysed (2x2 h against buffer without oxidant, 3-6 µg protein in each sample) and incubated for 1 h at 20°C with several reducing agents such as DTT (0.05–10 mM) or Trx *f*, *m* or from *E. coli* (0.75 µg for each reaction) in the presence of DTT (0.5 mM). Trx isoforms were pre-incubated with 5.5 mM DTT (30 min 20 °C). Reduction was followed by TCA precipitation and incubation with 10 mM AMS as described above. Results were visualized by Coomassie staining or silver staining after 8.5% non-reducing SDS-PAGE.

To analyse the direct interaction between oxidized Tic110 and Trx, freshly prepared dNTic110-proteoliposomes were oxidized (50 µM CuCl₂, 30 min, 20°C), pelleted (100,000 g, 30 min) and resuspended in buffer without oxidant (20 mM Tris-HCl (pH 8.0), 100 mM NaCl). Samples were incubated in the presence of Trx *f* C49S (8 µg in 200 µl reaction mixture) for 1 h at 20°C followed by flotation on sucrose step gradient and detection on a reducing gel (loading buffer supplemented with 100 mM DTT) by silver staining.

Leaves (0.1 g) of 10-day-old pea plants from the dark or light (30 min or 7 h illumination) were harvested and flash-frozen in liquid N₂. The frozen material was thoroughly ground in N₂ and extracted by addition of 1 ml buffer (100 mM Tris-HCl (pH 7.5), 0.2 mM EDTA, 1% SDS, 100 mM IAA) and incubated for 1 h at RT. The insoluble material was sedimented at 20,000 g for 10 min. 2x50 µl from each condition were precipitated with TCA (5% final concentration), washed with 100% acetone and dried. The pellet was solubilized in 100 mM Tris-HCl (pH 7.0), 1.5% SDS in the presence or absence of 2 mM TCEP for 30 min at RT. 10 mM AMS was added and samples were incubated for again 30 min in the dark at RT, and loaded on a 7.5% gel. Tic110 was detected by immunoblotting.

To analyse the redox state of Tic110 *in organello*, in the dark freshly prepared chloroplasts (10 µg chlorophyll for each sample) were treated with 50 µM CuCl₂ or 2 mM TCEP at 20 °C in wash medium (330 mM sorbitol, 50 mM HEPES/KOH (pH 7.6), 3 mM MgCl₂). After 30 min of incubation and solubilization (1% SDS), 10 mM AMS were added and the solution was incubated for 1 h in the dark at RT. The reaction was terminated by the addition of 100 mM DTT. Samples were subjected to SDS-PAGE (8.5%), and Tic110 was visualized by immunodecoration.

3.2.10. PEGylation assay

Tic20-proteoliposomes were treated with 10 mM PEG-Mal (5000 Da) in a buffer containing 100 mM Tris-HCl (pH 7.0), 1 mM EDTA, for the indicated times at RT in the dark in absence or presence of 1% SDS. The PEGylation reaction was stopped by addition of 100 mM DTT and SDS-PAGE sample buffer. NuPAGE Bis-Tris gels (0.36 M Bis-Tris-HCl (pH 6.5-6.8), 10% acrylamide) were employed using a MES running buffer (50 mM MES, 50 mM Tris, 1 mM EDTA, 1 mM sodium bisulfite, 0.1% SDS). Tic20 was visualized by silver staining.

3.2.11. Limited proteolysis assays with thermolysin

IE (10 µg total protein) or Tic20-proteoliposomes (4 µg protein) were pelleted (10 min, 256,000 g or 30 min, 400,000 g, respectively) and washed with 25 mM HEPES/KOH (pH 7.6), 5 mM MgCl₂ and 0.5 mM CaCl₂. Samples were incubated with 0.1 µg/µl thermolysin for the indicated time in the presence or absence of 1% Triton X-100 at RT. The reaction was stopped by addition of 10 mM EDTA. For the control, EDTA was added before thermolysin to the reaction mixture. Tic20 (and Tic110, Tic62 as controls in IE) was visualized by immunoblotting after SDS-PAGE.

3.2.12. Liposome preparation

Phosphatidylcholine (PC) was solubilized in chloroform:methanol (1:1) in a concentration of 20 mg/ml. To remove the solvent, samples were dried under N₂ flush for 30 min and in a vacuum exsiccator for 3 h in a glass tube. Until use, the PC film was stored at -20°C under argon. Lipid vesicles (20 mg/ml) were prepared in 10 mM Mops/Tris (pH 7.0), 100 mM NaCl, in the presence or absence of 1% SDS or in 20 mM Tris-HCl (pH 8.0), 100 mM NaCl. To prepare unilamellar liposome vesicles, samples were extruded 21 times through a polycarbonate filter with a diameter of 100 or 200 nm (Liposofast, Avestin, Ottawa, Canada). Purified proteins in a concentration of 0.5-0.8 mg/ml (or their buffer as a control) were mixed with liposomes in a 1:2 protein:lipid volume ratio and incubated for 1.5 h at 4°C. Samples were dialysed for 16 h at 4°C against the buffer without detergent, and the remaining detergent was removed during 2 h incubation at 4°C with Bio-Beads (20 mg/ 1 mg detergent). In the presence of SDS, incubation and dialysis was performed at RT.

3.2.13. Flotation assay

Liposome-associated and liposome-free proteins were separated by flotation through a sucrose gradient: Samples were adjusted to a sucrose concentration of 1.6 M and overlaid with the indicated sucrose step gradient (to a final volume of 12 or 4 ml). After centrifugation (100,000 g, 19 h, 4°C) 0.5 or 1 ml fractions were collected, TCA precipitated (5%) and washed with 100% acetone. Samples were resuspended in Laemmli-buffer, separated by SDS-PAGE and detected by silver-staining.

To verify the insertion of proteins into the liposomes, proteoliposomes were incubated in the presence of different buffers (control: 10 mM MOPS/Tris (pH 7.0) or 20 mM Tris-HCl (pH 8.0); high salt: 1 M MOPS/Tris (pH 7.0) or 1 M NaCl in 20 mM Tris-HCl (pH 8.0); high pH: 10 mM Na₂CO₃ (pH 11.0); denaturing: 6 M urea in 10 mM MOPS/Tris (pH 7.0) or in 20 mM Tris-HCl (pH 8.0)) for 30 min at RT and subjected to flotation.

3.2.14. Cross-linking

To analyse the oligomerization state of Hsp93, 20 µl samples from gel filtration (about 0.6 mg/ml protein) were incubated with 0.2% glutaraldehyde for 5 min at 37°C in 20 mM HEPES/KOH pH 7.6. The reaction was terminated by the addition of 50 mM Tris-HCl (pH 8.0). Samples were precipitated with TCA (5%), dried with 100 % acetone and loaded on a 5-10% SDS-PAGE and Coomassie-stained.

3.2.15. Swelling assay

Freshly prepared liposomes and proteoliposomes were diluted to 1 ml with a starting optical density of approximately 0.1 at 500 nm. The optical density of the samples was measured at 500 nm (OD_{500nm}) with a Shimadzu UV-2401PC Spectrophotometer (Columbia, USA) for the indicated time. At the beginning of the measurements 300 mM KCl were added. Additionally, Tic20-proteoliposomes were also incubated prior to measurements with 50 μ M $CuCl_2$ for 20 min at 20°C. To analyse the reversibility of oxidation, oxidized samples were subjected to dialysis with Millipore VSWP02500 filter discs according to the supplier's instructions (100 μ l sample on 25 ml buffer, for 30 min at RT) and reduced with 10 mM DTT (20 min, RT). Presented data are the average of at least three independent experiments. Standard deviations were calculated using the Excel 2007 software.

3.2.16. Electrophysiological measurements

3.2.16.1. Applied system

Electrophysiological measurements were performed using the IonoVation Bilayer Explorer (Osnabrück, Germany) according to the supplier's instructions. A disposable bilayer chamber ("bilayer slide"), consisting of two compartments (*cis* and *trans*), separated by a PTFE septum containing a microhole served for the preparation of the bilayer (Figure 6 A, B).

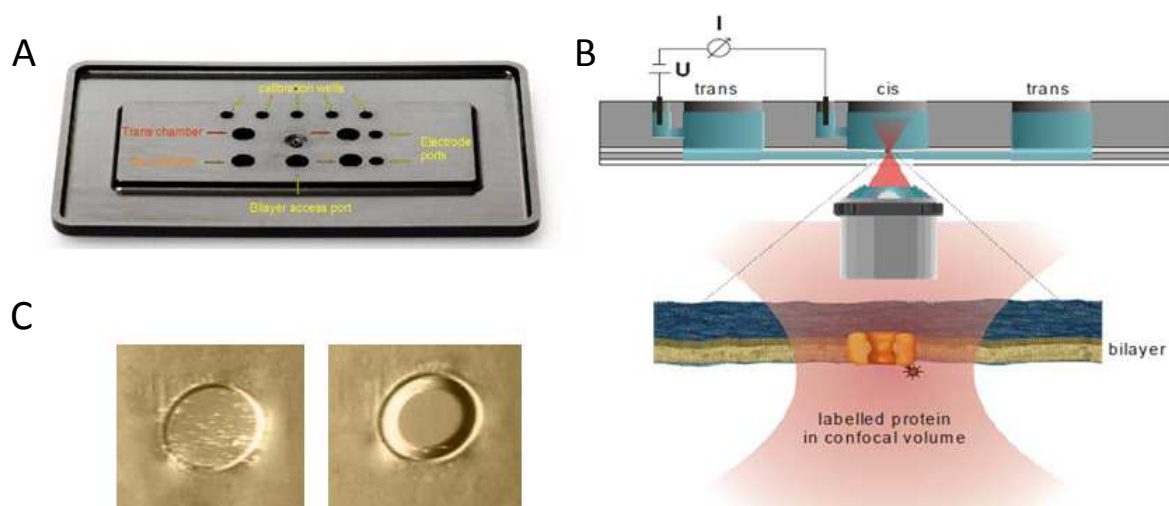


Figure 6. Principles of the IonoVation Bilayer Explorer

Figures were taken from IonoVation Bilayer Explorer V01 (2009) Manual from IonoVation. A) Bilayer chamber. Via the bilayer access port bilayer lipids and proteoliposomes can be added. B) Schematic view of the assembly of the bilayer slide. *Cis* and *trans* chambers are separated by a PTFE septum, serving for the preparation of the bilayer. Inserted protein allows current flow, which can be measured by the electrodes inserted to each compartment. C) Unordered lipid across the microhole (left) and a bilayer (right) can be also controlled using the light microscope.

Both compartments were filled with ca. 150 µl of saline buffer during measurements (10 mM MOPS/Tris (pH 7.0), 250/20 mM KCl, *cis/trans*). For electrical measurements Ag/AgCl electrodes with salt bridges were connected to the *cis* and *trans* compartments. A perfusion system with two 10 ml syringes was responsible for bilayer production and buffer exchange. For bilayer preparation ca. 0.2 µl of bilayer lipid in n-decane (5-10 mg/ml) was added directly to the microhole. Bilayer formation was also controlled by light microscopy (Olympus CKX41, Hamburg, Germany) (Figure 6 C). After the formation of a bilayer, proteoliposomes were added to the *cis* chamber (higher salt concentration). Fusion with the bilayer occurred by applying an osmotic gradient of 250/20 mM KCl between the two chambers (Figure 7). Patchmaster software (HEKA Elektronik, Lambrecht/Pfalz, Germany) controlled the experiment, i.e. preparing and verifying the bilayer formation and executing measurements.

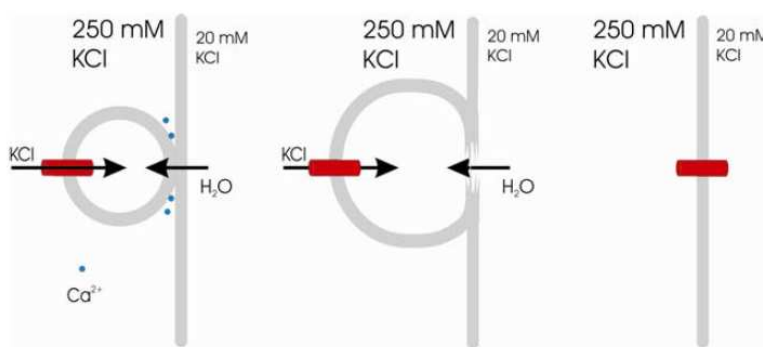


Figure 7. Schematic diagram of the fusion of proteoliposomes

The figure was taken from Ionovation Bilayer Explorer V01 (2009) Manual from IonoVation. The ionic gradient across the Teflon septum (250/20 mM KCl) allows the fusion of proteoliposomes with the bilayer if an open channel provides a pathway for the salt into the vesicle.

3.2.16.2. Conductance

Conductance of the channel was calculated from measurements under symmetric buffer conditions (10 mM MOPS/Tris (pH 7.0), 250 mM KCl). 15 different voltage values in a step gradient from -140 mV to +140 mV were applied, each voltage value for 5 min, and the current was measured. From the difference between two current levels in a gating event, the conductance was calculated using Ohm's law (Equation 1).

$$R = \frac{U}{I} \quad G = \frac{1}{R} = \frac{I}{U}$$

Equation 1. Ohm's law and the conductance

R	Resistance (Ω)
U	Voltage (V)
I	Current (A)
G	Conductance (S)

Conductance values of all gating events were plotted in a histogram and different conductance classes were determined according to the partial or complete closing of the channel. **Total conductance** of the channel was calculated from the absolute current measured between the two chambers. The **pore size** of the channel was estimated using the calculated conductance applying the model proposed by Hille (1992). His model assumes that the channel is a uniform cylinder with (r) radius and (l) length. Therefore, the resistance through the channel ($R_{channel}$) is given by Equation 2 A.

$$\text{A} \quad R_{channel} = \left(l + \frac{\pi \cdot r}{2} \right) \cdot \frac{\rho}{\pi \cdot r^2} \quad \text{B} \quad d = \frac{\rho \cdot G}{\pi} \cdot \left(\frac{\pi}{2} + \sqrt{\left(\left(\frac{\pi}{2} \right)^2 + \frac{4 \cdot \pi \cdot l}{\rho \cdot G} \right)} \right)$$

Equation 2. Calculation of the A) resistance and B) diameter of the channel (Hille, 1992)

$R_{channel}$	Resistance of the channel (Ω)
r	Pore radius (m)
l	Pore length (m)
ρ	Resistivity ($\Omega \text{ cm}$)
d	Pore diameter (m)
G	Conductance (S)

Equation 2 A was rearranged to calculate the channel diameter, exploiting that the conductance is the inverse of the resistance (Equation 2 B). Since there was no information about the length of the pore, two border values were used in the calculations: 1 nm and 5 nm, as cross sections of an expanded vestibule and a lipid bilayer, respectively. The resistivity of a solution containing 250 mM KCl is 247.5 $\Omega \text{ cm}$, according to Smart *et al.* (1997).

$$U_{rev} = \frac{R \cdot T}{F} \cdot \ln \frac{\sum P^+ \cdot c_{cis}^+ + \sum P^- \cdot c_{trans}^-}{\sum P^+ \cdot c_{trans}^+ + \sum P^- \cdot c_{cis}^-}$$

Equation 3. Goldman-Hodgkin-Katz equation

U_{rev}	Reverse potential (V)
R	Universal gas constant ($\text{J K}^{-1} \text{ mol}^{-1}$)
T	Temperature (K)
F	Faraday constant (C mol^{-1})
P	Permeability coefficient ($\text{m}^2 \text{ s}^{-1}$)
c	Concentration (mol L^{-1})
+/-	Index for cation/anion
cis/trans	Cis/trans chamber

3.2.16.3. Selectivity

The **selectivity** of the channel was determined under asymmetric buffer conditions (10 mM MOPS/Tris (pH 7.0), 250/20 mM KCl) with voltage values changing in a linear gradient from -100 mV to +100 mV and *vice versa*, eight times for each fusion. Voltage was plotted against

the measured current to read the intersection point (when the current is 0 pA), which defined the **reverse potential** of the channel. The Goldman-Hodgkin-Katz equation gave a rough estimation for the selectivity (Equation 3).

Since there were only two penetrating ions, Equation 3 was rearranged to Equation 4, and the ratio of the penetrating ions, therefore the selectivity was calculated.

$$\frac{P^+}{P^-} = \frac{c_{trans}^- - c_{cis}^- \cdot e^{\frac{U_{rev} \cdot F}{R \cdot T}}}{c_{trans}^+ \cdot e^{\frac{U_{rev} \cdot F}{R \cdot T}} - c_{cis}^+}$$

Equation 4. Rearranged Goldman-Hodgkin-Katz equation for two penetrating ions

U_{rev}	Reverse potential (V)
R	Universal gas constant ($J K^{-1} mol^{-1}$)
T	Temperature (K)
F	Faraday constant ($C mol^{-1}$)
P	Permeability coefficient ($m^2 s^{-1}$)
c	Concentration ($mol L^{-1}$)
+/-	Index for cation/anion
cis/trans	Cis/trans chamber

For data analysis, AxoScope 10.2 (Axon Instruments, Union City, USA), E-phys (developed by Thomas Steinkamp, University of Osnabrück, Germany) in combination with Origin 7.0 (OriginLab Corporation, Northampton, MA, USA) and Excel 2007 softwares were used. The presented data derived from two independent fusion events accounting for more than 4500 gating events and 16 voltage ramps.

3.2.17. Protein crystallization

Crystallization of Tic110 and Tic20 was performed in cooperation with Dr. Gergely Katona and Annette Duelli (University of Gothenburg, Sweden). For crystallization high concentration (above 10 mg/ml) and high purity of proteins had to be reached after purification. Therefore 2-3 times more cells were lysed and buffer volume, HisTrap column volume were also upscaled for this quantity. Except for these modifications, the purification protocol was the same as described in 3.2.8.

3.2.17.1. Cubic phase

For cubic phase crystallization, protein samples were mixed with 9-monoolein in a volume ratio of 2:3 in two 250 µl Hamilton syringes that were connected to each other with a mixer union (made at the Department of Biochemistry and Biophysics at the University of Gothenburg, Figure 8 A). 9-monoolein was melted at 55°C for 10 min followed by incubation at RT. The syringe used for the protein was pre-cooled, preventing precipitation at higher temperatures. Mixing was continued until a homogenous clear emulsion was present in the

syringes. Samples were incubated overnight at 20°C. Crystallization was tested in 24-well sitting drop plates (Crychem plate, Hampton Research, Aliso Viejo, CA, USA), applying the vapour diffusion method. 100-200 nl of the cubic phase were distributed on the plates using a Microsyringe-repeating dispenser (Hamilton, Figure 8 B) and mixed with 1 µl precipitant solution (MemStart, MemSys, MemGold I and II kits). The plates were sealed with Crystal Clear sealing tape (Hampton Research).

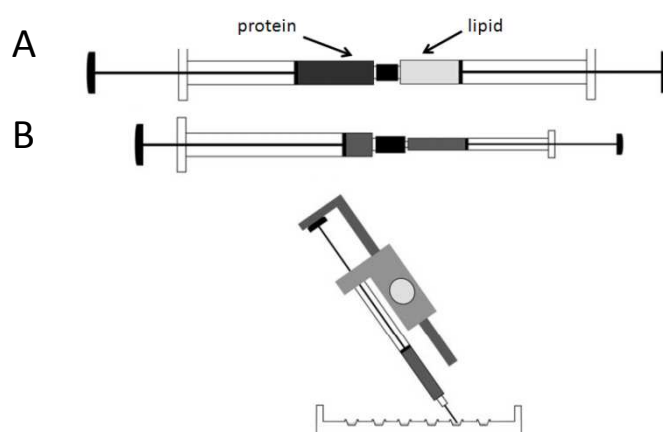


Figure 8. Tools for cubic phase crystallization

Figures were adapted from Nollert (2002). A) Protein and lipid (9-monoolein) were mixed with two 250 µl Hamilton syringes that were connected to each other with a mixer union. B) Mixed sample was taken up with a smaller syringe. Mixture was pipetted with the help of a Microsyringe-repeating dispenser onto the test plate.

3.2.17.2. *Bicelle*

For the bicelle method, detergent (CHAPS or CHAPSO) was diluted in 20 mM Tris-HCl (pH 8.0) followed by the addition of lipid (DMPG or DMPC). The mixture was thoroughly solubilized via repeated incubation at 37°C, on ice and vortexing. After the addition of protein, samples were incubated overnight at 4°C. Different composition of bicelles and bicelle-protein ratio were utilized to find the best condition. Crystallization test drops were set up via a Honeybee Sitting drop robot (Cartesian Technologies, Cambridgeshire, UK) in a 96-well plate containing 0.1 µl sample and 0.2 µl precipitant solution (from MemStart, MemSys, MemGold I and II kits) and covered by an Adhesive Crystallography Seal (ABgene, Thermo Fisher Scientific Inc., Epsom, UK).

Plates were controlled regularly for crystal formation. If crystals were grown, the experiments were reproduced with increased volumes. Crystals were mounted and flash-cooled in liquid nitrogen. In some cases, cryo-protectant was added in order to prevent freezing damage of crystals. Crystals were screened for well-diffracting protein crystals at the European Synchrotron Radiation Facility (ESRF).

4. Results

4.1. Tic110

4.1.1. Purification

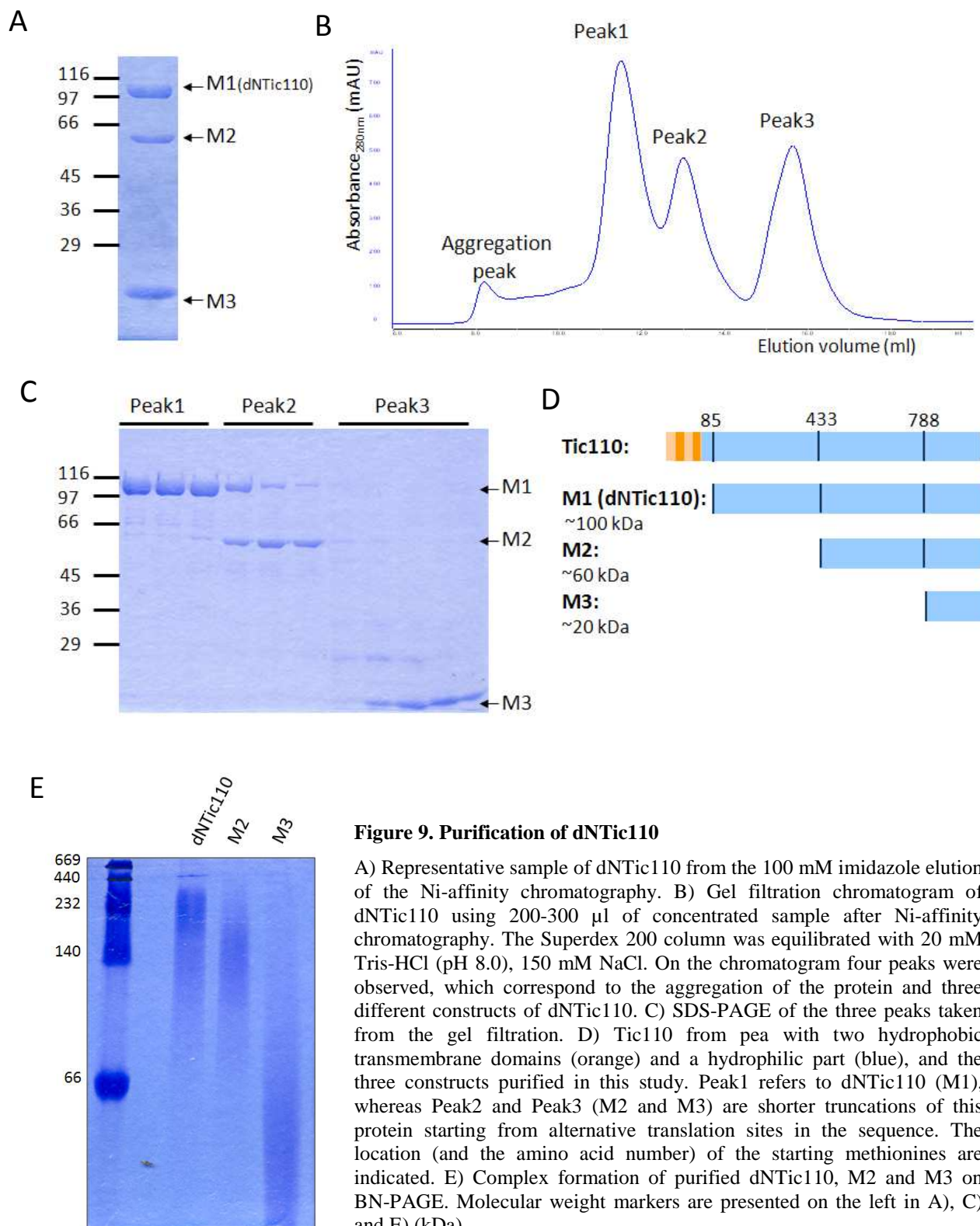
For the topological characterization of Tic110, dNTic110 - lacking the hydrophobic N-terminal domain of Tic110 - was overexpressed and purified in a soluble form, without any denaturing agents, following the protocol developed by Dr. Mónica Balsera (Balsera *et al.*, 2009a). Lower concentration of IPTG (0.2 mM) for the induction of *E. coli* and lower temperature (12°C) during protein expression allows the production of soluble dNTic110. Additionally, this construct does not contain the first two hydrophobic transmembrane helices, only the hydrophilic part of the protein.

After the Ni-affinity chromatography, three bands were visible on SDS-PAGE (Figure 9 A). These bands were separated after gel filtration on a Superdex 200 column (Figure 9 B, C). The first band represents dNTic110, whereas the other two bands are shorter truncations of the protein (M2 and M3), which were translated along with dNTic110 in *E. coli* (Figure 9 D). The simultaneous expression of the three protein forms was possible since the bacterial translation system recognized two alternative translation sites with a Shine-Dalgarno sequence (AGGAGG) followed by a start codon (AUG, methionine). Gel filtration furthermore removed the aggregated protein (Figure 9 B, “Aggregation peak”). Thereby, the purification protocol yielded a homogenous sample of dNTic110 (Figure 9 C lanes of “Peak1”). Additionally, note that no urea or other detergent was used for the purification, supporting the folding of the protein. CD spectroscopy (Balsera *et al.*, 2009a) also demonstrated that the presented purification protocol resulted in a folded protein, whose secondary structure does not change notably in the presence of detergent (0.03% DDM).

4.1.2. Complex formation

dNTic110 was subjected to BN-PAGE to analyse the oligomerization state of the protein. Although the protein behaves like a tetramer during size-exclusion chromatography (corresponding to a globular protein, Balsera *et al.*, 2009a), BN-PAGE analysis suggested dimer formation since the protein was present at 200-250 kDa (Figure 9 E). Furthermore, gel filtration followed by static light scattering also supported that dNTic110 is a dimer (Balsera *et al.*, 2009a). Subjecting the shorter constructs of dNTic110 (M2 and M3) to BN-PAGE,

resulted in M2 dimers and M3 monomers (Figure 9 E). Consequently, M2 still contains the domain responsible for the dimerization.



4.1.3. Insertion into liposomes

To investigate the membrane insertion of Tic110 without its hydrophobic part, proteoliposomes were prepared using purified dNTic110. The protein or its buffer (20 mM Tris-HCl (pH 8.0), 150 mM NaCl) was mixed with PC liposomes in the presence of 1% SDS. To obtain unilamellar membrane vesicles, liposomes were extruded through a 100 nm membrane prior to mixing with the protein. To remove detergent from the samples, overnight dialysis was performed at RT in 10 mM MOPS/Tris (pH 7.0), 100 mM NaCl.

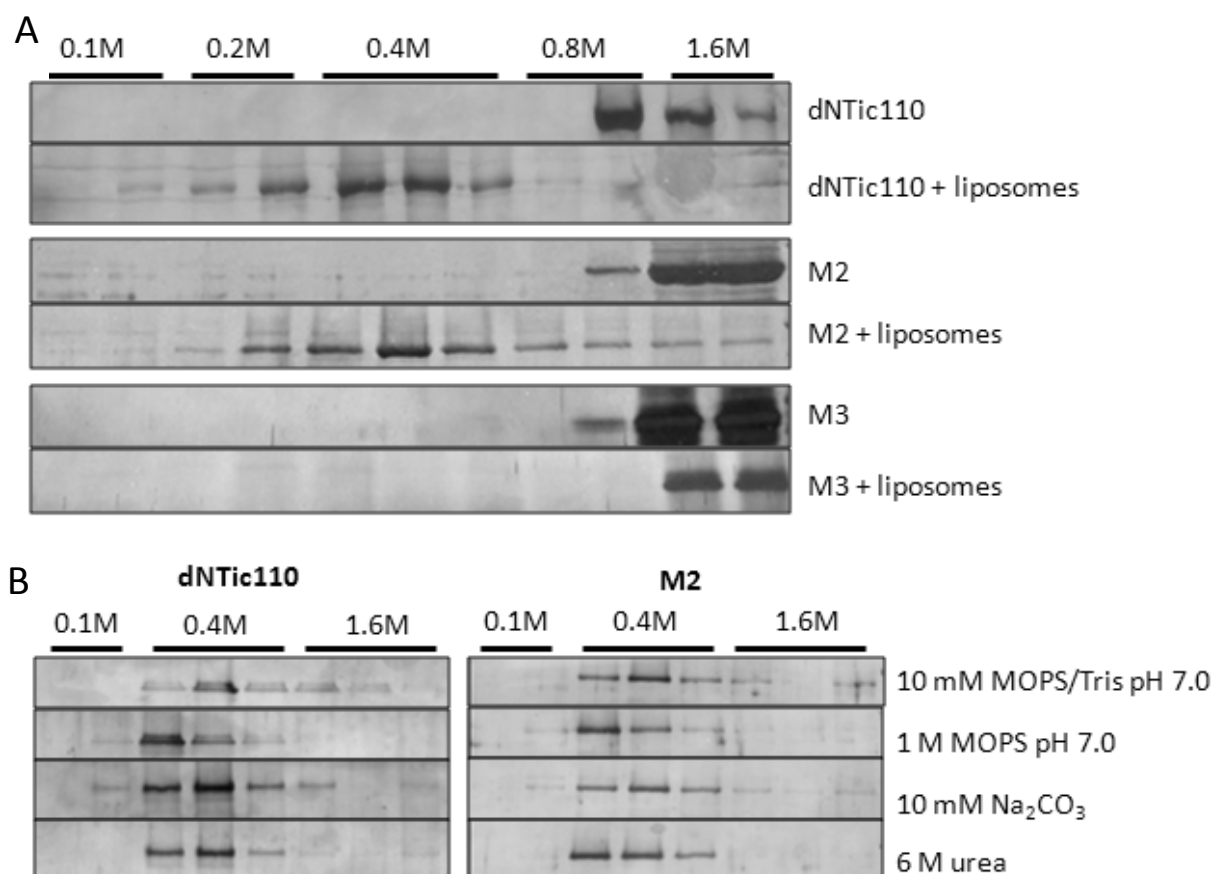


Figure 10. Insertion of Tic110 into liposomes

Figure was adapted partially from Balsera *et al.* (2009a). A) Flotation experiments of dNTic110, M2 and M3 in the absence or presence of liposomes in a sucrose step gradient. Samples containing 1.6 M sucrose were loaded at the bottom of the gradient (sucrose concentration of each step is indicated) and centrifuged to equilibrium (100,000 g, 19 h, 4°C). B) Flotation experiments of dNTic110- and M2-proteoliposomes incubated under the indicated buffer conditions for 30 min at RT prior to flotation. Samples of A) and B) were loaded on a 10% SDS-PAGE and silver-stained.

Samples were subjected to flotation to verify the insertion into the membrane (Figure 10). dNTic110 without liposomes stayed at the bottom of the gradient (in 1.6 M sucrose), whereas dNTic110 floated to the middle of the gradient (Figure 10 A) similarly to the empty liposomes (data not shown), indicating that dNTic110 was associated with the liposomes. M2 and M3 were also subjected to flotation similarly as dNTic110, to investigate, which part of Tic110

can still be inserted into the membrane. M2 floated with liposomes to the middle of the gradient, but stayed at the bottom in the absence of liposomes. On the contrary, M3 did not float in both cases.

To exclude that dNTic110 and M2 are not only loosely attached to the membrane, but are firmly inserted, proteoliposomes were incubated (30 min, RT) under the following conditions (Figure 10 B): control - 10 mM MOPS/Tris (pH 7.0); high ionic strength - 1 M MOPS/Tris (pH 7.0); high pH - 10 mM Na₂CO₃ (pH 11); denaturing - 6 M urea in 10 mM MOPS/Tris (pH 7.0). Since none of the used conditions could extract both proteins from the vesicles, they are deeply inserted into the membrane. These data clearly indicate that dNTic110 and M2 insert into the membrane, thus both constructs contain transmembrane domain(s).

dNTic110-proteoliposomes were also prepared in the absence of SDS, thereby no dialysis was needed. Flotation experiments after overnight incubation of the protein-liposome mixture showed that dNTic110 inserts into liposomes also without any detergent (data not shown).

4.1.4. Crystallization

Resolving the structure of Tic110 could strongly support Tic110 topological predictions and help to further understand the function of the protein. Since dNTic110 could be overexpressed in high yields and be purified to homogeneity, it was chosen for crystallization.

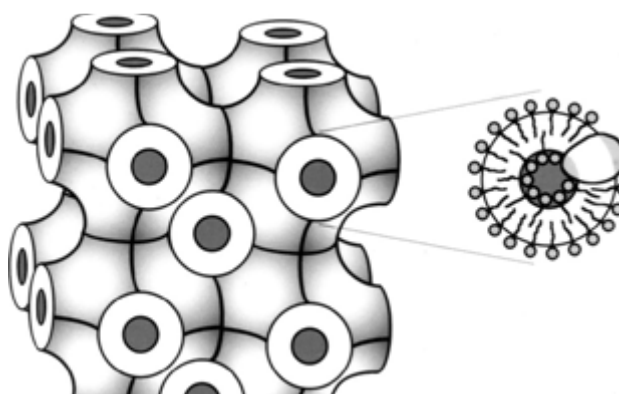


Figure 11. Schematic model of cubic phase

The figure was taken from Landau and Rosenbusch (1996). Cubic phase contains the lipid membrane (white) as an infinite three dimensional periodic minimal surface (consisting of 9-monoolein), and the continuous aqueous phase (gray) enclosed by the membrane. On the right, the enlarged lipid bilayer is presented with an inserted protein molecule having interactions both with the lipid and aqueous phase.

dNTic110 was expressed in larger volume of bacterial cultures (4-6 l) and purified by a 5 ml HisTrap HP column, to yield sufficient amounts of the protein. After gel filtration, the pure protein was concentrated to 10-20 mg/ml and used for crystallization tests. Since earlier studies succeeded neither under native conditions nor using detergent (0.03% DDM) (data not

shown), other approaches were set up. In cooperation with Dr. Gergely Katona and Annette Duelli (University of Gothenburg), cubic phase (Landau and Rosenbusch, 1996; Nollert, 2002) and bicelle (Faham and Bowie, 2002) methods were applied to crystallize the protein in a membrane-mimicking environment.

After mixing the protein with 9-monoolein, a cubic phase was formed, having a sponge-like structure (Figure 11) containing the lipid bilayer and an enclosed continuous aqueous phase. Hydrophobic interactions of the protein are allowed with the lipids, whereas hydrophilic domains face the aqueous phase.

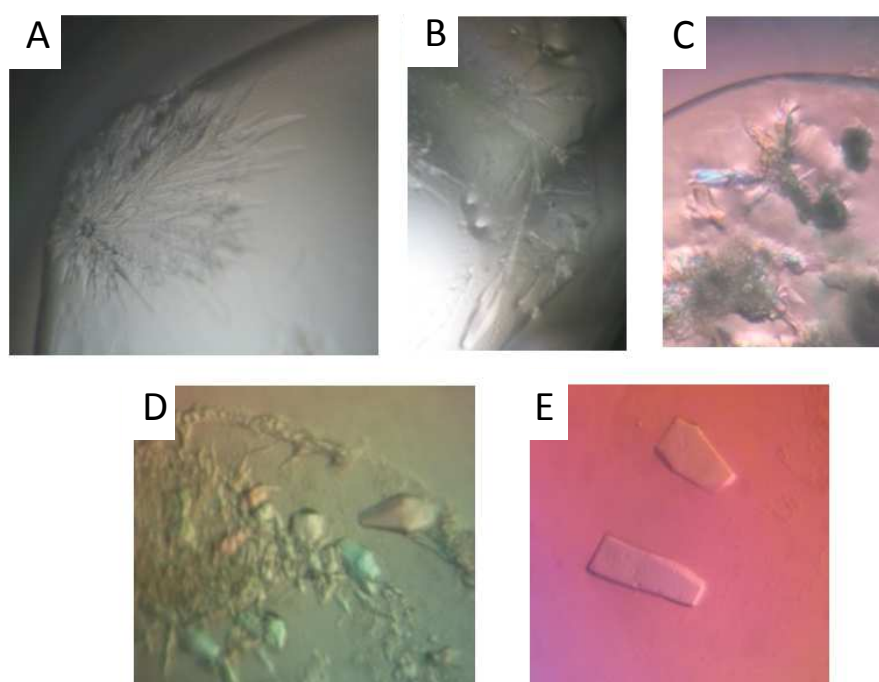


Figure 12. Crystallization of Tic110

Some representative crystals from A)-C) cubic phase and D)-E) bicelle crystallization test drops. Detailed composition of the drops: A) and B) 10 mg/ml dNTic110, precipitant: 0.1 M Zn-acetate, 0.1 M Na-acetate (pH 4.6), 12% w/v PEG 4000. No cryo-protectant was applied. C) 10 mg/ml dNTic110, precipitant: 0.5 M Li₂SO₄, 10% w/v PEG 8000. No cryo-protectant was applied. D) 10 mg/ml dNTic110; bicelle: 32 mg DMPC, 4 mg DMPG, 12 mg CHAPSO; 1:3 bicelle:protein volume ratio; precipitant: 0.1 M HEPES (pH 7.5), 12% w/v PEG 4000; cryo-protectant: 40% PEG 8000. E) 10 mg/ml dNTic110; bicelle: same as D); 1:3 bicelle:protein volume ratio; precipitant: 0.1 M Tris (pH 8.5), 10% w/v PEG 8000; cryo-protectant: 40% PEG 8000. Given amount of bicelle lipids and detergent was solubilized in 200 µl 20 mM Tris-HCl (pH 8.0).

For the second approach, the protein was added to a bicelle mixture consisting of a lipid (DMPG or DMPC) and an amphiphile molecule (CHAPS or CHAPSO) forming small bilayer disks. Therefore, the membrane protein incorporated into bicelles may be in a more bilayer-like environment than in detergent micelles. The advantage of this method - in contrast to the cubic phase - is that all steps during preparation are performed at 4°C (whereas cubic phase

should be at RT). At this temperature Tic110 is more stable, degradation or aggregation occurs much slower.

A large number of growing crystals were observed in the test plates of both methods, under different crystallization conditions. Crystals were mounted, flash-cooled in liquid nitrogen and stored until the measurements in ESRF. Some resulting crystals are presented in Figure 12 with the detailed description of their composition. However, our measurement did not lead to a conclusive result yet, since part of the samples contained only salt, some others did not have a proper diffraction to determine the content of the crystal. Hence more tests have to be performed to screen for the best condition of crystal growth. However, the presence of crystals under different conditions is very promising and indicates that these methods may lead to the determination of the Tic110 crystal structure.

4.1.5. Oxidation states

4.1.5.1. In vitro

To analyse the oxidation states of Tic110, a sulfhydryl-reactive agent, AMS, was applied. This molecule binds covalently to free -SH groups of Cys, thereby increasing the molecular weight of the protein by 0.5 kDa for each Cys. As a result, if a protein contains a disulfide bridge, 1 kDa difference can be observed between its oxidized and reduced form. This approach revealed that purified dNTic110 has different oxidation states (Figure 13 A and Balsera et al., 2009a): dNTic110 was incubated with 50 μ M CuCl₂, or with 10 mM DTT and subjected to non-reducing SDS-PAGE after incubation with AMS. A clear difference between the two oxidation states was observed: the reduced protein had a lower mobility on the non-reducing gel, since all of the Cys reacted with AMS. The oxidized sample contained three bands: the one with lowest mobility corresponded to the reduced form, whereas the two other bands with lower molecular weights indicated one or two disulfide bridges in the molecule. The purified protein was in the reduced state, since it had similar molecular weight to the reduced sample.

Oxidized glutathione (GSSG) in different concentrations and under different conditions also oxidized dNTic110, indicated by the shift in the non-reducing gels after AMS labelling (Figure 13 B). After dialysis of these samples, they were reversibly reduced by DTT.

To further investigate the reversibility of the oxidation, a physiological reducing agent, Trx was used. In chloroplasts, Trxs are responsible for the regulation of the action of several proteins (for more detail see Section 1.2.3.2) via reducing or oxidizing their redox active Cys.

It is feasible that the disulfide bridge in Tic110 could also be a Trx target. To investigate this possibility, dNTic110 was oxidized with CuCl_2 , dialysed to remove oxidant and incubated with the two chloroplast Trx isoforms (*f* and *m*) and with Trx from *E. coli* (performed by Dr. Mónica Balsera, Figure 13 C, Balsera *et al.*, 2009a). For optimal enzyme activity, Trx was reduced before the reaction with DTT, consequently 500 μM DTT was remained in the reaction mixture, which however did not reduce the oxidized dNTic110 in the absence of Trxs (data not shown). All three Trx isoforms reduced the oxidized protein, clearly indicating that Tic110 is a Trx target *in vitro*. Note that reduction of dNTic110 did not occur without the preliminary reduction of Trx.

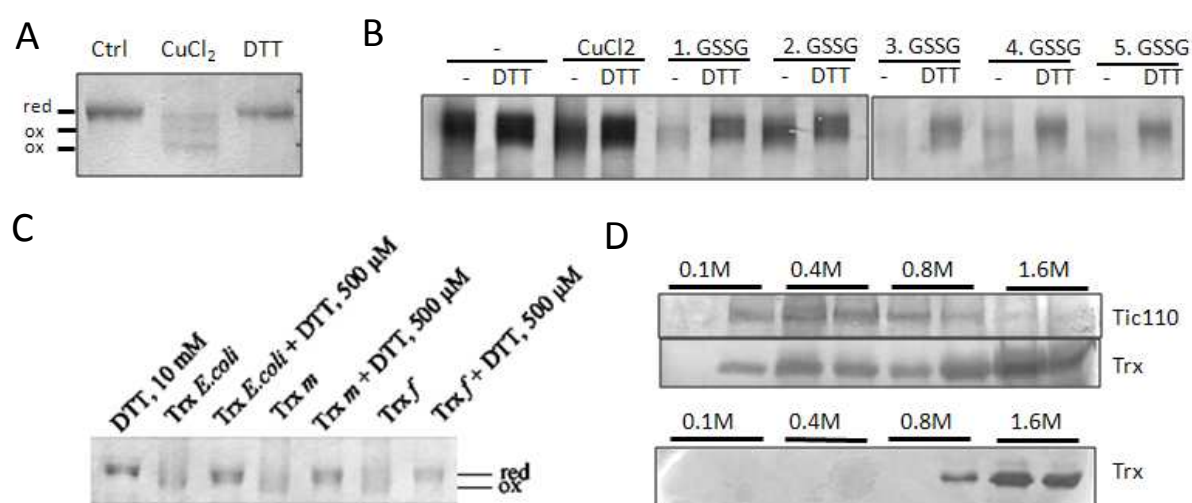


Figure 13. Oxidation states of Tic110 *in vitro*

A) dNTic110 was oxidized by 50 μM CuCl_2 or reduced by 10 mM DTT for 1 h at 20°C, followed by TCA precipitation (5%) and wash with 100% acetone. Air-dried pellet was incubated with 10 mM AMS, 2 mM EDTA, 100 mM Tris-HCl (pH 7.0) in the dark (1 h, RT). Samples were subjected to non-reducing SDS-PAGE and Coomassie-stained. Red and ox indicate the reduced and oxidized forms of the protein. B) dNTic110 was oxidized by 50 μM CuCl_2 (1 h, 20°C), or by oxidized glutathione (GSSG) under the following conditions: 1.: 15 mM GSSG, 2 h, 20°C; 2.: 50 mM GSSG, 2 h, 20°C; 3.: 5 mM GSSG, 1 h, 20°C; 4.: 5 mM GSSG, o/n, 20°C; 5.: 5 mM GSSG, o/n, 4°C. Oxidation followed by dialysis with 20 mM Tris-HCl (pH 8.0), 150 mM NaCl to remove the oxidant. The dialysed samples were incubated afterwards in buffer or with 10 mM DTT for 1 h at 20°C and TCA precipitated (5%). After washing with 100% acetone, the dried pellet was resuspended and incubated in 10 mM AMS, 2 mM EDTA, 100 mM Tris-HCl (pH 7.0) for 30 min at RT in the dark. Non-reducing SDS-PAGE of the samples was silver-stained. C) The figure was taken from Balsera *et al.* (2009a), experiments were performed by Dr. Mónica Balsera. With CuCl_2 oxidized dNTic110 was dialysed and subjected to the indicated conditions followed by TCA precipitation, wash with 100% acetone and incubation with 10 mM AMS. Trx: thioredoxin; red and ox: reduced and oxidized protein, respectively. The non-reducing SDS-PAGE was Coomassie-stained. Note the difference in the running behaviour of the protein in each lane of A)-C). D) dNTic110 was inserted into liposomes, oxidized by 50 μM CuCl_2 (30 min, 20°C) and incubated with Trx *f*C49S mutant (1h, 20°C). Sample was subjected to overnight flotation in a sucrose step gradient (sucrose concentration of each step is indicated). Samples were loaded on an SDS-PAGE under reducing conditions and silver-stained. Lower gel represents the same experiment but using empty liposomes.

To demonstrate the direct interaction between Trx and Tic110, dNTic110-proteoliposomes were oxidized with CuCl_2 and incubated with Trx *f* C49S. dNTic110 inserts into the lipid bilayer during electrophysiological measurements with a mixed orientation (Balsera *et al.*, 2009a), suggesting that the previous insertion into liposomes is likewise bidirectional. Thus, some Cys that face the stromal side in chloroplasts - and therefore may be targets for Trx recognition - are facing the outside of liposomes. Trx *f* C49S has a mutation in its active site, which does not allow the release of the target protein, therefore a covalent intermediate complex (in this case of dNTic110 and Trx) remains after the reaction (Figure 5 B). The reaction mixture was subjected to flotation on a sucrose gradient and samples were analysed by silver staining on a reducing gel (allowing the dissociation of the complex). Trx *f* floated together with dNTic110 (Figure 13 D), whereas Trx in the absence of dNTic110 did not attach to the liposomes. Therefore, we can conclude that Trx binds directly to dNTic110 *in vitro*.

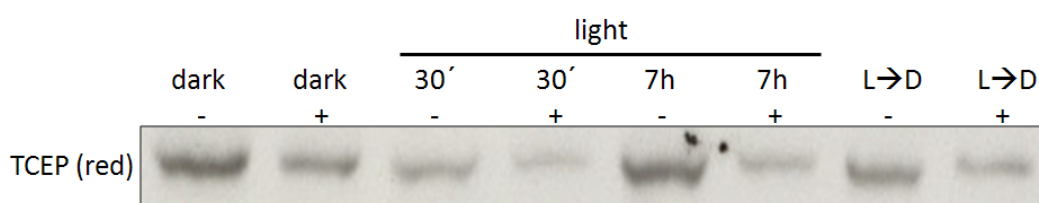


Figure 14. Oxidation states of Tic110 *in vivo*

Oxidation state of Tic110 in 10-day-old pea plants was analysed in leaves taken from the dark or after the indicated time of illumination (light, $100 \mu\text{mol photons m}^{-2} \text{s}^{-1}$). Some of the illuminated plants were afterwards incubated in the dark (L→D), and samples were taken after 1 h. Leaves were thoroughly ground in liquid nitrogen and extracted by 100 mM Tris-HCl (pH 7.5), 0.2 mM EDTA, 1% SDS, 100 mM IAA (1 h, RT), and the insoluble material was sedimented at 20,000 g for 10 min. After TCA precipitation (5%), samples were washed with 100% acetone and dried. The pellet was solubilized and incubated in 100 mM Tris-HCl (pH 7.0), 1.5% SDS in the presence or absence of 2 mM TCEP (30 min, RT). 10 mM AMS were added and the mixture was incubated for 30 min in the dark at RT. The reaction was stopped by adding 100 mM DTT. Samples were loaded on a 7.5% gel. Tic110 was detected by immunoblotting.

4.1.5.2. *In vivo*

Since the redox state of chloroplasts changes during light and dark cycles, it can be speculated that the redox states of Tic110 are dependent on illumination *in vivo*. To investigate this notion, pea leaves were taken from the dark or after different times of illumination and the oxidation state of Tic110 was analysed. To prevent Cys residues from oxidation after isolation, IAA was also present in the extraction buffer, which reacts with all free -SH groups. Samples were treated with TCEP (a reducing agent) or with buffer, followed by incubation with 10 mM AMS. TCEP reduces disulfide bridges, thus the running behaviour of samples with disulfide bridge(s) was different in the reduced samples compared to untreated ones.

Leaves isolated from the dark, contained reduced Tic110 since the samples in the absence or presence of TCEP migrated at the same level (Figure 14). On the contrary, after 30 min and 7 h of illumination Tic110 was oxidized, indicated by the shift between the reduced and untreated samples. Incubation in the dark for 1 h following the light period was not sufficient to reduce the protein again, since the difference between the bands was still observable. To summarize, Tic110 is reduced in the dark and oxidized in the light *in vivo*.

4.1.6. Cysteines involved in disulfide bridge formation

dNTic110 contains nine Cys residues, six of which are fully conserved in land plants: Cys¹³⁴, **Cys⁴⁴⁵**, **Cys⁴⁹²**, Cys⁵⁰⁶, Cys⁶⁷⁴ and **Cys⁸⁹⁰** in pea sequence (bold represents Cys, which are conserved in all green plants) (Balsera *et al.*, 2009a and Figure 35). Therefore, these residues are potential candidates for disulfide bridge formation. To elucidate, which Cys are involved in disulfide bridge(s), the following Cys point mutations were generated in dNTic110 separately: C445S, C470S, C492S, C506S and C674S. Furthermore, a C-terminal deletion mutant of dNTic110 (dNdCTic110) was generated, lacking Cys⁸⁵⁴ and Cys⁸⁹⁰. These mutant proteins were subjected to similar experiments as dNTic110 and results were compared with the wild-type protein.

The oxidation of C445S, C470S, C506S and C674S resulted in a similar oxidation pattern as compared to dNTic110 (Figure 15 A compared to Figure 13 A). However, C506S had already a similar pattern to that of the oxidized protein without any treatment. Interestingly, C492S oxidation resulted in an additional high molecular weight band, which may correspond to a dimer of the protein formed by an intramolecular disulfide bridge. Additionally, another high molecular weight band was also present in the non-oxidized sample (both bands are marked with asterisks in Figure 15 A). dNdCTic110 was hardly visible on the gel after oxidation, most of the sample stayed most probably in the stacking gel indicating the formation of non-dissociable aggregates.

In order to verify the reversibility of the oxidation, oxidized samples were dialysed to remove the oxidant and treated with Trxs, similarly to dNTic110 (compare Figure 15 B with Figure 13 C). Oxidized C445S, C470S, C506S and C674S were reduced via all Trx isoforms. In contrast, the additional band in the oxidized C492S sample (indicated by an asterisk in Figure 15 B) did not disappear after reduction, not even after the treatment with 10 mM DTT, indicating that this product is not formed via a disulfide bond. dNdCTic110 could not be used for this experiment, since there was no more protein observable after dialysis and reduction

with 10 mM DTT (data not shown), which may be due to the excessive aggregation of the protein upon oxidation. Taken together, the mutation of Cys⁴⁹² and the deletion of the C-terminus of dNTic110 caused noticeable changes in the behaviour of dNTic110 upon oxidation.

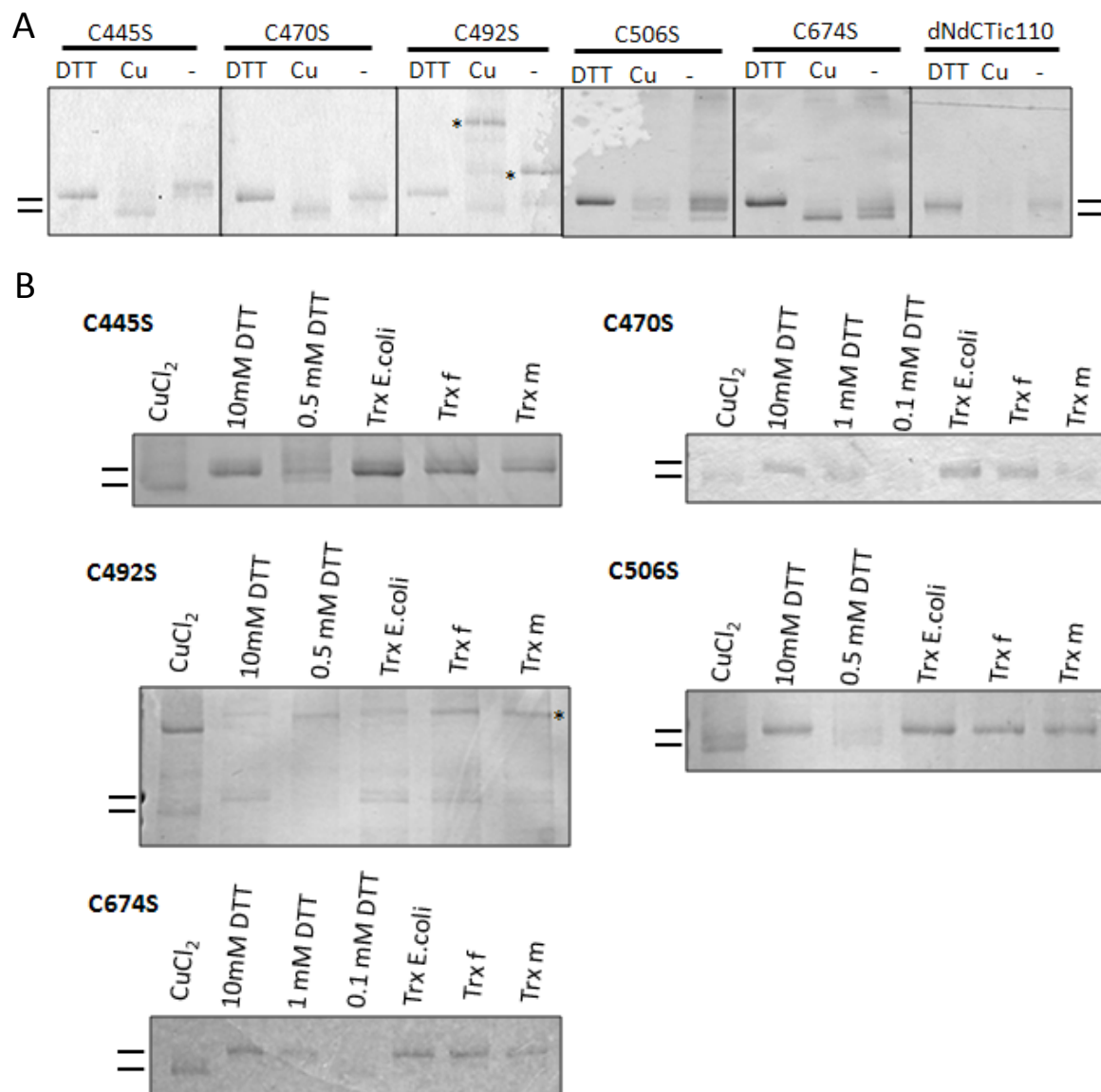


Figure 15. Oxidation states of Tic110 mutants

A) dNTic110 Cys mutants (C445S, C470S, C492S, C506S, C674S) and dNdCTic110 were purified and oxidized by 50 μ M CuCl₂ or reduced by 10 mM DTT for 1 h at 20°C, followed by TCA precipitation (5% TCA) and wash with 100% acetone. Air-dried pellets were incubated with 10 mM AMS (1 h, RT) in the dark. Samples were subjected to 8.5% non-reducing SDS-PAGE and Coomassie-stained. The size of the oxidized (lower band) and reduced (higher band) protein is depicted on the left and on the right. Asterisks indicate high molecular weight complexes of the C492S construct. B) CuCl₂ oxidized proteins (first lane) were dialysed against 20 mM Tris-HCl (pH 8.0), 150 mM NaCl and subjected to the indicated conditions (1 h, 20°C) followed by TCA precipitation and wash with acetone. The pellet was incubated with 10 mM AMS, 2 mM EDTA, 100 mM Tris-HCl (pH 7.0) for 1 h at RT in the dark. Note that thioredoxin (Trx) was pre-incubated with 5.5 mM DTT (30 min, 20°C), therefore 0.5 mM DTT remained in the samples. The size of the oxidized (lower band) and reduced (higher band) protein is depicted on the left. 8.5% non-reducing SDS-PAGE was Coomassie-stained. Asterisk indicates a high molecular weight complex of the C492S construct.

4.1.7. Effect on the channel activity and import rates

The presented oxidation states of Tic110 may have different roles in chloroplasts. One possibility is to alter the channel activity of the protein. The channel activity of Tic110 has been already characterized by the group of Prof. Richard Wagner at the University of Osnabrück, Germany (Heins *et al.*, 2002; Balsera *et al.*, 2009a). The electrodes of the equipment used are sensitive to the applied oxidants and reducing agents (Dr. Tom Alexander Götze, personal communication), therefore direct oxidation and reduction of Tic110 during measurements could not be performed.

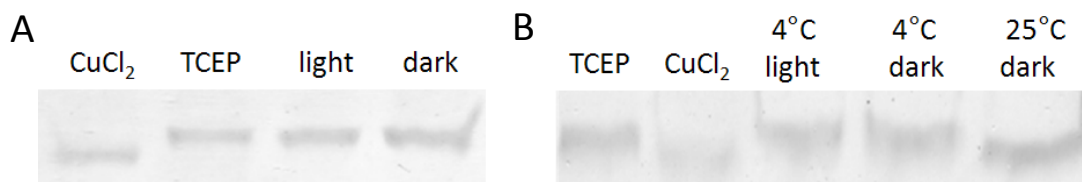


Figure 16. Oxidation states of Tic110 in organello

A) Chloroplasts from 10-day-old pea plants from the dark or from the light were isolated and treated with 10 mM AMS in the presence of 1% SDS (1 h, RT, in the dark). Reaction was stopped via the addition of 100 mM DTT. Control samples were pre-treated with 50 μ M CuCl₂ or 2 mM TCEP (1 h, RT) prior to AMS. Samples were subjected to 8.5% SDS-PAGE and Tic110 was visualized by immunoblotting. B) Chloroplasts from 10-day-old pea plants were isolated in the dark and incubated under the indicated conditions for 30 min. Light: 900 μ mol photons m⁻² s⁻¹ illumination. Samples were treated further as in A). Control samples are the same as in A).

As another approach, *in vitro* protein import experiments with isolated pea chloroplasts could permit the comparison of import rates between different conditions. Since Tic110 is reduced in the dark and oxidized upon illumination (Figure 14), our aim was to compare protein import into chloroplasts isolated from plants from the dark or from the light. Prior to performing this experiment, the oxidation state of Tic110 was analysed in isolated chloroplasts. Surprisingly, AMS-labelling revealed that Tic110 from both dark and light incubated plants is reduced (Figure 16 A, compare samples with oxidized (CuCl₂) and reduced (DTT) Tic110). If chloroplasts were incubated in the dark or in the light at 4°C, experiments led to similar results: Tic110 was reduced in both samples (Figure 16 B). However, incubation of chloroplasts at RT resulted in oxidation, pointing out that Tic110 is oxidized in a temperature dependent manner *in organello*. Since incubation of chloroplasts at higher temperatures makes them less import competent, the comparison of chloroplasts with oxidized (from RT) and reduced (from 4°C) Tic110 is not possible. Thus, performing import experiments into isolated chloroplasts was not an eligible tool to examine the effect of Tic110

oxidation states on import rates. Therefore, to find out whether the channel activity (or import efficiency) is altered upon oxidation, further experiments have to be designed.

4.1.8. Effect on the interaction with the motor complex

The second possible role for the oxidation states of Tic110 is the altered interaction with other components of the TIC translocon (e.g. the motor complex), or with the preprotein. To elucidate this potential effect, components of the motor complex (Hsp93, Tic40) were cloned, overexpressed and purified for *in vitro* interaction assays.

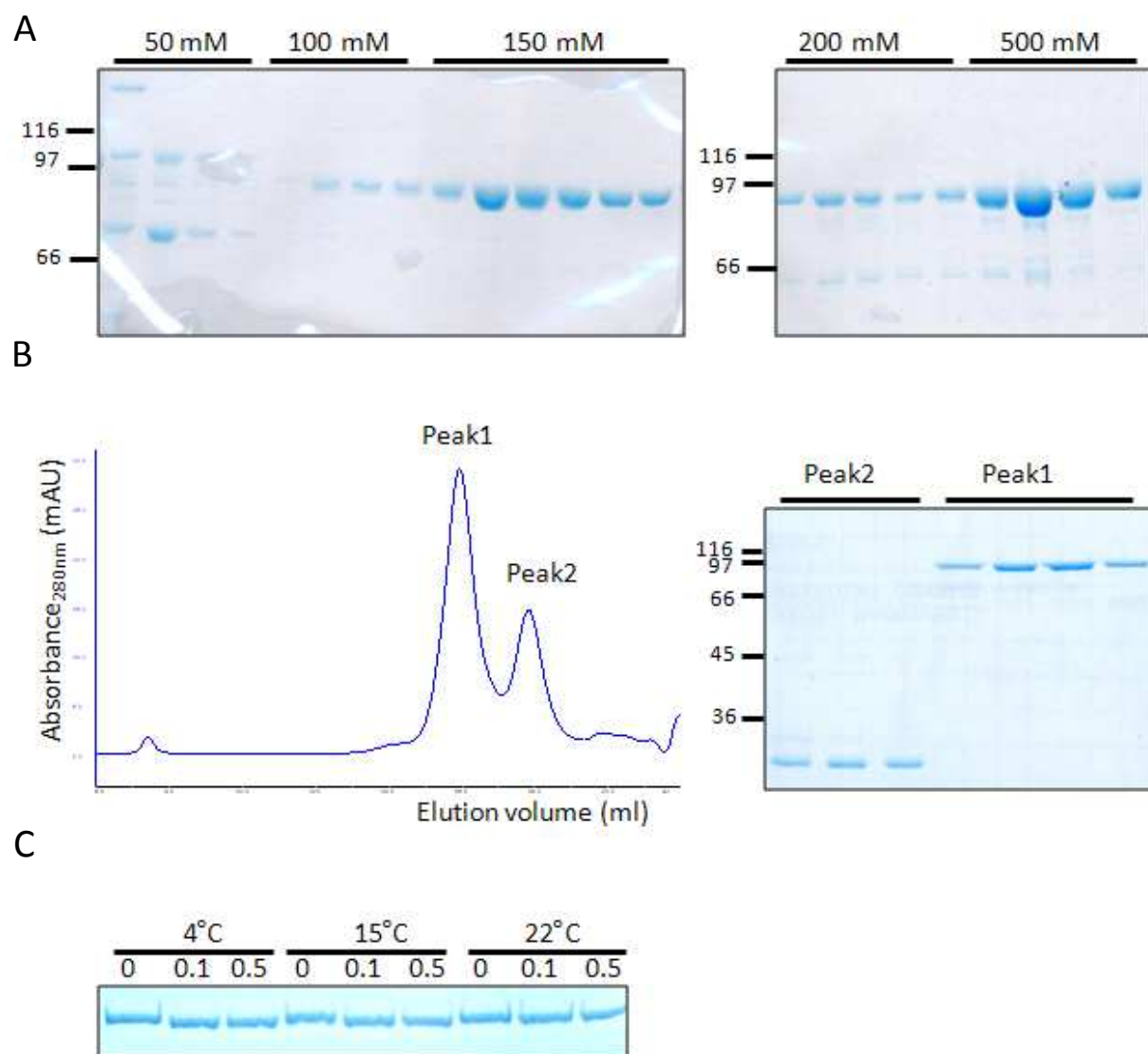


Figure 17. Purification of Hsp93

A) Elutions of the Ni-affinity purification of Hsp93 with increasing imidazole concentrations in 20 mM Tris-HCl (pH 8.0), 150 mM NaCl. B) Gel filtration of Hsp93 samples from 150 mM imidazole elution after Ni-affinity chromatography on a Superose 6 column in the same buffer (on the left). Samples from the two peaks are loaded on a 10% SDS-PAGE and Coomassie-stained (on the right). Molecular weight markers are indicated on the left side of the gel. C) Thrombin cleavage test of purified Hsp93. Samples (5 μ g protein) were incubated overnight with the indicated amount of thrombin (unit) at the indicated temperatures. Note changes in the mobility of the untreated and treated samples.

4.1.8.1. Hsp93

Ni-affinity chromatography of Hsp93 resulted in a pure protein after elution with 150 mM imidazole (Figure 17 A). These samples were subjected to gel filtration on a Superose 6 column (Figure 17 B), which successfully separated Hsp93 (“Peak1”) from a lower molecular weight contaminating protein (“Peak2”) present in the elution samples. Since Hsp93 was cloned into a pET14b vector containing a thrombin cleavage site, the His-tag was cleaved by overnight incubation with thrombin (Figure 17 C). All of the applied temperatures and protease concentrations resulted in cleavage, therefore 4°C and the lowest enzyme concentration was employed in further experiments (4°C incubation is preferable as at this temperature less aggregation or degradation of the protein could occur).

HSP100 protein family members usually form hexamers in the presence of ATP or ADP (Schirmer *et al.*, 1996). Accordingly, the oligomerization state of Hsp93 was analysed in the absence or presence of nucleotides (Figure 18). Without nucleotide pre-incubation, the protein behaves as a dimer during gel filtration (Figure 18 A, compare peaks with indicated molecular weight markers). However, after incubation with 5 mM ADP a shift was observed in the protein peak, which corresponded to the size of a hexamer. A similar result was observed in the presence of 5 mM ATP (data not shown). However, hexamers seemed to be very unstable, since dilution of the samples led to dissociation (data not shown). Furthermore, there was no hexamer detected on BN-PAGE using the hexamer and dimer samples from gel filtration (Figure 18 B), and only a minor fraction could be cross-linked as a hexamer with formaldehyde (Figure 18 C). Additionally, a very small amount of hexamers was also observed in the dimer samples. Interestingly, the presence of the His-tag in the protein sequence inhibited hexamer formation (data not shown).

To investigate the oligomerization state of Hsp93 in chloroplasts, stroma was isolated and subjected to gel filtration (Figure 18 D). Immunoblotting of elution samples revealed that Hsp93 is mainly present in two different molecular weight complexes, similarly to the *in vitro* studies: Most of the protein was present at an elution volume corresponding to the dimer, whereas a smaller amount of the protein eluted at a lower volume indicating higher molecular weight complexes (e.g. hexamers). Note that although the isolated stroma was not incubated with ADP or ATP, there is still a fraction of hexamers. It could be attributed to the effect of ATP/ADP present in the isolated chloroplasts.

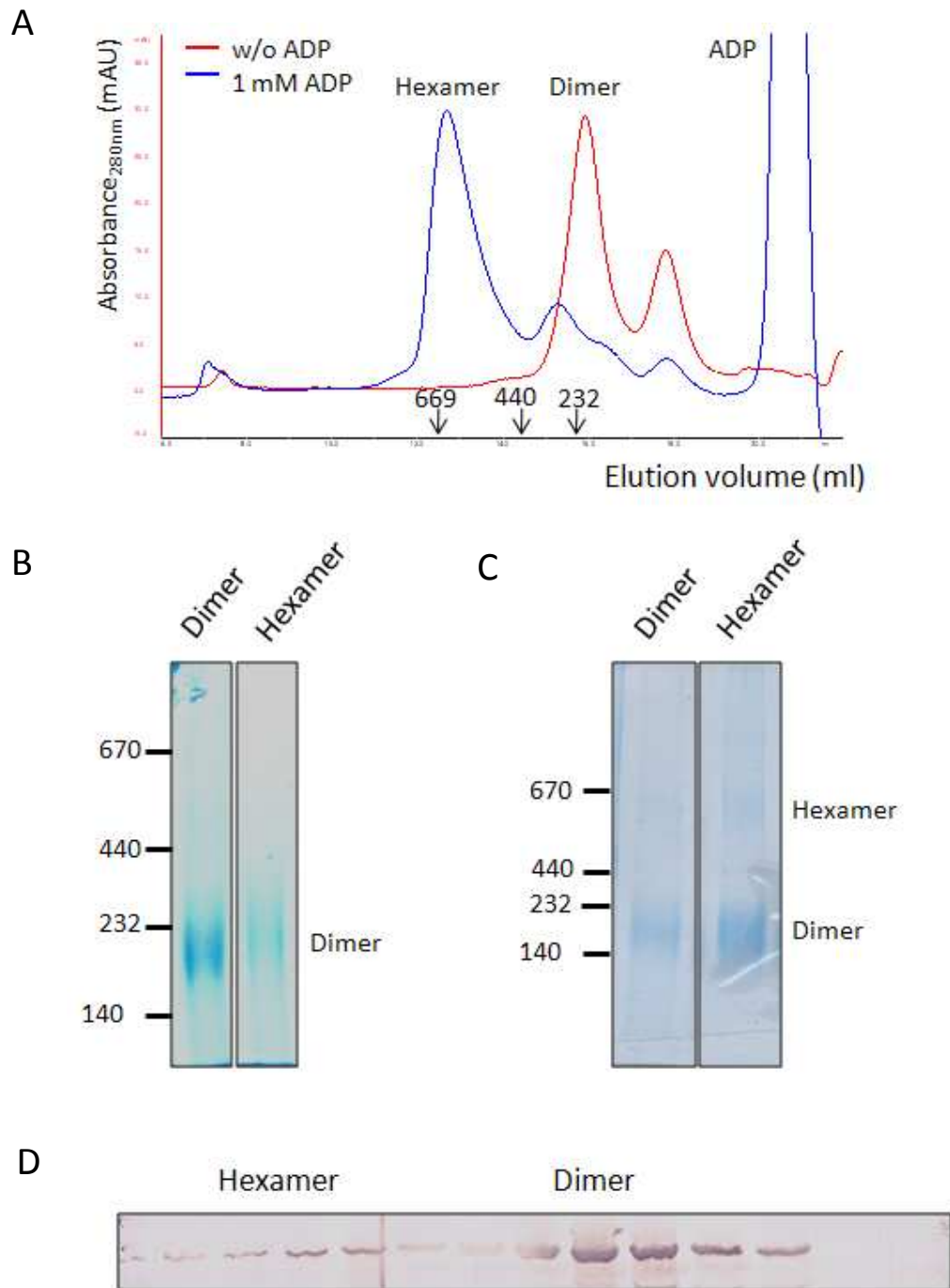


Figure 18. Oligomerization state of Hsp93

A) Hsp93 oligomerization in the absence or presence of ADP. Red line (same as Figure 17 B) shows the protein without nucleotide (w/o ADP). Blue line: the purified and cleaved protein was incubated with 5 mM ADP, 5 mM MgCl_2 for 15 min at RT and loaded on a Superose 6 column equilibrated with 20 mM Tris-HCl (pH 8.0), 150 mM NaCl, 5 mM MgCl_2 and 1 mM ADP. Elution volumes of molecular weight markers (kDa) are indicated. Hexamer and dimer peak fractions from gel filtration were taken and B) subjected to 5-10% BN-PAGE or C) cross-linked with 0.2% glutaraldehyde for 5 min at 37°C in 20 mM HEPES (pH 7.6). The reaction was stopped with 50 mM Tris-HCl (pH 8.0). Samples were precipitated with 5% TCA, washed with 100% acetone and loaded on a 5-10% SDS-PAGE. D) Stroma was isolated from chloroplasts (corresponding to 1 mg chlorophyll, in 5 mM Tris-HCl (pH 8.0)), concentrated to 200 μl and loaded on a Superdex 200 column with 20 mM Tris-HCl (pH 8.0), 150 mM NaCl. Samples from every second elution fraction were loaded on a 10% SDS-PAGE and the gel was immunoblotted against Hsp93.

4.1.8.2. Tic40

Tic40sol was cloned and overexpressed without the Tic40 transmembrane domain to obtain a soluble protein, which however contains all the interaction sites predicted to interact with Tic110 and Hsp93 (Section 1.2.2.3). After the purification of Tic40sol with Ni-affinity chromatography, two additional bands of higher molecular weight were also observed (Figure 19 A). Tic40 in IE is also present in multiple bands (Stahl *et al.*, 1999; Ko *et al.*, 2005), which were attributed to different conformations of the protein. Therefore, LC-MS/MS analysis was performed and revealed that they were identical to Tic40sol (Figure 19 B), but somehow these two forms had a different mobility on SDS-PAGE.

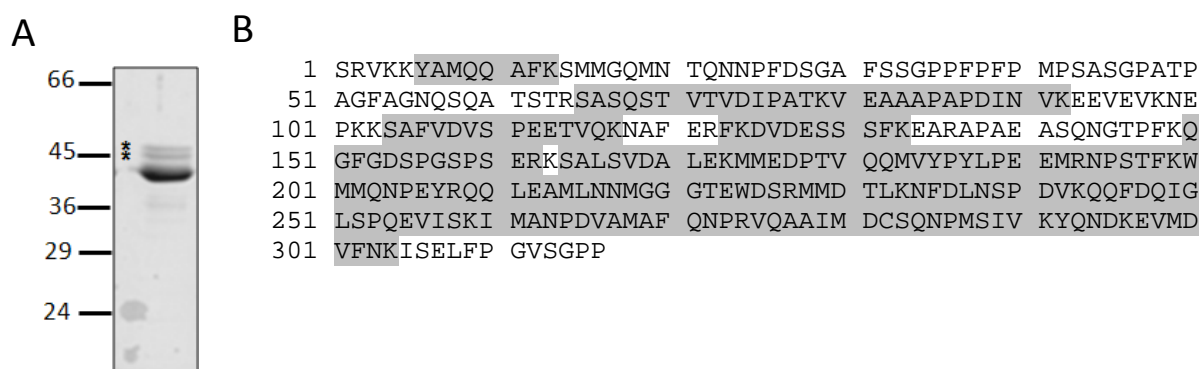


Figure 19. Purification of Tic40sol

A) Elution sample from Ni-affinity purification of Tic40sol. Asterisks indicate two additional bands, which were sequenced by LC-MS/MS. B) Sequence of Tic40sol without its transmembrane domain. Resulted oligopeptides from LC-MS/MS are shaded. (Sequencing gave the same results for both bands.)

4.1.8.3. Interaction assays

After the successful purification of dNTic110, Hsp93 and Tic40sol, their interaction was investigated under different conditions. As a first approach, proteins were incubated under native conditions followed by a gel filtration to detect possible complexes. The three proteins were incubated with each other in all possible combinations in different molar ratios and in the absence or presence of ADP. In this study some representative examples of these experiments are presented.

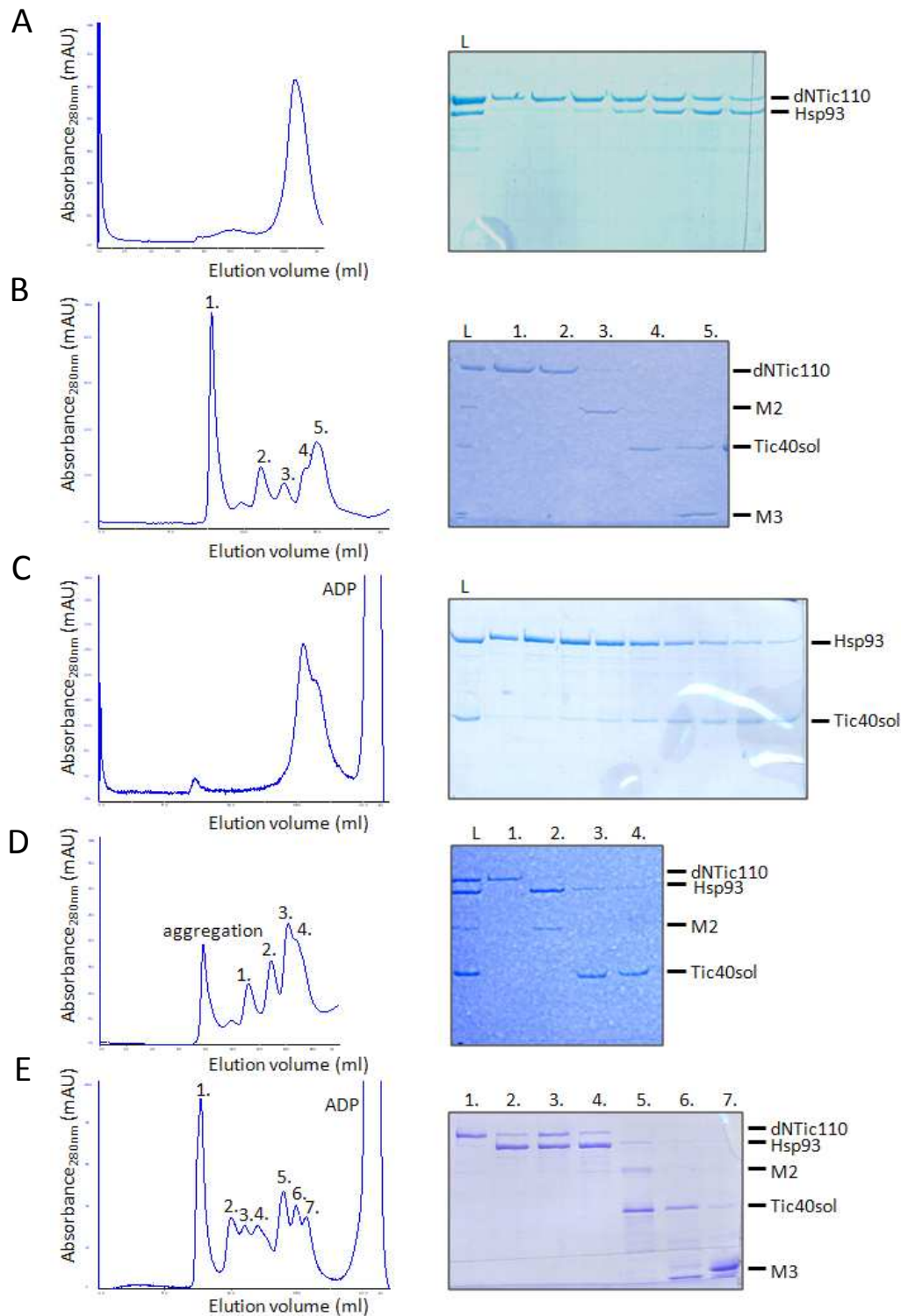


Figure 20. Interaction studies of dNTic110, Hsp93 and Tic40sol under native conditions

A) dNTic110 and Hsp93, B) dNTic110 and Tic40sol, C) Hsp93 and Tic40sol, D) dNTic110, Hsp93 and Tic40sol were incubated for 30 min at 20°C. Reaction mixture of C) contained 5 mM ADP and 5 mM MgCl_2 additionally to the buffer. Samples were loaded on a Superose 6 (A and C) or Superdex 200 (B and D) column equilibrated with 20 mM Tris-HCl (pH 8.0), 150 mM NaCl and additional 1 mM ADP, 5 mM MgCl_2 in the case of C). E) Hsp93 (20 mg/ml) was incubated with 5 mM ADP, 5 mM MgCl_2 (10 min, RT) followed by the addition of dNTic110 and Tic40sol and repeated incubation (10 min, RT). Sample was loaded on a Superdex 200 column with 20 mM Tris-HCl (pH 8.0), 150 mM NaCl, 1 mM ADP, 5 mM MgCl_2 . Aliquots from peak fractions of A)-E) were loaded on a 10% SDS-PAGE and Coomassie-stained (on the right). Note that dNTic110 was not subjected to gel filtration before these experiments, therefore its shorter truncations (M2 and M3) were also visible in the samples. L: loaded sample. Peak 1. in B) and E): aggregation of dNTic110.

Incubation of dNTic110 and Hsp93 resulted in one peak after loading the sample on a Superose 6 column (Figure 20 A). SDS-PAGE revealed that they are present in separate complexes, however their peaks could not be effectively resolved, because of their similar molecular weight. dNTic110 and Tic40sol did not form a common complex, their peaks clearly separated from each other on the gel filtration chromatogram (Figure 20 B). Similarly to this, Hsp93 and Tic40sol were also observed in two different complexes, which could be determined after SDS-PAGE of the resulted peak fractions (Figure 20 C). As a result, Tic40sol could be attributed to the “shoulder” of the peak. In the presented experiment ADP was also added to the mixture, however, Hsp93 did not form higher molecular weight complexes, only a dimer. This was possibly due to the concentration of the protein (~ 3 mg/ml), which might not be productive for oligomerization (Section 4.1.8.1).

Incubation of all three proteins together resulted also in separate complexes, both in the absence or presence of ADP (Figure 20 D and E). In the presence of ADP, a higher concentration of Hsp93 was used (~ 20 mg/ml), therefore the protein was present in three peaks (2.-4. in Figure 20 E). They were corresponding to the hexamer (2.), the dimer (4.) and a peak in-between (3.). The third peak contains also dNTic110 (Figure 20 E, SDS-PAGE). It can be speculated that the two proteins are therefore in a common complex. However, there was no shift observed in the elution volume of dNTic110, which should have been caused by the molecular weight increment upon interaction. Therefore, this amount of Hsp93 came most probably from peaks 2. and 4., since its amount is lower on the SDS-PAGE as that of the two other bands from the two neighboring peaks. A similar common peak was observed with Tic40sol and M2 (5. in Figure 20 E), but also without any shift in the elution volume. After thorough experiments using all combinations of the three proteins with different molar ratios, in the absence or presence of ADP, it was concluded that the interaction of the three proteins could not be detected under these conditions. Therefore, another approach had to be developed to examine the interaction of these proteins.

Since Tic110 is a membrane protein, a membrane-mimicking environment was used to further investigate its interactions. In a membrane-environment the protein might have a more native-like conformation (which does not necessarily highly differ from the conformation in the buffer, Balsera *et al.*, 2009a), allowing hydrophobic interactions with the “membrane”. Therefore, possible new contact areas could emerge on the surface responsible for association with other proteins. To mimic a membrane environment, two different methods were used.

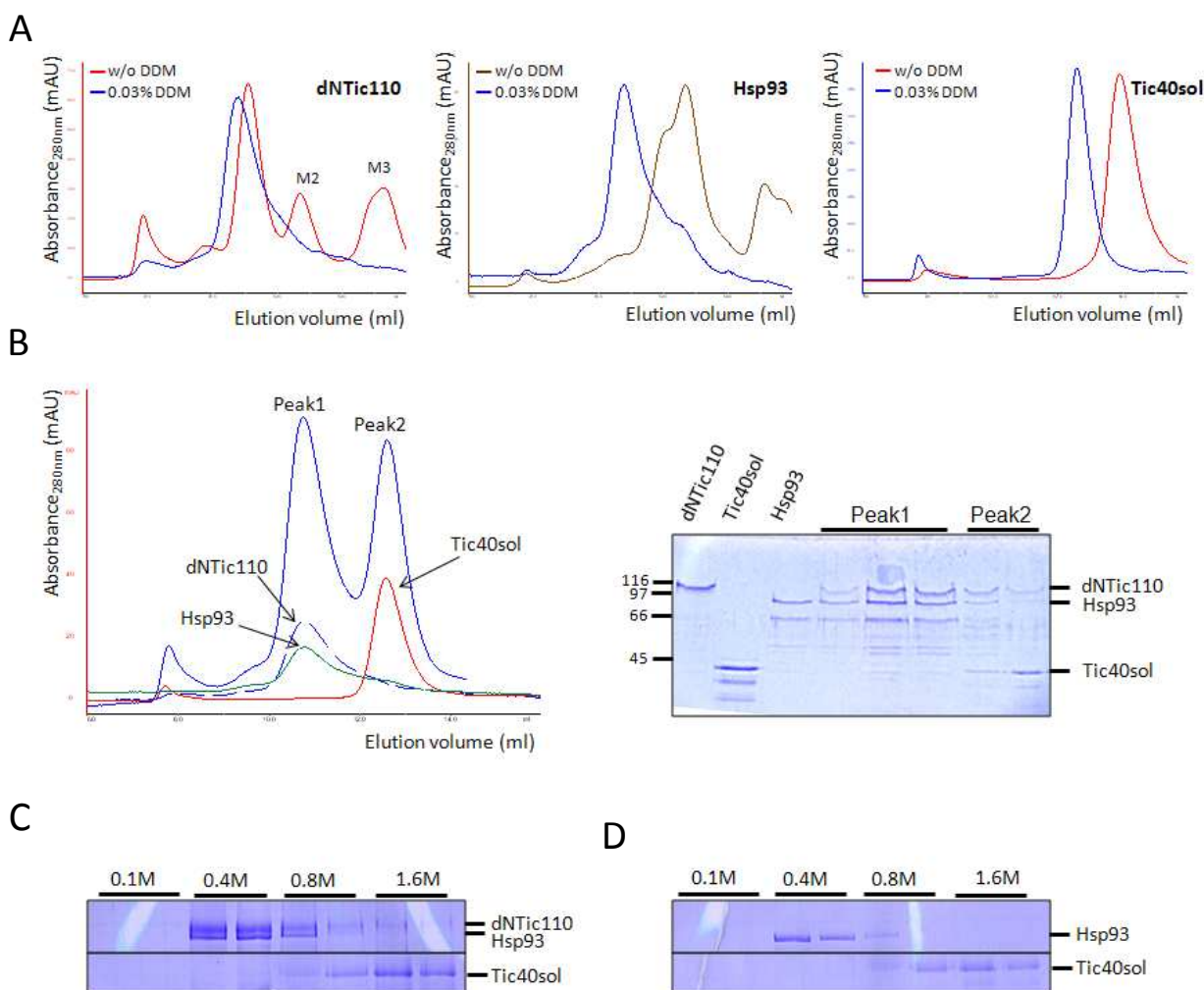


Figure 21. Interaction studies of dNTic110, Hsp93 and Tic40sol in membrane-mimicking environments

A) Gel filtration of dNTic110, Hsp93 or Tic40sol - separately - in the absence (w/o) or presence of 0.03% dodecylmaltoside (DDM). Samples were incubated prior to gel filtration with the detergent for 20 min at 20°C. Note that there are two independent chromatograms depicted on each figure. B) Gel filtration of dNTic110, Hsp93 and Tic40sol in the presence of 0.03% DDM. dNTic110 was pre-incubated with DDM (15 min, 20°C), followed by the addition of Hsp93 and Tic40sol (20 min, 20°C). Gel filtration profiles of the three proteins separately (incubated with DDM) are also depicted on the chromatogram to allow comparison of the elution volumes. Used protein samples and aliquots of peak elution fractions are loaded on a 10% SDS-PAGE and Coomassie-stained (on the right). A) and B): Gel filtration was performed with Superdex 200 in 20 mM Tris-HCl (pH 8.0), 150 mM NaCl with or without 0.03% DDM. C) dNTic110-proteoliposomes and D) empty liposomes were incubated with Hsp93 and Tic40sol (1 h, 20°C) and subjected to flotation on a sucrose step gradient with the indicated sucrose concentrations. After centrifugation (100,000 g, 19 h), samples were precipitated with 5% TCA, washed with acetone, loaded on a 10% SDS-PAGE and Coomassie-stained.

Firstly, interaction studies were performed in the presence of a detergent (DDM). Before joint incubation, the behaviour of dNTic110, Hsp93 and Tic40sol was analysed separately in the presence of a 0.03% DDM: They were incubated with DDM and subjected to gel filtration (Figure 21 A). The resulted chromatograms were compared with their gel filtration profile in the absence of detergent. This analysis revealed that all three proteins interacted with the detergent, since their elution peak shifted in the presence of DDM. To explore their interaction with each other, dNTic110 was pre-incubated with DDM, followed by the addition

of Hsp93 and Tic40sol. Gel filtration in the presence of DDM resulted in two peaks, the first (“Peak1” in Figure 21 B) contained dNTic110 and Hsp93, and the second (“Peak2”) only Tic40sol. Since both dNTic110 and Hsp93 separately ran at the same elution volume in the presence of detergent, it cannot be distinguished in “Peak1” whether there is a complex of these proteins present (Figure 21 B, compared chromatograms).

As a second membrane-mimicking approach, dNTic110-proteoliposomes were incubated with Hsp93 and Tic40sol and the reaction mixture was floated on a sucrose gradient (Figure 21 C). Tic40sol stayed at the bottom of the gradient, whereas dNTic110 and Hsp93 floated together to the middle. However, Hsp93 behaved similarly in the absence of dNTic110 indicating a Tic110-independent interaction with the liposomes (Figure 21 D).

Taken together, interaction of Tic40 with any other component could not be detected in a membrane-mimicking environment, whereas the interaction of Hsp93 with the detergent and liposomes prevented the clear detection of a complex with dNTic110. Therefore, to demonstrate the direct interaction between Tic110 and the motor complex, and to further look into the role of Tic110 oxidation states in complex formation, another approach has to be developed.

4.1.9. Effect on the interaction with preproteins

To elucidate whether the reduction or oxidation of Tic110 could alter the binding of preproteins, IE vesicles were applied. Since the IE preparation results in right-side-out vesicles (Waegemann *et al.*, 1992), the interaction of preproteins with the intermembrane space side of IE can be studied, mimicking the incoming preprotein during import. IE were oxidized with CuCl₂ or reduced with DTT, and the vesicles were incubated (after removing oxidant and reducing agent by washing) with two different *in vitro* radioactively translated preproteins (³⁵S-pSSU and ³⁵S-pOE33). Flotation was performed in a sucrose step gradient, and the localization of Tic110 and preproteins was compared in the oxidized and reduced samples (Figure 22). Tic110 floated to the middle of the gradient. The majority of the preproteins stayed at the bottom of the gradient in all samples, however, a fraction was also co-localized with Tic110. There was a higher amount of pSSU bound to IE compared to pOE33, however it could be also a reason of the lower amount of pOE33 used in this assay. Comparing the amount of the floated preproteins in the oxidized and reduced samples (Figure 22 left and right), there was no clear difference in the case of pSSU visible, however, less pOE33 floated in the oxidized samples than in the reduced. This could be also attributed to the

lower amount of Tic110 in those samples. Although the same amount of IE (and therefore Tic110) was used in all experiments, the oxidation caused severe aggregation of Tic110, which remained in the stacking gel (data not shown). If this portion of Tic110 was not reachable for the preprotein, it is reasonable that a lower amount of pOE33 was bound to the oxidized samples.

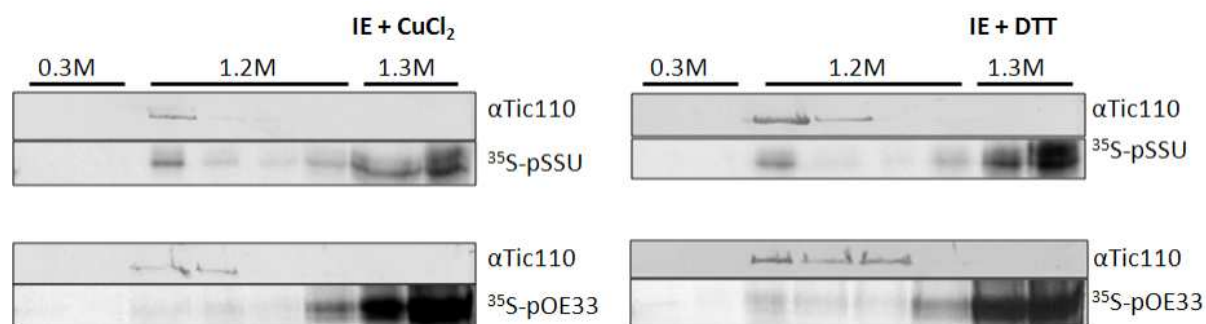


Figure 22. Binding of preproteins to inner envelopes (IE)

IE were oxidized by 50 μ M CuCl_2 (left) and reduced by 10 mM DTT (right) for 20 min at 20°C. Samples were pelleted (256,000 g, 10 min), washed (25 mM HEPES/KOH (pH 7.6), 3 mM MgCl_2) and incubated with radioactively labelled (^{35}S) pSSU (upper figures) and pOE33 (lower figures) for 20 min at RT. Reaction mixtures were loaded at the bottom of a sucrose step gradient in the presence of 1.6M sucrose (sucrose concentrations are indicated) and centrifuged (100,000 g, 17 h) to equilibrium. Tic110 and preproteins were detected by immunoblotting and autoradiography, respectively.

In summary, it was demonstrated that preproteins bind to IE, however, there was no clear difference observed in the oxidized and reduced samples, since the aggregation of Tic110 made the evaluation unreliable.

4.2. Tic20

4.2.1. Purification

Tic20 was purified to homogeneity after solubilizing cell lysate pellet with 1% LS and using Ni-affinity chromatography in the presence of 0.3% LS, following the protocol established by Dr. Philipp Benz (Figure 23 A, Benz, 2009, Kovács-Bogdán *et al.*, submitted). The protein was eluted from the Ni Sepharose after incubation with 100 and 200 mM imidazole. Other, less harsh detergents (such as 1% DDM, 1% DeMa or 1% CHAPS) were also employed for the purification. In those cases, solubilization of the protein from the cell lysate pellet could be achieved. However, Tic20 was not eluted from the Ni Sepharose even with 500 mM imidazole, indicating that it was precipitated on the column (Figure 23 B shows a representative result with DDM). Therefore, experiments presented here were performed in the presence of 0.3% LS.

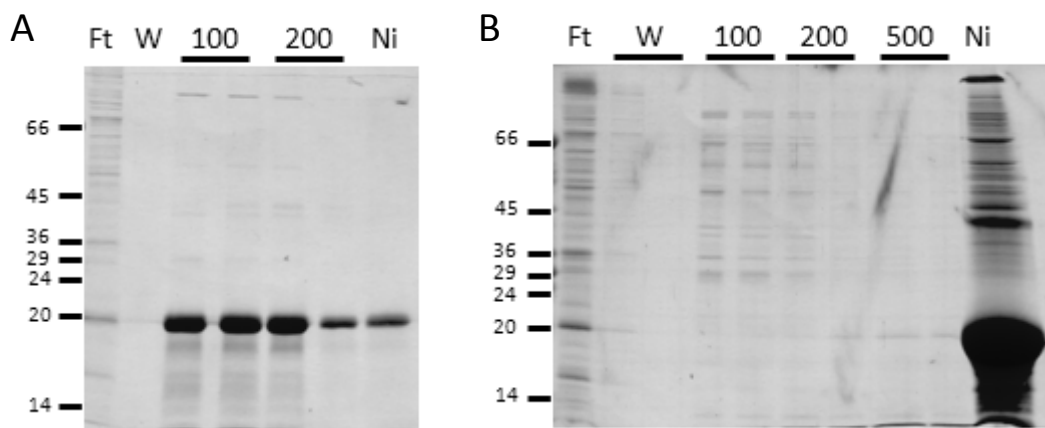


Figure 23. Purification of Tic20

Tic20 was overexpressed in BL21 (DE3) cells, bacteria were lysed and the total membrane fraction was sedimented by centrifugation. The resulting pellet was solubilized with A) 1% LS or B) 1% DDM. After pelleting insoluble material, supernatant was incubated with Ni Sepharose. The matrix was subsequently washed with 20 mM Tris-HCl (pH 8.0), 150 mM NaCl, 0.3% LS or 1% DDM (W: last washing steps) and bound proteins were eluted from the matrix by increasing concentrations of imidazole (as indicated in mM). Ft: flow-through after pelleting Ni Sepharose. Ni: Ni Sepharose after purification, eluted with Laemli buffer. Molecular weight markers are given in kDa on the left.

For control experiments (presented in following sections) a protein had to be used, which can be inserted into the membrane but is not supposed to form a channel. Therefore, two other proteins, NtTic110 and tpSSU-NtTic110-mSSU, were chosen. NtTic110 is the N-terminal part of Tic110 containing the first two hydrophobic and one amphipathic transmembrane domains. This construct inserts into the membrane during *in vitro* protein import experiments (Lübeck *et al.*, 1997). Furthermore, as the full length Tic110 and dNTic110 possess very similar channel activities (Heins *et al.*, 2002; Balsera *et al.*, 2009a), it is unlikely that the N-

terminal part alone forms a channel. tpSSU-NtTic110-mSSU contains additionally the transit peptide of SSU at the N-terminus and a part of the mature SSU at the C-terminus of NtTic110.

Both proteins were purified following a similar protocol as for the purification of Tic20, to achieve comparable results. NtTic110 was eluted from the Ni Sepharose with 100 and 200 mM imidazole similarly to Tic20 (Figure 24 A), however, tpSSU-NtTic110-mSSU could be eluted with 150 mM imidazole (Figure 24 B). Note that another additional band was also visible at about 20 kDa in a comparable amount to tpSSU-NtTic110-mSSU. This protein may refer to a shorter truncation of tpSSU-NtTic110-mSSU containing also a His-tag, which was translated in the bacteria along with the full length protein. Sequencing of this band via LC-MS/MS further supported the hypothesis that this is a part of tpSSU-NtTic110-mSSU (data not shown).

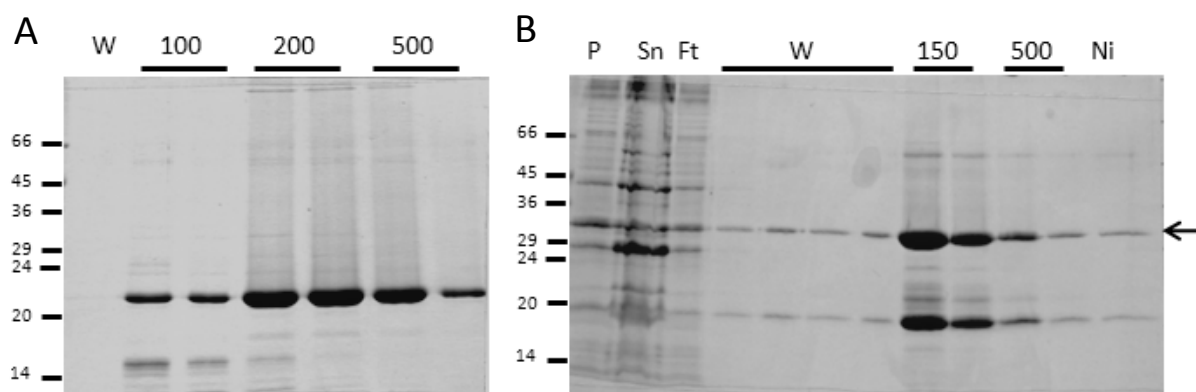


Figure 24. Purification of A) NtTic110 and B) tpSSU-NtTic110-mSSU

A) NtTic110 and B) tpSSU-NtTic110-mSSU were purified from the pellet (P) after the lysis of *E. coli* using Ni-affinity chromatography. Pellet was solubilized in 20 mM Tris-HCl (pH 8.0), 300 mM NaCl and 1% LS, whereas wash and elution of Ni Sepharose was performed in the same buffer but with 0.3% LS, similarly to Tic20 (Figure 23). Sn: supernatant after pelleting cell lysate. Ft: flow-through after pelleting the Ni Sepharose. W: last washing steps. Elution was performed with the indicated concentration of imidazole (in mM). Ni: Ni Sepharose after purification, eluted with Laemli buffer. Molecular weight markers are given in kDa on the left. Arrow indicates tpSSU-NtTic110-mSSU.

4.2.2. Insertion into liposomes

To better characterize Tic20 in a membrane-mimicking environment, heterologously overexpressed and purified Tic20 was reconstituted into liposomes *in vitro*. Liposomes were made using PC in 20 mM Tris-HCl (pH 8.0), 100 mM NaCl and mixed with freshly purified Tic20 (containing also 100 mM imidazole and 0.3% LS). To remove detergent, samples were dialysed overnight against 20 mM Tris-HCl (pH 8.0), 100 mM NaCl, followed by incubation with Bio-Beads. As a negative control, liposomes were mixed with the buffer of Tic20, and treated the same way as Tic20 containing samples.

Flotation experiments were performed to verify a stable insertion. Tic20-proteoliposomes were placed at the bottom of a sucrose gradient ranging from 1.6 M (bottom) to 0.1 M (top) sucrose. After overnight centrifugation, Tic20 migrated to the middle of the gradient (Figure 25 A) similarly to the empty liposomes (data not shown), indicating an interaction with the liposomes. In contrast, the protein alone (in the elution buffer from Ni-affinity purification, containing also 0.3% LS) remained at the bottom of the gradient (Figure 25 A).

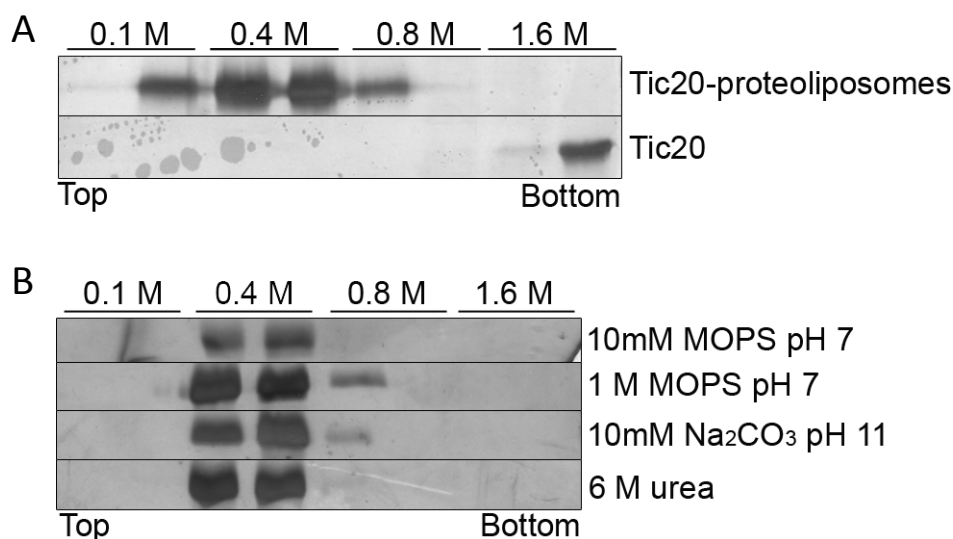


Figure 25. Insertion of Tic20 into liposomes

Figure was adapted from Kovács-Bogdán *et al.* (submitted). A) Flotation experiments of Tic20-proteoliposomes and Tic20 without liposomes in a sucrose gradient. Samples containing 1.6 M sucrose were loaded at the bottom of the sucrose step gradient (each step contained the indicated concentration of sucrose) and centrifuged to equilibrium (100,000 g, 19 h, 4°C). Fractions were analysed by silver-staining. B) Flotation experiments of Tic20-proteoliposomes (similar to (A)) incubated under the indicated conditions for 30 min at RT before centrifugation. 6 M urea was buffered to pH 8.0 with 10 mM MOPS/Tris.

To verify that Tic20 is firmly inserted into the liposome membrane and not only loosely bound to the vesicle surface, proteoliposomes were incubated under high ionic strength, high pH and denaturing conditions prior to flotation (Figure 25 B). None of the applied conditions changed the migration behaviour of Tic20 in the gradient. Therefore, it can be concluded that the protein was not only bound to the surface by ionic or hydrophobic interactions but deeply inserted into the liposomal membrane. Thus, the Tic20-proteoliposomes described here represented a suitable *in vitro* system for the analysis of Tic20 in a membrane-mimicking environment.

Similar experiments were performed with NtTic110 and tpSSU-NtTic110-mSSU as negative controls for Tic20-proteoliposome experiments. Both proteins were reconstituted into liposomes, and the insertion was verified under different conditions (high salt, high pH,

denaturing) similarly to Tic20-proteoliposomes. Flotation on the sucrose gradient after all of the used conditions demonstrated the correct insertion of these proteins (Figure 26). The 20 kDa contaminating band present in the tpSSU-NtTic110-mSSU samples also floated (data not shown), indicating that the remaining part of Tic110 still contained transmembrane domains.

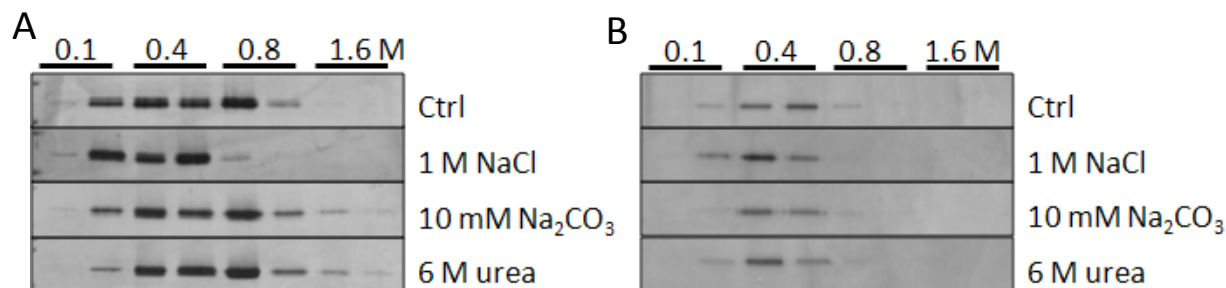


Figure 26. Insertion of A) NtTic110 and B) tpSSU-NtTic110-mSSU into liposomes

A) NtTic110- and B) tpSSU-NtTic110-mSSU-proteoliposomes were incubated under the indicated conditions for 30 min at RT. Ctrl: 20 mM Tris-HCl (pH 8.0), 100 mM NaCl. 1 M NaCl and 6 M urea were buffered to pH 8.0 with 20 mM Tris-HCl. Samples containing 1.6 M sucrose were loaded at the bottom of the sucrose step gradient (each step contained the indicated concentration of sucrose) and centrifuged to equilibrium (100,000 g, 19 h, 4°C). Fractions were analysed by silver-staining.

4.2.3. Complex formation in proteoliposomes

Tic20 forms high molecular weight complexes (> 700 kDa) on 2D BN-PAGE after the solubilization of IE and chloroplasts (Kikuchi *et al.*, 2009; Benz, 2009; Kovács-Bogdán *et al.*, submitted). An open question is whether Tic20 is the only component of this complex or it has other interaction partners.

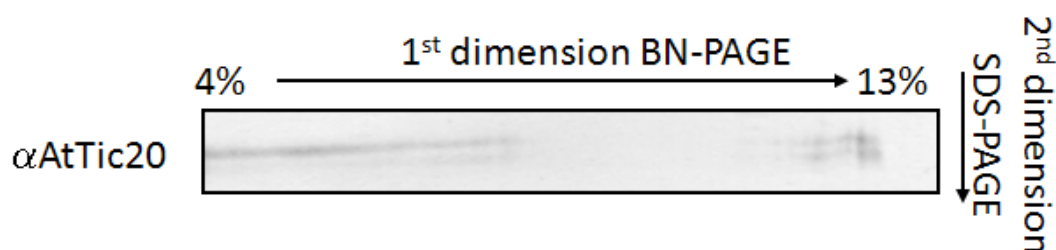


Figure 27. Complex formation of Tic20 in proteoliposomes

Figure was adapted from Kovács-Bogdán *et al.* (submitted). Two-dimensional BN/SDS-PAGE of Tic20-proteoliposomes (20-30 µg protein). Samples were solubilized in 5% digitonin and separated by 4-13% BN-PAGE followed by 12.5% SDS-PAGE. Specific antibody was used for immunodetection.

Without the involvement of other interaction partners, complex formation of Tic20 was analysed *in vitro* using Tic20-proteoliposomes. Freshly prepared proteoliposomes were solubilized in the presense of 5% digitonin and subjected to 2D BN-PAGE analysis, similarly to Benz (2009) and Kovács-Bogdán *et al.* (submitted). The migration behaviour of the protein resembles that earlier observed in IE: the majority of the protein localizes in high molecular

weight complexes, however, a portion is also detected at lower molecular weights (Figure 27). Thus, Tic20 had the inherent ability to homo-oligomerize in the presence of a lipid bilayer and did not need another interaction partner, supporting the hypothesis that the major components of the one megadalton complex in IE are homo-oligomers composed of Tic20.

4.2.4. Orientation in proteoliposomes

According to computational predictions (Kouranov *et al.*, 1998 and TMHMM Server), CD spectroscopy and PEGylation assays (Benz 2009; Kovács-Bogdán *et al.*, submitted), Tic20 is a mainly α -helical protein containing 4 hydrophobic transmembrane domains inserted into the membrane with its N- and C-termini facing to the stroma. However, it is also interesting, in which direction Tic20 is inserted into the liposome membrane in the proteoliposomes reconstituted in this study. For this purpose, PEG-Mal, a membrane non-permeable reagent was applied, which covalently binds to –SH groups (of Cys or other –SH containing molecules, such as DTT) and has a molecular weight of 5 kDa. Under native conditions, Cys residues only facing outside the membrane are labelled with PEG-Mal. The reaction can be visualized by the change of the mobility on SDS-PAGE. Assuming that Tic20 in *Arabidopsis* has the same topology as in pea (Benz, 2009; Balsera *et al.*, 2009b; Kovács-Bogdán *et al.*, submitted), no Cys residues are oriented towards the intermembrane space, Cys¹²⁹ is located in helix one, Cys²⁵¹ is oriented to the stromal side of helix four and Cys²⁶⁴ is located in the stroma.

After incubation of Tic20-proteoliposomes with PEG-Mal in the presence of SDS two Cys were clearly labelled, whereas the third appeared as a faint band (Cys1, Cys2 and Cys3 in Figure 28 A). However, some contaminations - being visible after silver staining - interfered with a clear evaluation, since they have a similar size as the labelled bands (0' control in Figure 28 A). Under native conditions, one Cys was labelled after only 5 min and the other two bands appeared with increased incubation time. Interestingly, the appearing bands under native conditions were fainter compared to the samples containing SDS, indicating that only a part of Tic20 was labelled. This effect could be caused by a non-homogenous orientation of the protein in liposomes. The difference of the labelled amount of Tic20 under native and denaturing conditions suggests that the protein was mostly in a right-side-out orientation in the liposomes (which cannot be labelled), similarly to its orientation in the IE. Note that the observed shift in the running behavior is higher than 5 kDa, which can be attributed to an aberrant mobility of the modified protein in the Bis-Tris/SDS-PAGE used in the assay.

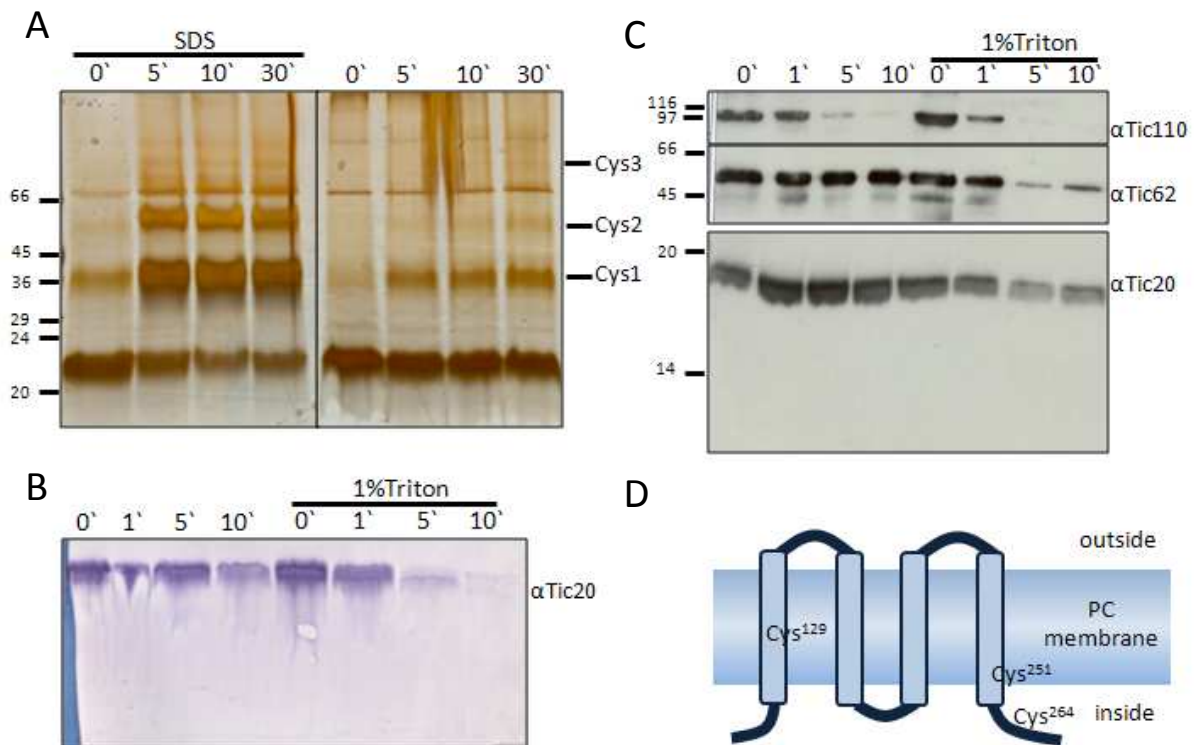


Figure 28. Orientation of Tic20 in liposomes

A) Tic20 liposomes were treated for the indicated time points with 10 mM PEG-Mal in the presence or absence of 1% SDS. The reaction was stopped by addition of 100 mM DTT. For the 0' controls DTT was added prior to PEGylation. Samples were applied to SDS-PAGE (Bis-Tris/MES Nu-PAGE) and silver-stained. PEGylated protein is indicated with the corresponding number of labelled cysteines (Cys1, Cys2, Cys3). B) Tic20-proteoliposomes (4 µg protein) and C) IE vesicles (10 µg total protein) were subjected to limited proteolysis with thermolysin (0.1 µg/µl) at RT for the indicated time points in the absence or presence of 1% Triton X-100. The reaction was stopped by addition of 10 mM EDTA. For the 0' controls EDTA was added before thermolysin to the reaction mixture. Tic20 (and Tic110, Tic62 as controls in IE) were detected by immunoblotting after SDS-PAGE. Molecular weight markers were indicated on the left (kDa). D) Topological model of Tic20 inserted into the phosphatidylcholine (PC) liposomes in a right-side-out orientation (similarly to IE). The possible localization of cysteines (Cys) of Tic20 in *Arabidopsis* is indicated.

As a second approach to determine the orientation of Tic20, proteoliposomes and IE vesicles were subjected to limited proteolysis experiments with thermolysin (Figure 28 B and C). Under native conditions, Tic20 could hardly be proteolytically degraded in the liposomes, without any detectable degradation band. After Triton X-100 pre-treatment, the protein was degraded and some lower bands were observed. In the case of IE, Tic20 was not degraded (even after 10 min) under native conditions, indicating that the protein is deeply inserted into the membrane. Treatment with the detergent allowed degradation, however still not to 100% after 10 min incubation. Since the protein could be slightly degraded in proteoliposomes but not in IE under the same conditions after 10 min, it could be hypothesized that Tic20 is also deeply inserted into liposomes, but partly in a bidirectional manner: A lower amount of the protein is accessible to the protease (inside-out inserted), whereas the rest is protected (right-

side-out inserted, Figure 28 D). These data further supported results from PEGylation experiments that the majority of Tic20 in proteoliposomes is oriented similarly to Tic20 in IE.

4.2.5. Channel activity

Even though Tic20 has long been suggested to form a channel in the IE membrane, this notion was solely based on structural analogy to other four-transmembrane helix proteins (Kouranov *et al.*, 1998; Reumann and Keegstra, 1999), and no experimental evidence has been provided so far. Therefore, Tic20-proteoliposomes were used to investigate the channel activity with two different experimental approaches: with swelling assays and electrophysiology.

4.2.5.1. Swelling assays

Addition of high concentrations of salt causes a change in the size of liposomes, which can be followed by measuring the optical density at 500 nm (OD_{500nm}). This can be used to detect the presence of a pore-forming protein inserted into the liposomes: Shrinkage after the addition of salt is prevented by the equilibration of the osmotical gradient between both sides of the membrane if the channel is permeable for the penetrating ions (Pencer *et al.*, 2001; Ertel *et al.*, 2005).

For swelling assays, liposomes and Tic20-proteoliposomes were diluted with their buffer (20 mM Tris-HCl (pH 8.0), 100 mM NaCl) to an OD_{500nm} of about 0.1. In the beginning of the experiment samples were incubated until the OD_{500nm} reached equilibrium. After addition of 300 mM KCl, their OD_{500nm} dropped initially, due to shrinkage caused by the osmotic shock (Figure 29). The OD_{500nm} of protein-free liposomes remained at this low level (Figure 29, dark blue), showing no change in their size; whereas in the case of Tic20-proteoliposomes the OD_{500nm} increased constantly with time (Figure 29, red). This increase strongly supported the presence of a channel in the Tic20-proteoliposomes that was permeable for ions, thereby creating an equilibrium between the inner compartment of the proteoliposomes and the surrounding buffer.

The effect of other salts (e.g. LiCl, NaCl, KCl, CsCl, CaCl₂), amino acids (glycine, arginine) and sucrose on Tic20-proteoliposomes was also analysed, however, in the case of those no channel activity could be observed. It indicates that *in vitro* the channel might be only active in the presence of K⁺, however, it does not exclude a role to transport other compounds *in vivo*.

Tic20 in *Arabidopsis* contains a deeply inserted Cys in the membrane (Figure 28 D). The oxidation of this Cys therefore might cause intermolecular disulfide bridges within the

homooligomer. If the channel is closed upon oxidation, it should be observed via the change in the OD_{500nm} . Hence, Tic20-proteoliposomes were treated with 0.5 mM $CuCl_2$, followed by swelling assay. Similarly to empty and Tic20-containing liposomes, the OD_{500nm} dropped after the addition of 300 mM KCl, but it did not increase during the measurement (Figure 29, green), indicating that the channel was closed after oxidation with $CuCl_2$. The oxidation of empty liposomes did not result in any change (data not shown). Interestingly, decreasing the concentration of $CuCl_2$ to 0.1 mM did not close the channel, since an increase in the OD_{500nm} after the initial drop was still observed (data not shown). To analyse the reversibility of the oxidation, $CuCl_2$ oxidized Tic20-proteoliposomes were dialysed to remove oxidant and reduced (treated with DTT). These proteoliposomes still did not show any channel activity with swelling assays, indicating that an irreversible oxidation had occurred (data not shown).

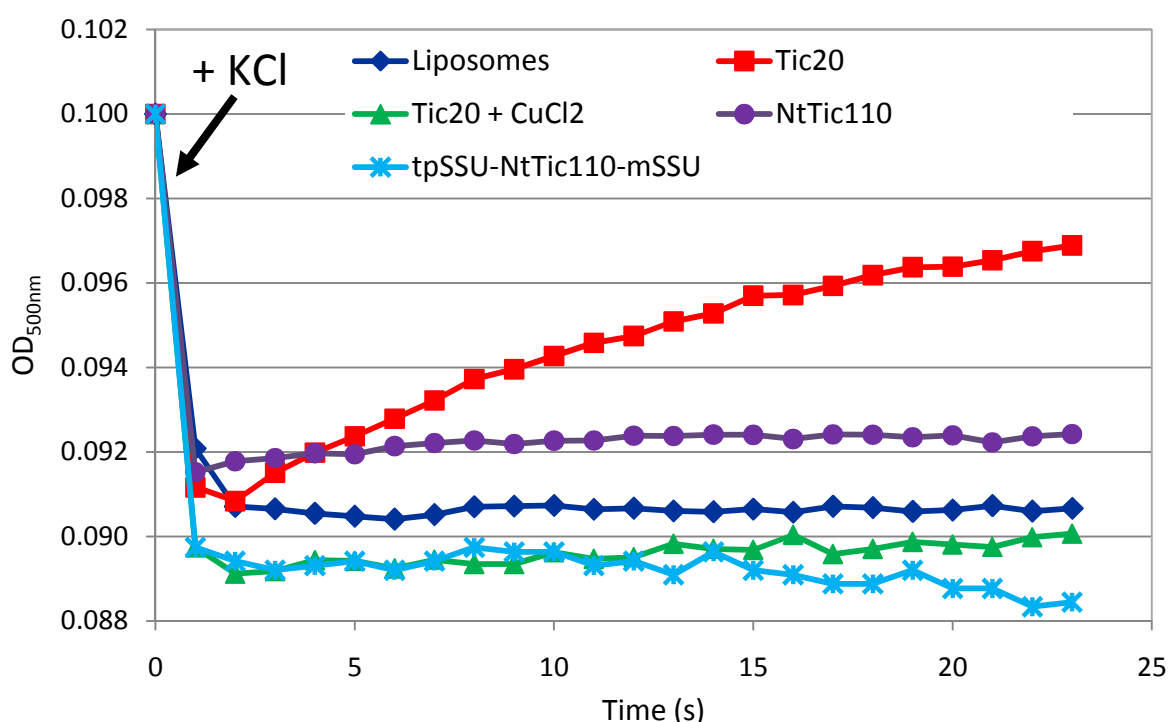


Figure 29. Swelling assays

Figure was partially adapted from Kovács-Bogdán *et al.* (submitted). Tic20-, NtTic110- and tpSSU-NtTic110-mSSU-proteoliposomes and empty liposomes were diluted with 20 mM Tris-HCl (pH 8.0), 100 mM NaCl to 1 ml to have an optical density at 500 nm (OD_{500nm}) of about 0.1. After reaching equilibrium, 300 mM KCl was added (arrow) and OD_{500nm} was measured in every minute. To close the channel, Tic20-proteoliposomes were pre-incubated with 0.5 mM $CuCl_2$ for 20 min at 20°C (Tic20 + $CuCl_2$) and swelling assay was performed. Presented data are the average of at least three experiments, except tpSSU-NtTic110-mSSU, which is a representative result; standard deviations are below 3%.

To exclude the possible effects in the swelling assay of (i) contaminating channel-forming proteins derived from the bacterial membrane and (ii) a protein inserted into the liposomes (but not forming a channel), negative controls were set up: NtTic110 and tpSSU-NtTic110-

mSSU were purified and reconstituted into liposomes, for both following a similar protocol as with Tic20 (Sections 4.2.1 and 4.2.2). Proteoliposomes were then subjected to swelling assay similarly to Tic20. They behaved similarly to the empty liposomes during swelling assays (Figure 29, purple and light blue): after addition of salt, the OD_{500nm} decreased and remained at a constant level, except for a small initial increase in the case of NtTic110. These observations strongly suggest that the observed change in the OD_{500nm} is a result of Tic20 channel activity.

4.2.5.2. Electrophysiology

As a second approach to investigate channel activity, electrophysiological measurements were performed. During these measurements, liposomes containing a pore-forming protein fuse with the lipid bilayer according to the osmotical gradient present on both sides of the membrane (Figure 7). Electrodes installed in connection with *cis* and *trans* chambers allow to measure a channel inserted into the bilayer, since the ion flow through the membrane can be measured as a current flow.

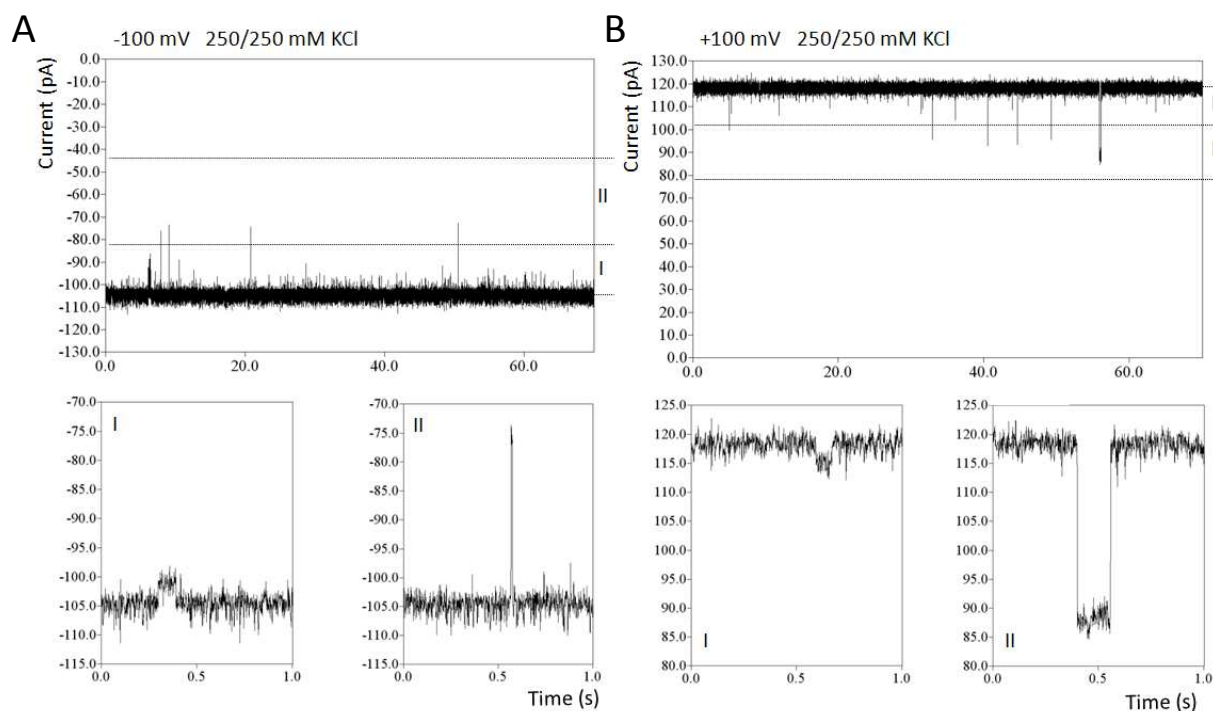


Figure 30. Single gating events of Tic20

Figure was adapted from Kovács-Bogdán *et al.* (submitted). Current traces of a Tic20 channel in lipid bilayer at A) -100 mV and B) +100 mV. Dotted lines indicate thresholds of each conductance class (I and II). Lower panels show representative gating events belonging to each class. Measurements were performed under symmetrical buffer conditions (20 mM MOPS/Tris (pH 7.0), 250 mM KCl). Presented current traces are representative results from two independent fusions accounting for more than 4500 gating events.

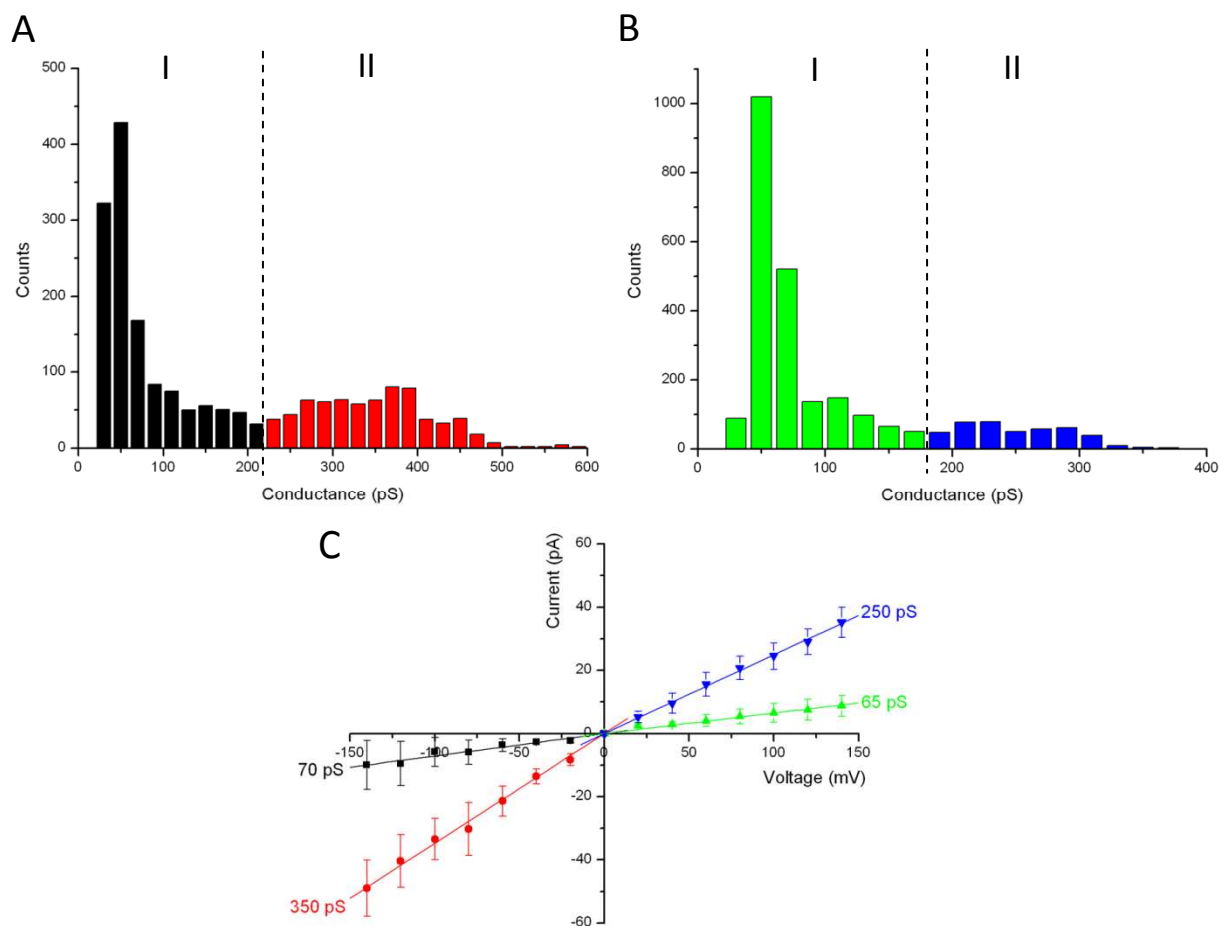


Figure 31. Conductance of Tic20

Figure was adapted from Kovács-Bogdán *et al.* (submitted). Conductance histograms of all gating events of Tic20 at (A) negative and (B) positive voltages. Colours represent different conductance classes (I and II). (C) Current-voltage relationship diagram of all analysed gating events ordered in the four indicated conductance classes using the same colour code as in (A) and (B). Indicated conductance values correspond to the slope of fitted linear in each class. Measurements were performed under symmetrical buffer conditions (20 mM MOPS/Tris (pH 7.0), 250 mM KCl). Presented data derive from two independent fusions accounting for more than 4500 gating events.

After the fusion of Tic20-proteoliposomes with a lipid bilayer, ion channel activity was observed (Figure 30). The total conductance under symmetrical buffer conditions (10 mM MOPS/Tris (pH 7.0), 250 mM KCl) was dependent on the direction of the applied potential: 1260 pS (± 70 pS) and 1010 pS (± 50 pS) under negative and positive voltage values, respectively. The channel was mostly in the completely open state, however, individual single gating events were also frequently observed, varying in a broad range between 25 pS to 600 pS (Figure 30 and Figure 31). All detected gating events were depicted in two histograms (Figure 31 A and B for negative and positive voltages, respectively). Two conductance classes (I and II) were defined both at negative and positive voltage values with thresholds of 220 pS and 180 pS, respectively. After sorting all gating events in the corresponding conductance classes, a current-voltage relationship diagram was depicted (Figure 31 C), which defined the conductance values for each classes: 70 pS or 65 pS for the smaller and 350 pS or 250 pS for

the higher conductance classes at negative or positive voltage values, respectively. Note that gating events belonging to the smaller conductance classes (I) occurred more frequently. The remarkable difference in higher conductance classes under negative and positive voltages suggested that the measured pore was asymmetric. This was probably due to interactions of the permeating ions with the channel, which presumably exhibited an asymmetric potential profile along the pore.

The selectivity of Tic20 was investigated under asymmetric salt conditions (10 mM MOPS/Tris (pH 7.0), 250/20 mM KCl). The reverse potential can be read from voltage ramp diagrams (measuring the current while changing the voltage) at 0 pA current value. Therefore, the obtained reverse potential was 37.0 ± 1.4 mV (Figure 32 A). According to the Goldman-Hodgking-Katz approach (Equation 3), this corresponds to a selectivity of 6.5:1 for $K^+ : Cl^-$ ions, thus indicating cation selectivity, similar to Tic110 (Balsera *et al.*, 2009a). In line with the conductance values, the channel is intrinsically rectifying (behaving differently under negative and positive voltage values), supporting asymmetric channel properties.

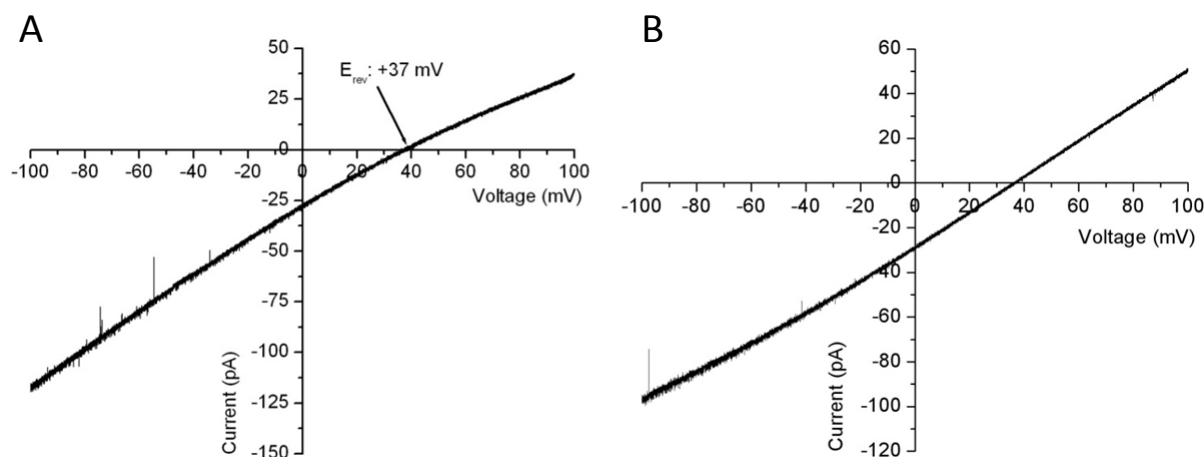


Figure 32. Voltage ramp of Tic20

Figure was partially adapted from Kovács-Bogdán *et al.* (submitted). A) A representative voltage ramp of Tic20 demonstrating the cation selectivity of the channel with a positive reverse potential (E_{rev}). B) Voltage ramp of Tic20 when the protein is inserted into the bilayer in the other direction. Note that the presented ramp folds to another direction than in A). Measurements were performed under asymmetrical buffer conditions (20 mM MOPS/Tris (pH 7.0), 250/20 mM KCl). Presented voltage ramps are representative results from two independent fusions accounting for 16 voltage ramps.

To determine the channel's orientation within the bilayer, two side-specific characteristics were taken into account: the highest total conductance under symmetrical buffer conditions was measured under negative voltage values, and the channel rectifies in the same direction under asymmetrical buffer conditions (compare folding of voltage ramp in Figure 32 A and B).

The pore size was roughly estimated according to Hille (1992) (Equation 2). Considering the highest conductance class (350 pS), a channel length of 1-5 nm and a resistivity of 247.5 Ω cm for a solution containing 250 mM KCl, furthermore taking into account that the conductivity of the electrolyte solution within the pore is ~5 times lower than in the bulk solution (Smart *et al.*, 1997), the pore size was estimated to vary between 8-14 Å.

The negative control proteoliposomes (containing NtTic110 or tpSSU-NtTic110-mSSU) did not show any channel activity during electrophysiological measurements (data not shown), indicating that the observed channel is not the result of a possible bacterial contamination.

4.2.6. Crystallization

The detailed structure of Tic20 would clearly support our observations according to the channel formation of Tic20, would furthermore elucidate the oligomerization state of the protein and also the possible interaction sites for other proteins. To determine the crystal structure of Tic20 we applied similarly to dNTic110 the bicelle method in cooperation with Dr. Gergely Katona and Annette Duelli (University of Gothenburg, Sweden).

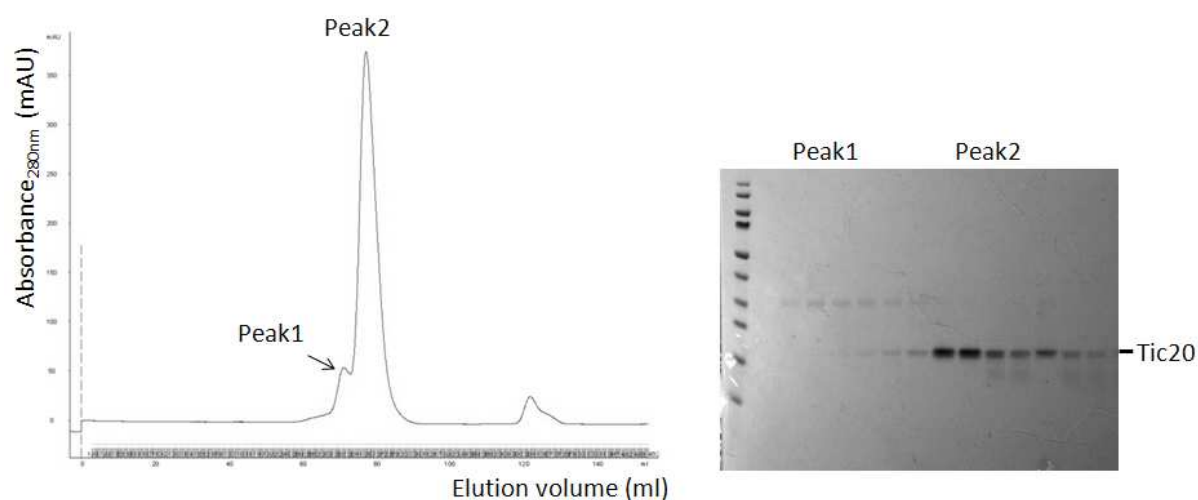


Figure 33. Gel filtration of Tic20

Gel filtration chromatogram (left) of Tic20 with Superdex 200 in 20 mM Tris-HCl (pH 8.0), 150 mM NaCl, 0.3% LS. Samples from resulted peaks were loaded on SDS-PAGE (right). Pure samples of Tic20 (Peak2) were concentrated and used for crystallization.

For the structural analysis, a highly concentrated and pure protein was needed without any possible aggregations. Therefore, after the Ni-affinity purification, Tic20 was subjected to gel filtration using a Superdex 200 column equilibrated with 20 mM Tris-HCl (pH 8.0), 150 mM NaCl and 0.3% LS. Another contaminating protein was observed at about 40 kDa, which

could be successfully separated by gel filtration (Figure 33, Peak1). Furthermore, there was no aggregation peak observed at lower elution volumes.

Highly concentrated (>10 mg/ml) and freshly prepared Tic20 was mixed with different composition of bicelles and crystallization test plates were set up. Crystal growth was observed in several test drops (some examples are presented in Figure 34). Crystals were mounted, flash-cooled in liquid nitrogen and stored until measurements in the ESRF. Since the grown crystals contained either salt or did not have a good diffraction to determine the content, further tests have to be performed to find out the best crystallization conditions for the formation of Tic20 crystals, which can be used to resolve its structure.

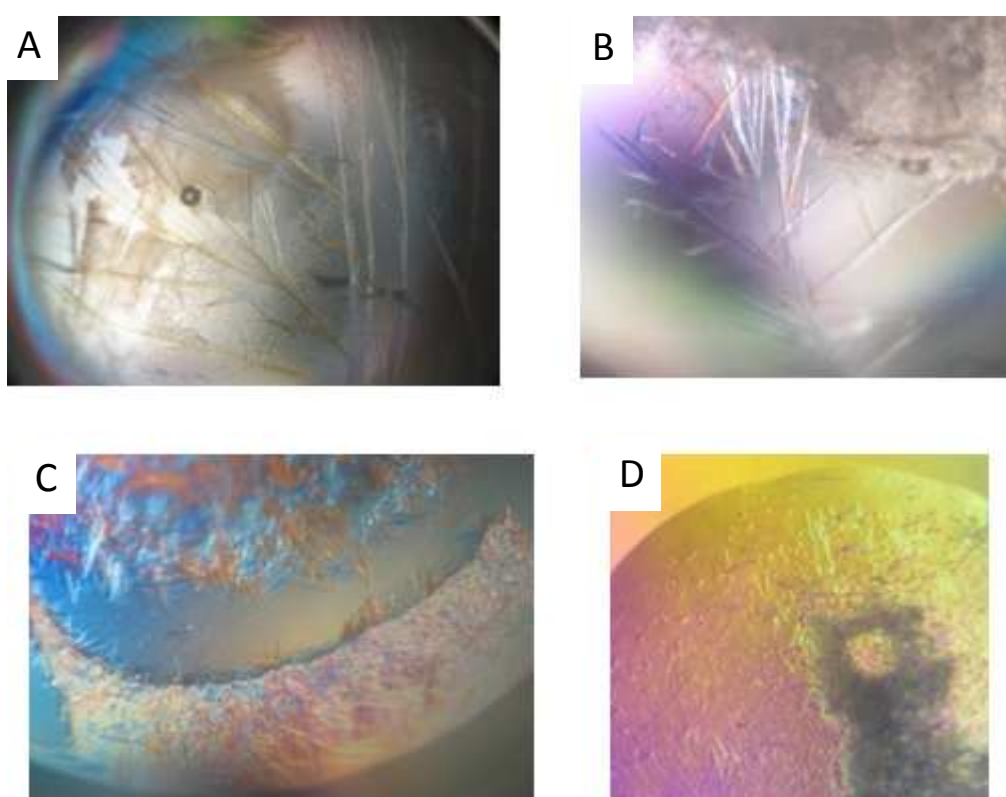


Figure 34. Crystallization tests of Tic20

Some representative crystals from bicelle crystallization test drops. Detailed composition of the drops: A) and B) 14 mg/ml Tic20; bicelle: 32 mg DMPC, 4 mg DMPG, 12 mg CHAPSO; 1:3 bicelle:protein volume ratio; precipitant: 0.2 M Zn-acetate, 10% w/v PEG 8000, 0.1 M MES (pH 6.0); cryo-protectant: PEG 8000. C) 15 mg/ml Tic20; bicelle: same as A); 1:3 bicelle:protein volume ratio; precipitant: 0.1 M $MgCl_2$, 0.1 M Na-acetate (pH 4.6), 30% PEG 400; cryo-protectant: PEG 400. D) 12 mg/ml Tic20; bicelle: 54 mg DMPC, 6 mg DMPG, 20 mg CHAPSO; 1:3 bicelle:protein volume ratio; precipitant: 0.1 M NaCl, 0.05 M $MgCl_2$, 0.1 M Na-acetate (pH 4.1), 30% PEG 400; cryo-protectant: PEG 400. Given amount of bicelle lipids and detergent was solubilized in 200 μ l 20 mM Tris-HCl (pH 8.0).

5. Discussion

5.1. Topology and structure of Tic110

The localization of the hydrophilic part of Tic110 (dNTic110) has been debated for a long time. Three different theories placed it (i) to the stromal side as a soluble part of the protein, responsible for chaperone recruitment (Jackson *et al.*, 1998; Inaba *et al.*, 2003); (ii) to the intermembrane space, for contacting the incoming transit peptide and the TOC translocon (Lübeck *et al.*, 1996); and (iii) to the membrane building the protein import channel (Heins *et al.*, 2002). The data presented in this work (namely that dNTic110 inserts into the membrane *in vitro* without the hydrophobic N-terminus of Tic110 and without any other components or detergents), together with the results from gel filtration of dNTic110 in the absence or presence of detergent, limited proteolysis experiments of IE combined with LC-MS/MS, Cys labelling assays (using PEG-Mal) of IE and computational predictions, led Dr. Mónica Balsera (Balsera *et al.*, 2009a) to determine the topology of Tic110 (Figure 35). This model is also compatible with the models of earlier publications: dNTic110 is hydrophilic, however, the presence of amphipathic helices allows the insertion into the membrane. Additionally, these amphipathic helices inserted into liposomes also in the absence of detergents, indicating the high membrane affinity of this part. Loops between the transmembrane domains are located both to the intermembrane space - presenting contact sites for the transit peptide and the TOC translocon -, and to the stromal side, for recruiting chaperones. According to this model, M2, a shorter form of Tic110, also contains two amphipathic helices, which explains its insertion into liposomes (Figure 10). On the contrary, M3 does not contain any transmembrane domains, therefore it was not inserted.

Tic110 migrates on BN-PAGE at 200-250 kDa (Kikuchi *et al.*, 2009; Benz, 2009; Kovács-Bogdán *et al.*, submitted) either as a dimer or involving other components in the complex. BN-PAGE (Figure 9 E) and size exclusion chromatography followed by static light scattering (Balsera *et al.*, 2009a) of the purified dNTic110 supported the first hypothesis. Furthermore, the M2 truncation of Tic110 also formed a dimer, whereas M3 was a monomer, indicating that the domain responsible for the oligomerization is located between residues Met⁴³³ and Met⁷⁸⁸ in the pea sequence.

The crystal structure of Tic110 would answer several questions about the structure and function of the protein. Crystallization from lipidic phases is a very promising approach to

crystallize Tic110, since several membrane protein structures have already been resolved using this method (for detailed review see Johansson *et al.*, 2009). Therefore, the preliminary work performed during this study to crystallize Tic110, might lead in the future to protein crystals with high resolution.

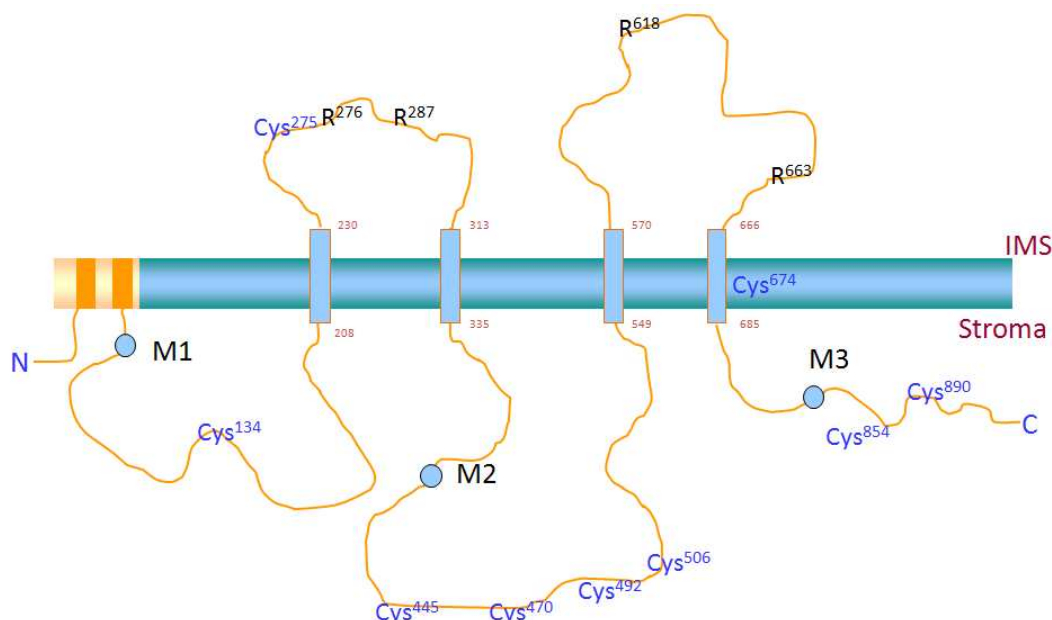


Figure 35. Topological model of Tic110

The topological model of Tic110 was adapted from Balsera *et al.* (2009a). Tic110 contains two hydrophobic (orange) and four amphipathic (blue) transmembrane helices. M1 is the first amino acid of dNTic110 used in this study. M2 and M3 represent the start methionines of two shorter forms, which were overexpressed in *E. coli* along with dNTic110. Cysteines (Cys) in the pea sequence are indicated. Note that only one Cys is located in the intermembrane space (IMS) and one is deeply inserted into the membrane. Arginin (R) cleavage sites for trypsin proteolysis under native conditions are located in the IMS side.

5.2. Redox characterization of Tic110

5.2.1. Oxidation states

The notion that Tic110 is redox regulated via its highly conserved Cys residues became more apparent after the demonstration of different Tic110 redox states *in vitro* and *in vivo*. Furthermore, reduction of the protein with physiological reducing agents, such as Trxs, pointed out that Tic110 could be a target for Trx regulation. Tic110 is the second demonstrated Trx target in the TIC translocon (after Tic55), further suggesting multiple ways of regulation of protein import at the level of the TIC translocon. However, the *in vivo* role of Trxs in the regulation of Tic110 function should be a matter of further investigation. Another question is, whether only one isoform reduces Tic110 specifically or Tic110 is the substrate of all chloroplastic Trx isoforms as presented by *in vitro* assays.

Surprisingly, Tic110 is reduced in the dark and oxidized in the light *in vivo*. On the contrary, Trx target proteins are typically reduced in the light and oxidized in the dark. However, there are also some described Trx targets, e.g. RB60 (Trebitsh *et al.*, 2000) and 2-Cys-peroxiredoxin (Horling *et al.*, 2002), which have a similar oxidation pattern in the light/dark cycle as Tic110, supporting the possibility of Trx regulation.

Interestingly, there are no Trx isoforms described in mitochondria regulating protein import. However, a disulfide exchange system in the mitochondrial IMS has been thoroughly characterized (Mesecke *et al.*, 2005): A class of mitochondrial IMS proteins - containing conserved Cys residues -, after being imported through the TOM (Translocase of the Outer Mitochondrial membrane) complex into the IMS, take part in an oxidative folding via the Mia40/Erv1 system. Similar oxidative folding pathway exists in the bacterial cell envelope catalysed by Dsb proteins (Kadokura and Beckwith, 2010) and in the endoplasmic reticulum mediated by a protein disulfide isomerase and Ero1 (Tu *et al.*, 2000). Such pathway or proteins with a Dsb-like activity has not been identified in the chloroplast envelope protein import machinery yet. However, the presence of a sulfhydryl-oxidizing system is feasible in the thylakoid lumen (Balsera *et al.*, 2009b, Herrmann *et al.*, 2009).

5.2.2. Cysteines involved in disulfide bridge formation

Since Tic110 contains nine Cys residues (six of which are highly conserved in land plants) (Figure 35), an intriguing challenge is to elucidate which Cys are involved in disulfide bridge formation. Experiments using mutants of Tic110 resulted in two interesting and promising observations: Firstly, dNTic110 C492S mutants build high molecular weight complexes (possibly dimers) after oxidation, which could not be reversibly reduced. Secondly, oxidation of the C-terminal deletion of dNTic110 (dNdCTic110) leads to notably high amounts of aggregations. These observations can be interpreted that the changed (C492S) or deleted (Cys⁸⁵⁴ or Cys⁸⁹⁰) Cys might be responsible for the disulfide bridge formation. It can be hypothesized that in the absence of these Cys, the other Cys partner in the disulfide bridge might irreversibly bind to another Cys or to other residues upon oxidation. However, dNdCTic110 could also aggregate because of its possibly different conformation, which is not stable upon oxidation.

One further possibility to analyse the relevance of different Cys residues, might be the complementation of *Arabidopsis tic110* mutants with Tic110 having exchanged Cys residues. According to the data presented here, mutation of Cys⁴⁹² and/or Cys⁸⁹⁰ (the highly conserved

Cys deleted with the C-terminal truncation) would be the most promising candidates. A difference in the phenotype of wild type and mutant Tic110 complemented plants (maybe under stress conditions) could indicate the relevance of the Cys of interest.

However, these two candidate Cys residues are not in a CXXC motif (and none of the Cys present in Tic110). Instead they can be positioned close enough in the three dimensional structure to enable oxidation, since they are both on the stromal side of the membrane. This, or other possible disulfide pairs would be verified by the resolved crystal structure of Tic110.

5.2.3. Roles of the oxidation states

This study also attempted to define the role of the oxidation states of Tic110. Three different possibilities could be investigated: possible alterations (i) in the channel and protein import activity, (ii) in the interaction with the Hsp93/Tic40 motor complex or (iii) in the interaction with preproteins. However, this work could not clearly define the role of different oxidation states, but the accomplished results might significantly help further investigations in this area.

5.2.3.1. Effect on the channel activity and import rates

Singh and Ashley (2006) observed that the channel activity of human CLIC1 (chloride intracellular channel) responds to changes in the redox potential in the surrounding buffer, which refers to a redox sensitive Cys in the sequence. Similarly to this, Tic110 channel activity might be regulated upon oxidation.

The sensitivity of the used equipment to oxidants and reductants during electrophysiological measurements hindered determination of the effect of Tic110 oxidation states on the channel and import activity. Therefore, other possible oxidants/reductants have to be analysed. Using GSSG during electrophysiological measurements - similarly to Singh and Ashley (2006) - might have an effect on the channel activity, since the incubation of Tic110 with GSSG led to an oxidized protein (Figure 13 B). This option still has to be investigated in the future.

Furthermore, since isolated chloroplasts are highly sensitive to higher temperatures (at which Tic110 is found to be oxidized), the oxidation of Tic110 in chloroplasts should be analysed in more details. Isolation of chloroplasts from dark and light treated plants did not give a solution, since Tic110 was reduced in both samples (Figure 16 A).

5.2.3.2. Effect on the interaction with the motor complex and preproteins

Interaction between Tic110, Tic40 and Hsp93 could not be demonstrated during this work, which might be attributed to different reasons:

- The complex is very dynamic and therefore could not be stabilized under the applied conditions. This effect becomes clear after performing 2D BN-PAGE: Tic110 localizes at a 200-250 kDa complex (Kikuchi *et al.*, 2009; Benz, 2009; Kovács-Bogdán *et al.*, submitted), which cannot contain all motor components, since Tic110 and Tic40 are supposed to form dimers (present work, Balsera *et al.*, 2009a, Schwenkert *et al.*, 2011), whereas Hsp93 is a dimer or a hexamer. Furthermore, there is still no report about the isolation of the whole TIC complex (or a core of it), which however, could be performed with the core of the TOC complex (Schleiff *et al.*, 2003b).
- The applied nucleotide during the experiments might also critically influence the association, since Tic40 was demonstrated to bind stronger to Hsp93 in the presence of ATP but not in the presence of ADP.
- Dilution during gel filtration could be also a drawback to identify the complexes, since the oligomerization of Hsp93 seemed to be strongly dependent on the concentration (Section 4.1.8.1).
- The complex may need another additional component for proper hetero-oligomerization. One candidate is Hsp70, which was recently demonstrated to play an important role in the import process (Su and Li, 2010; Shi and Theg, 2010). Another possible partner is a preprotein, which might be a link between these proteins, however, their complex was also identified in the absence of preproteins after co-immunoprecipitation (Kessler and Blobel, 1996; Nielsen *et al.*, 1997; Su and Li, 2010).
- Other parts of the proteins, such as the N-terminal part of Tic110 or the membrane inserted domain of Tic40 might be also needed for stable interaction. However, earlier studies supported the opposite: (Chou *et al.*, 2003) demonstrated that the soluble part and the alleged TPR-like domain of Tic40 binds to dNTic110, and the second Sti1 domain of Tic40 stimulates the ATP hydrolysis of Hsp93. Possible reasons for the discrepancy with the here presented data might be the different conditions and organisms (*Arabidopsis* and pea) used.
- Domains of the proteins, which are not involved in the interaction, might also shield the active sites during *in vitro* experiments.
- A not correctly folded protein may also prevent association. To support the correct conformation of Tic110, interaction tests were also performed in a membrane-mimicking

environment. However, non-protein mediated membrane attachment of Hsp93 alone prevented a clear conclusion (Figure 21).

There are however other possibilities to further investigate the interaction between Tic110 and the motor components: Using a cross-linking approach, the association of the components would be stabilized, therefore their interaction could be detected. However, the non-specificity of this approach has to be considered, therefore, a cross-linker with a short spacer arm should be chosen. A second approach might be a yeast-two-hybrid assay to analyse their interaction. However, in this system different oxidation states of Tic110 cannot be generated, which prevents to study the main aim of this investigation: whether the interaction is altered under different redox conditions. A third possibility is to use Hsp70 or a preprotein in the analysis (see above). Furthermore, applying specific domains of these proteins (which are predicted to be responsible for protein-protein interaction) might exclude the shielding effect of other parts of the proteins. Finally, setting up an efficient system for *in vivo* characterization of the complex, would be the best possibility to elucidate the role of Tic110 redox states in the interaction with the motor components.

To analyse whether there is a difference in the binding of preproteins to Tic110 (or IE), an oxidizing agent should be used, which does not cause significant aggregation of the protein. Another possibility is the isolation of IE vesicles without reducing agents, which might lead to an oxidized Tic110 in the sample. However, the different oxidation states of other IE proteins might have an additional effect. This could be excluded by using Tic110-proteoliposomes for interaction assays.

5.2.4. Oligomerization state of Hsp93

A side-project of this study involved the characterization of Hsp93 oligomerization states. The protein was present mostly as a dimer *in vitro* and also in isolated pea stroma suggesting that this conformation is the most stable unit. It is in good agreement with earlier studies analysing Hsp93 in *Arabidopsis* chloroplast and plastid stroma (Peltier *et al.*, 2004). In the presence of ADP or ATP, hexamer formation was observed indicating the functional assembly of the HSP100 protein family (Schirmer *et al.*, 1996; Andersson *et al.*, 2006). Furthermore, the residual ATP or ADP in the stroma of isolated pea chloroplasts also enabled the formation of a minor fraction of hexamers. Similarly, Majeran *et al.* (2008) could also detect Hsp93 hexamers in mesophyll chloroplasts of maize. Interestingly, the N-terminal His-tag prevented hexamerization of Hsp93 *in vitro*. This effect might answer why in earlier studies the tag used

for purification was proteolitically degraded (Andersson *et al.*, 2006), or the protein was purified without a tag (Parsell *et al.*, 1994). An interesting question is how Hsp93 functions during the import process and which form (ATP bound or free) binds to the preprotein, Tic110 or Tic40. The hexameric state might play an important role, since Hsp93 binds stronger to Tic40 *in vitro* in the presence of ATP (Chou *et al.*, 2003).

5.3. Channel-forming components of the TIC complex

More than a decade after the identification of Tic20, this work provides the first experimental evidence for Tic20 channel function, using two different *in vitro* approaches in the presence of liposomes, confirming earlier *in silico* predictions (TMHMM server and Kouranov *et al.*, 1998). Based on these data combined with earlier studies (e.g. cross-links to imported preprotein, protein import defects in the knock down mutants and co-localization with the imported preprotein after chloroplast solubilization (Kouranov *et al.*, 1998; Reumann and Keegstra, 1999; Kikuchi *et al.*, 2009)) it is very feasible that Tic20 forms a protein translocation channel in the IE membrane. Although *in vitro* data support only ion selectivity, a more complex environment *in vivo* (e.g. other interaction partners associated with the channel) would enable protein translocation. Furthermore, cation selectivity of the channel also indicates a role in protein translocation, since the transit peptide is positively charged. The calculated pore size of 8-14 Å is in a similar range as the size of other protein translocation channels, such as Toc75 (in the outer envelope membrane 14-26Å, Hinnah *et al.*, 2002) and Tic110 in the IE (15-31 Å, Heins *et al.*, 2002). Thus, the Tic20 pore would be sufficient for the translocation of precursor proteins through the membrane.

According to cross-linking results (Kouranov *et al.*, 1998), Tic20 is connected to TOC translocon components. Therefore, after entering the intermembrane space via the TOC complex, some preproteins might be transported through the IE via Tic20. On the contrary, Kikuchi *et al.* (2009) presented that Tic20 migrates on BN-PAGE at the same molecular weight as the imported pSSU. The authors interpreted these results in a way that Tic20 might function at an intermediate step between the TOC translocon and the channel of Tic110. However, being a substantial part of the general import pathway seems unlikely due to the very low abundance of Tic20 (Kovács-Bogdán *et al.*, submitted). It can be speculated that such abundant proteins as pSSU, which are imported at a very high rate, may interact incidentally with nearby proteins. Due to the severe phenotype of *attic20-I* mutants it can be hypothesized that Tic20 might be specifically required for the translocation of some essential

proteins. Thus, to clarify this question, substrate proteins of Tic20 should be a matter of further investigation.

Localization of Tic20 and Tic110 in independent complexes, their different stoichiometry (Kovács-Bogdán *et al.*, submitted) and the channel activity of both proteins independently (this work and Balsera *et al.*, 2009a) clearly demonstrates that the two channel-forming proteins function separately in two complexes (Figure 36). It is very feasible that Tic110 forms the protein conducting channel as a dimer, since purified dNTic110 behaves as a dimer on BN-PAGE (Figure 9 E) and during gel filtration followed by static light scattering (Balsera *et al.*, 2009a). Furthermore, after mild solubilization of IE and chloroplasts Tic110 localizes in a 200-250 kDa complex (Kikuchi *et al.*, 2009; Benz, 2009; Kovács-Bogdán *et al.*, submitted), which might contain Tic110 dimers. However, at a similar molecular weight on BN-PAGE not only Tic110 but also Hsp93, Tic62 and Tic55 were described (Caliebe *et al.*, 1997; Kückler *et al.*, 2002). The molecular weight of a complex containing all of these components would be much higher. Therefore, components of the TIC complex might associate with Tic110 very dynamically resulting in different compositions under different conditions, or alternatively, there are more complexes present at the same molecular weight.

Tic20 is a part of a one megadalton complex (Kikuchi *et al.*, 2009; Benz, 2009; Kovács-Bogdán *et al.*, submitted). An open question is whether this complex consists of only Tic20 or it might associate with other components. Tic22, the only TIC component located in the intermembrane space, is a potential candidate for interaction, since both proteins were identified together in cross-linking experiments (Kouranov *et al.*, 1998). However, only minor amounts of Tic20 and Tic22 were shown to co-localize after gel filtration of solubilized envelope membranes. Furthermore, PIC1/Tic21 might also be present in this complex, since Kikuchi *et al.* (2009) described PIC1/Tic21 as a minor subunit of the one megadalton complex. Hence the role of this protein is highly debated, whether it is a protein translocation channel or a metal permease in the IE (Teng *et al.*, 2006; Duy *et al.*, 2007; Duy *et al.*, 2011), this question should be a matter of investigation. Moreover, the presence of chaperones in the Tic20 complex - providing driving force through the channel - is also worth considering. One candidate might be Cpn60, which protein co-localizes with Tic20 after solubilization of envelopes followed by gel filtration (Kouranov *et al.*, 1998). However, according to the study presented here, the majority of Tic20 in proteoliposomes localizes in high molecular weight complexes, without the involvement of any other proteins. Thus, this observation gives the support for the hypothesis that the major components of the one megadalton complex in IE

are homo-oligomers composed of Tic20. The lower molecular weight complex observed also on the 2D BN-PAGE of Tic20-proteoliposomes might indicate that another partner(s) (which was not present in the proteoliposomes) is needed to catalyse the proper oligomerization of Tic20.

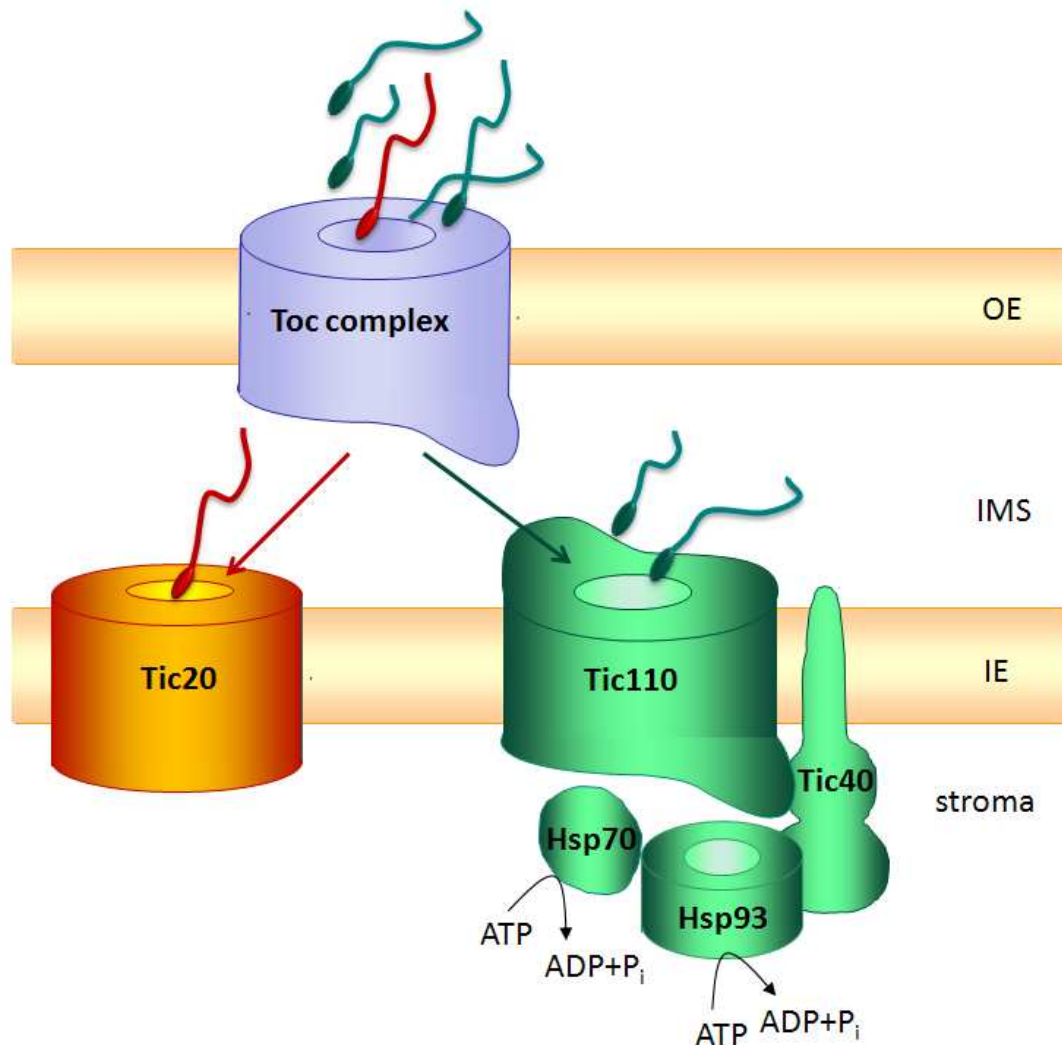


Figure 36. Two distinct protein import channels of the TIC complex

Hypothetical model of Tic20 and Tic110 channels in the inner envelope (IE) of chloroplasts based on Kovács-Bogdán *et al.* (submitted). After passing the TOC complex in the outer envelope (OE), preproteins are imported either via Tic110 (green) or Tic20 (red/orange) through the IE. The import through the Tic110 channel is facilitated by the motor complex(es), whereas the identity of Tic20 interaction partners is still a matter of investigation. IMS: intermembrane space.

Regulation of Tic20 could be mediated by other (probably dynamically) associated components. The presence of highly conserved Cys on the stromal side indicate Trx regulation (Balsera *et al.*, 2009b). This notion is also supported by the observation that the oxidation of Tic20-proteoliposomes prevented the channel activity during swelling assays.

However, this oxidation seemed to be non-reversible. Therefore, the regulation possibilities of Tic20 channel activity should be a matter of further investigation.

The presence of two protein translocation channels would match the one found in the inner mitochondrial membrane, where three different specific translocases exist responsible for defined groups of inner membrane proteins (Neupert and Herrmann, 2007; Mokranjac and Neupert, 2010): Firstly, the TIM22 translocon mediates the insertion of the solute carrier family and the membrane embedded Tim subunits. Secondly, the TIM23 complex catalyses the import of membrane proteins, having mostly only one transmembrane domain with a N_{in}-C_{out} orientation (stop-transfer mechanism). Thirdly, some precursors (e.g. subunit 9 of the F₀F₁-ATPase, Oxa1) following import into the matrix (via TIM23) integrate into the inner membrane with the help of the Oxa1 complex (conservative sorting). The situation in chloroplasts does not seem as clear-cut, but a separation determined by the final destination and/or intrinsic properties of translocated proteins is feasible.

Additionally, TOC complexes with different isoform composition differentiate between housekeeping and photosynthetic proteins (Kubis *et al.*, 2003; Kubis *et al.*, 2004): Phenotype analyses of *Arabidopsis* lacking one of the Toc159 or Toc34 isoforms revealed that TOC complexes consisting of AtToc132/AtToc120 and AtToc34 are involved in the import of non-photosynthetic proteins, whereas AtToc159 and AtToc33 play a role preferentially in the import of photosynthetic proteins. However, a similar differentiation between the function of Tic110 and Tic20 is unlikely, according to the very low amount of Tic20 in both photosynthetic and non-photosynthetic tissues (Kovács-Bogdán *et al.*, submitted).

Unfortunately, due to the lethality of *attic110* and the very severe phenotype of *attic20-I* homozygous knockout mutants, their separate mode of action will be very difficult to investigate *in vivo*. One possibility would be the generation of *tic110* and *tic20* knock-out mutants of *Physcomitrella patens*, since there are two isoforms of *PpTic110* and three isoforms of *PpTic20* present (Kalanon and McFadden, 2008). The function of a selected isoform might be therefore complemented partially in single knock-out mutants to prevent lethality. Additionally, resolving the crystal structures of both proteins would further support experiments demonstrating independent channel formation, and would give more information about possible interaction sites.

5. References

- Akita,M., Nielsen,E., Keegstra,K., 1997. Identification of protein transport complexes in the chloroplastic envelope membranes via chemical cross-linking. *J. Cell Biol.* 136, 983-994.
- Alte,F., Stengel,A., Benz,J.P., Petersen,E., Soll,J., Groll,M., Bölter,B., 2010. Ferredoxin:NADPH oxidoreductase is recruited to thylakoids by binding to a polyproline type II helix in a pH-dependent manner. *Proc. Natl. Acad. Sci. U. S. A* 107, 19260-19265.
- Andersson,F.I., Blakytyn,R., Kirstein,J., Turgay,K., Bukau,B., Mogk,A., Clarke,A.K., 2006. Cyanobacterial ClpC/HSP100 protein displays intrinsic chaperone activity. *J. Biol. Chem.* 281, 5468-5475.
- Arnon,D.I., 1949. Copper enzymes in isolated chloroplasts - Polyphenoloxidase in *Beta Vulgaris*. *Plant Physiol* 24, 1-15.
- Balsera,M., Goetze,T.A., Kovács-Bogdán,E., Schürmann,P., Wagner,R., Buchanan,B.B., Soll,J., Bölter,B., 2009a. Characterization of Tic110, a channel-forming protein at the inner envelope membrane of chloroplasts, unveils a response to Ca^{2+} and a stromal regulatory disulfide bridge. *J. Biol. Chem.* 284, 2603-2616.
- Balsera,M., Soll,J., Buchanan,B.B., 2009b. Protein import in chloroplasts: An emerging regulatory role for redox. *Advances in Botanical Research* 52, 277-332.
- Bartsch,S., Monnet,J., Selbach,K., Quigley,F., Gray,J., von Wettstein,D., Reinbothe,S., Reinbothe,C., 2008. Three thioredoxin targets in the inner envelope membrane of chloroplasts function in protein import and chlorophyll metabolism. *Proc. Natl. Acad. Sci. U. S. A* 105, 4933-4938.
- Becker,T., Hritz,J., Vogel,M., Caliebe,A., Bukau,B., Soll,J., Schleiff,E., 2004. Toc12, a novel subunit of the intermembrane space preprotein translocon of chloroplasts. *Mol. Biol. Cell* 15, 5130-5144.
- Bédard,J., Kubis,S., Bimanadham,S., Jarvis,P., 2007. Functional similarity between the chloroplast translocon component, Tic40, and the human co-chaperone, Hsp70-interacting protein (Hip). *J. Biol. Chem.* 282, 21404-21414.
- Benz,J.P., 2009. Characterization of two components of the chloroplastic Tic complex. Dissertation
- Benz,J.P., Lintala,M., Soll,J., Bölter,B., 2011. A new concept for ferredoxin–NADP(H) oxidoreductase binding to plant thylakoids. *Trends Plant Sci.* 15, 608-613.
- Benz,J.P., Stengel,A., Lintala,M., Lee,Y.H., Weber,A., Philippar,K., Gügel,I.L., Kaieda,S., Ikegami,T., Mulo,P., Soll,J., Bölter,B., 2009. *Arabidopsis* Tic62 and ferredoxin-NADP(H) oxidoreductase form light-regulated complexes that are integrated into the chloroplast redox poise. *Plant Cell* 21, 3965-3983.

- Blatch,G.L., Lasse,M., 1999. The tetratricopeptide repeat: a structural motif mediating protein-protein interactions. *Bioessays* 21, 932-939.
- Block,M.A., Dorne,A.J., Joyard,J., Douce,R., 1983. Preparation and characterization of membrane fractions enriched in outer and inner envelope membranes from spinach chloroplasts. II. Biochemical characterization. *J. Biol. Chem.* 258, 13281-13286.
- Blum,H., Beier,H., Gross,H.J., 1987. Improved Silver Staining of Plant-Proteins, Rna and Dna in Polyacrylamide Gels. *Electrophoresis* 8, 93-99.
- Bock,R., Timmis,J.N., 2008. Reconstructing evolution: gene transfer from plastids to the nucleus. *Bioessays* 30, 556-566.
- Bruce,B.D., 2000. Chloroplast transit peptides: structure, function and evolution. *Trends Cell Biol.* 10, 440-447.
- Caliebe,A., Grimm,R., Kaiser,G., Lübeck,J., Soll,J., Heins,L., 1997. The chloroplastic protein import machinery contains a Rieske-type iron-sulfur cluster and a mononuclear iron-binding protein. *EMBO J.* 16, 7342-7350.
- Cavalier-Smith,T., 2000. Membrane heredity and early chloroplast evolution. *Trends Plant Sci.* 5, 174-182.
- Chen,X., Smith,M.D., Fitzpatrick,L., Schnell,D.J., 2002. *In vivo* analysis of the role of atTic20 in protein import into chloroplasts. *Plant Cell* 14, 641-654.
- Chigri,F., Hörmann,F., Stamp,A., Stammers,D.K., Bölder,B., Soll,J., Vothknecht,U.C., 2006. Calcium regulation of chloroplast protein translocation is mediated by calmodulin binding to Tic32. *Proc. Natl. Acad. Sci. U. S. A* 103, 16051-16056.
- Chiu,C.C., Chen,L.J., Li,H.M., 2010. Pea chloroplast DnaJ-J8 and Toc12 are encoded by the same gene and localized in the stroma. *Plant Physiol* 154, 1172-1182.
- Chiu,C.C., Li,H.M., 2008. Tic40 is important for reinsertion of proteins from the chloroplast stroma into the inner membrane. *Plant J.* 56, 793-801.
- Chou,M.L., Chu,C.C., Chen,L.J., Akita,M., Li,H.M., 2006. Stimulation of transit-peptide release and ATP hydrolysis by a cochaperone during protein import into chloroplasts. *J. Cell Biol.* 175, 893-900.
- Chou,M.L., Fitzpatrick,L.M., Tu,S.L., Budziszewski,G., Potter-Lewis,S., Akita,M., Levin,J.Z., Keegstra,K., Li,H.M., 2003. Tic40, a membrane-anchored co-chaperone homolog in the chloroplast protein translocon. *EMBO J.* 22, 2970-2980.
- Cline,K., Henry,R., Li,C., Yuan,J., 1993. Multiple pathways for protein transport into or across the thylakoid membrane. *EMBO J.* 12, 4105-4114.
- Constan,D., Froehlich,J.E., Rangarajan,S., Keegstra,K., 2004. A stromal Hsp100 protein is required for normal chloroplast development and function in *Arabidopsis*. *Plant Physiol* 136, 3605-3615.

- Dávila-Aponte, J.A., Inoue, K., Keegstra, K., 2003. Two chloroplastic protein translocation components, Tic110 and Toc75, are conserved in different plastid types from multiple plant species. *Plant Mol. Biol.* 51, 175-181.
- De Los, R.P., Ben Zvi, A., Slutsky, O., Azem, A., Goloubinoff, P., 2006. Hsp70 chaperones accelerate protein translocation and the unfolding of stable protein aggregates by entropic pulling. *Proc. Natl. Acad. Sci. U. S. A* 103, 6166-6171.
- Duy, D., Stübe, R., Wanner, G., Philippar, K., 2011. The chloroplast permease PIC1 regulates plant growth and development by directing homeostasis and transport of iron. *Plant Physiol* 155, 1709-1722.
- Duy, D., Wanner, G., Meda, A.R., von Wiren, N., Soll, J., Philippar, K., 2007. PIC1, an ancient permease in *Arabidopsis* chloroplasts, mediates iron transport. *Plant Cell* 19, 986-1006.
- Ertel, F., Mirus, O., Bredemeier, R., Moslavac, S., Becker, T., Schleiff, E., 2005. The evolutionarily related beta-barrel polypeptide transporters from *Pisum sativum* and *Nostoc* PCC7120 contain two distinct functional domains. *J. Biol. Chem.* 280, 28281-28289.
- Faham, S., Bowie, J.U., 2002. Bicelle crystallization: a new method for crystallizing membrane proteins yields a monomeric bacteriorhodopsin structure. *J. Mol. Biol.* 316, 1-6.
- Fellerer, C., Schweiger, R., Schöngruber, K., Soll, J., Schwenkert, S. Cytosolic HSP90 cochaperones HOP and FKBP interact with freshly synthesized chloroplast preproteins of *Arabidopsis*. *Mol. Plant*, in press.
- Firlej-Kwoka, E., Strittmatter, P., Soll, J., Bölder, B., 2008. Import of preproteins into the chloroplast inner envelope membrane. *Plant Mol. Biol.* 68, 505-519.
- Flügge, U.I., Hinz, G., 1986. Energy dependence of protein translocation into chloroplasts. *Eur. J. Biochem.* 160, 563-570.
- Gould, S.B., Waller, R.F., McFadden, G.I., 2008. Plastid evolution. *Annu. Rev. Plant Biol.* 59, 491-517.
- Gross, J., Bhattacharya, D., 2009. Mitochondrial and plastid evolution in eukaryotes: an outsiders' perspective. *Nat. Rev. Genet.* 10, 495-505.
- Halperin, T., Ostersetzer, O., Adam, Z., 2001. ATP-dependent association between subunits of Clp protease in pea chloroplasts. *Planta* 213, 614-619.
- Hedges, S.B., Blair, J.E., Venturi, M.L., Shoe, J.L., 2004. A molecular timescale of eukaryote evolution and the rise of complex multicellular life. *BMC. Evol. Biol.* 4, 2.
- Heins, L., Mehrle, A., Hemmler, R., Wagner, R., Kuchler, M., Hörmann, F., Sveshnikov, D., Soll, J., 2002. The preprotein conducting channel at the inner envelope membrane of plastids. *EMBO J.* 21, 2616-2625.

- Herrmann,J.M., Kauff,F., Neuhaus,H.E., 2009. Thiol oxidation in bacteria, mitochondria and chloroplasts: common principles but three unrelated machineries? *Biochim Biophys Acta* 1793, 71-77.
- Hille,B., 1992. *Ionic channels of excitable membranes*, Sinauer Associates Inc., Sunderland, Massachusetts.
- Hinnah,S.C., Wagner,R., Sveshnikova,N., Harrer,R., Soll,J., 2002. The chloroplast protein import channel Toc75: pore properties and interaction with transit peptides. *Biophys. J.* 83, 899-911.
- Hirabayashi,Y., Kikuchi,S., Oishi,M., Nakai,M., 2011. *In vivo* studies on the roles of two closely related *Arabidopsis* Tic20 proteins, AtTic20-I and AtTic20-IV. *Plant Cell Physiol.* 52, 469-78.
- Hirohashi,T., Hase,T., Nakai,M., 2001. Maize non-photosynthetic ferredoxin precursor is mis-sorted to the intermembrane space of chloroplasts in the presence of light. *Plant Physiol* 125, 2154-2163.
- Hisabori,T., Motohashi,K., Hosoya-Matsuda,N., Ueoka-Nakanishi,H., Romano,P.G., 2007. Towards a functional dissection of thioredoxin networks in plant cells. *Photochem. Photobiol.* 83, 145-151.
- Horling,F., König,J., Dietz,K.J., 2002. Type II peroxiredoxin C, a member of the peroxiredoxin family of *Arabidopsis thaliana*: its expression and activity in comparison with other peroxiredoxins. *Plant Physiology and Biochemistry* 40, 491-499.
- Hörmann,F., Küchler,M., Sveshnikov,D., Oppermann,U., Li,Y., Soll,J., 2004. Tic32, an essential component in chloroplast biogenesis. *J. Biol. Chem.* 279, 34756-34762.
- Inaba,T., Alvarez-Huerta,M., Li,M., Bauer,J., Ewers,C., Kessler,F., Schnell,D.J., 2005. *Arabidopsis tic110* is essential for the assembly and function of the protein import machinery of plastids. *Plant Cell* 17, 1482-1496.
- Inaba,T., Li,M., Alvarez-Huerta,M., Kessler,F., Schnell,D.J., 2003. atTic110 functions as a scaffold for coordinating the stromal events of protein import into chloroplasts. *J. Biol. Chem.* 278, 38617-38627.
- Jackson,D.T., Froehlich,J.E., Keegstra,K., 1998. The hydrophilic domain of Tic110, an inner envelope membrane component of the chloroplastic protein translocation apparatus, faces the stromal compartment. *J. Biol. Chem.* 273, 16583-16588.
- Jarvis,P., 2008. Targeting of nucleus-encoded proteins to chloroplasts in plants. *New Phytol.* 179, 257-285.
- Johansson,L.C., Wöhri,A.B., Katona,G., Engström,S., Neutze,R., 2009. Membrane protein crystallization from lipidic phases. *Curr. Opin. Struct. Biol.* 19, 372-378.
- Johnson,A.E., van Waes,M.A., 1999. The translocon: a dynamic gateway at the ER membrane. *Annu. Rev. Cell Dev. Biol.* 15, 799-842.

- Kadokura,H., Beckwith,J., 2010. Mechanisms of oxidative protein folding in the bacterial cell envelope. *Antioxid. Redox. Signal.* 13, 1231-1246.
- Kalanon,M., McFadden,G.I., 2008. The chloroplast protein translocation complexes of *Chlamydomonas reinhardtii*: a bioinformatic comparison of Toc and Tic components in plants, green algae and red algae. *Genetics* 179, 95-112.
- Kasmati,A.R., Topel,M., Patel,R., Murtaza,G., Jarvis,P., 2011. Molecular and genetic analyses of Tic20 homologues in *Arabidopsis thaliana* chloroplasts. *Plant J.*, in press.
- Keegstra,K., Youssif,A.E., 1986. Isolation and characterization of chloroplast envelope membranes. In: Weissbach,A., Weissbach,H. (Eds.), *Methods Enzymology - Plant Molecular Biology*, Vol 118, pp. 316-325.
- Kessler,F., Blobel,G., 1996. Interaction of the protein import and folding machineries of the chloroplast. *Proc. Natl. Acad. Sci. U. S. A* 93, 7684-7689.
- Kessler,F., Blobel,G., Patel,H.A., Schnell,D.J., 1994. Identification of two GTP-binding proteins in the chloroplast protein import machinery. *Science* 266, 1035-1039.
- Kikuchi,S., Oishi,M., Hirabayashi,Y., Lee,D.W., Hwang,I., Nakai,M., 2009. A 1-megadalton translocation complex containing Tic20 and Tic21 mediates chloroplast protein import at the inner envelope membrane. *Plant Cell* 21, 1781-1797.
- Ko,K., Taylor,D., Argenton,P., Innes,J., Pedram,B., Seibert,F., Granell,A., Ko,Z., 2005. Evidence that the plastid translocon Tic40 components possess modulating capabilities. *J. Biol. Chem.* 280, 215-224.
- Kouranov,A., Chen,X., Fuks,B., Schnell,D.J., 1998. Tic20 and Tic22 are new components of the protein import apparatus at the chloroplast inner envelope membrane. *J. Cell Biol.* 143, 991-1002.
- Kovacheva,S., Bedard,J., Patel,R., Dudley,P., Twell,D., Rios,G., Koncz,C., Jarvis,P., 2005. *In vivo* studies on the roles of Tic110, Tic40 and Hsp93 during chloroplast protein import. *Plant J.* 41, 412-428.
- Kovacheva,S., Bedard,J., Wardle,A., Patel,R., Jarvis,P., 2007. Further *in vivo* studies on the role of the molecular chaperone, Hsp93, in plastid protein import. *Plant J.* 50, 364-379.
- Kovács-Bogdán, E., Benz, P., Soll, J., and Bölder, B. Tic20 forms a channel independent of Tic110 in chloroplasts. *BMC Plant Biol.*, submitted.
- Kovács-Bogdán,E., Soll,J., Bölder,B., 2010. Protein import into chloroplasts: The Tic complex and its regulation. *Biochim. Biophys. Acta* 1803, 740-747.
- Kubis,S., Baldwin,A., Patel,R., Razzaq,A., Dupree,P., Lilley,K., Kurth,J., Leister,D., Jarvis,P., 2003. The *Arabidopsis ppi1* mutant is specifically defective in the expression, chloroplast import, and accumulation of photosynthetic proteins. *Plant Cell* 15, 1859-1871.

- Kubis,S., Patel,R., Combe,J., Bedard,J., Kovacheva,S., Lilley,K., Biehl,A., Leister,D., Rios,G., Koncz,C., Jarvis,P., 2004. Functional specialization amongst the *Arabidopsis* Toc159 family of chloroplast protein import receptors. *Plant Cell* 16, 2059-2077.
- Küchler,M., Decker,S., Hörmann,F., Soll,J., Heins,L., 2002. Protein import into chloroplasts involves redox-regulated proteins. *EMBO J.* 21, 6136-6145.
- Laemmli,U.K., 1970. Cleavage of structural proteins during the assembly of the head of bacteriophage T4. *Nature* 227, 680-685.
- Landau,E.M., Rosenbusch,J.P., 1996. Lipidic cubic phases: a novel concept for the crystallization of membrane proteins. *Proc. Natl. Acad. Sci. U. S. A* 93, 14532-14535.
- Lee,D.W., Kim,J.K., Lee,S., Choi,S., Kim,S., Hwang,I., 2008. *Arabidopsis* nuclear-encoded plastid transit peptides contain multiple sequence subgroups with distinctive chloroplast-targeting sequence motifs. *Plant Cell* 20, 1603-1622.
- Leister,D., 2003. Chloroplast research in the genomic age. *Trends Genet.* 19, 47-56.
- Lubben,T.H., Keegstra,K., 1986. Efficient *in vitro* import of a cytosolic heat shock protein into pea chloroplasts. *Proc. Natl. Acad. Sci. U. S. A* 83, 5502-5506.
- Lübeck,J., Heins,L., Soll,J., 1997. A nuclear-coded chloroplastic inner envelope membrane protein uses a soluble sorting intermediate upon import into the organelle. *J. Cell Biol.* 137, 1279-1286.
- Lübeck,J., Soll,J., Akita,M., Nielsen,E., Keegstra,K., 1996. Topology of IEP110, a component of the chloroplastic protein import machinery present in the inner envelope membrane. *EMBO J.* 15, 4230-4238.
- Madueno,F., Napier,J.A., Gray,J.C., 1993. Newly imported Rieske iron-sulfur protein associates with both Cpn60 and Hsp70 in the chloroplast stroma. *Plant Cell* 5, 1865-1876.
- Majeran,W., Zybaylov,B., Ytterberg,A.J., Dunsmore,J., Sun,Q., van Wijk,K.J., 2008. Consequences of C4 differentiation for chloroplast membrane proteomes in maize mesophyll and bundle sheath cells. *Mol. Cell Proteomics.* 7, 1609-1638.
- Martin,T., Sharma,R., Sippel,C., Waagemann,K., Soll,J., Vothknecht,U.C., 2006. A protein kinase family in *Arabidopsis* phosphorylates chloroplast precursor proteins. *J. Biol. Chem.* 281, 40216-40223.
- Martin,W., Herrmann,R.G., 1998. Gene transfer from organelles to the nucleus: how much, what happens, and why? *Plant Physiol* 118, 9-17.
- Martin,W., Rujan,T., Richly,E., Hansen,A., Cornelsen,S., Lins,T., Leister,D., Stoebe,B., Hasegawa,M., Penny,D., 2002. Evolutionary analysis of *Arabidopsis*, cyanobacterial, and chloroplast genomes reveals plastid phylogeny and thousands of cyanobacterial genes in the nucleus. *Proc. Natl. Acad. Sci. U. S. A* 99, 12246-12251.

- Mata-Cabana,A., Florencio,F.J., Lindahl,M., 2007. Membrane proteins from the cyanobacterium *Synechocystis* sp. PCC 6803 interacting with thioredoxin. *Proteomics*. 7, 3953-3963.
- May,T., Soll,J., 2000. 14-3-3 proteins form a guidance complex with chloroplast precursor proteins in plants. *Plant Cell* 12, 53-64.
- Mesecke,N., Terziyska,N., Kozany,C., Baumann,F., Neupert,W., Hell,K., Herrmann,J.M., 2005. A disulfide relay system in the intermembrane space of mitochondria that mediates protein import. *Cell* 121, 1059-1069.
- Mokranjac,D., Neupert,W., 2010. The many faces of the mitochondrial TIM23 complex. *Biochim. Biophys. Acta* 1797, 1045-1054.
- Motohashi,K., Kondoh,A., Stumpp,M.T., Hisabori,T., 2001. Comprehensive survey of proteins targeted by chloroplast thioredoxin. *Proc. Natl. Acad. Sci. U. S. A* 98, 11224-11229.
- Neupert,W., Herrmann,J.M., 2007. Translocation of proteins into mitochondria. *Annu. Rev. Biochem.* 76, 723-749.
- Nielsen,E., Akita,M., Dávila-Aponte,J., Keegstra,K., 1997. Stable association of chloroplastic precursors with protein translocation complexes that contain proteins from both envelope membranes and a stromal Hsp100 molecular chaperone. *EMBO J.* 16, 935-946.
- Nollert,P., 2002. From test tube to plate: a simple procedure for the rapid preparation of microcrystallization experiments using the cubic phase method. *J. Appl. Cryst.* 35, 637-640.
- Parsell,D.A., Kowal,A.S., Lindquist,S., 1994. *Saccharomyces cerevisiae* Hsp104 protein. Purification and characterization of ATP-induced structural changes. *J. Biol. Chem.* 269, 4480-4487.
- Peltier,J.B., Ripoll,D.R., Friso,G., Rudella,A., Cai,Y., Ytterberg,J., Giacomelli,L., Pillardy,J., van Wijk,K.J., 2004. Clp protease complexes from photosynthetic and non-photosynthetic plastids and mitochondria of plants, their predicted three-dimensional structures, and functional implications. *J. Biol. Chem.* 279, 4768-4781.
- Pencer,J., White,G.F., Hallett,F.R., 2001. Osmotically induced shape changes of large unilamellar vesicles measured by dynamic light scattering. *Biophys. J.* 81, 2716-2728.
- Qbadou,S., Becker,T., Mirus,O., Tews,I., Soll,J., Schleiff,E., 2006. The molecular chaperone Hsp90 delivers precursor proteins to the chloroplast import receptor Toc64. *EMBO J.* 25, 1836-1847.
- Ratnayake,R.M., Inoue,H., Nonami,H., Akita,M., 2008. Alternative processing of *Arabidopsis* Hsp70 precursors during protein import into chloroplasts. *Biosci. Biotechnol. Biochem.* 72, 2926-2935.
- Reumann,S., Keegstra,K., 1999. The endosymbiotic origin of the protein import machinery of chloroplastic envelope membranes. *Trends Plant Sci.* 4, 302-307.

- Ruprecht,M., Bionda,T., Sato,T., Sommer,M.S., Endo,T., Schleiff,E., 2010. On the impact of precursor unfolding during protein import into chloroplasts. *Mol. Plant* 3, 499-508.
- Saiki,R.K., Gelfand,D.H., Stoffel,S., Scharf,S.J., Higuchi,R., Horn,G.T., Mullis,K.B., Erlich,H.A., 1988. Primer-directed enzymatic amplification of DNA with a thermostable DNA polymerase. *Science* 239, 487-491.
- Sambrook,J., Fritsch,E.F., Maniatis,T., 1989. *Molecular Cloning - A Laboratory Manual.*, Cold Spring Harbour Laboratory Press, New York.
- Schagger,H., von Jagow,G., 1991. Blue native electrophoresis for isolation of membrane protein complexes in enzymatically active form. *Anal. Biochem.* 199, 223-231.
- Schindler,C., Hracky,R., Soll,J., 1987. Protein transport in chloroplasts: ATP is prerequisite. *Z. Naturforsch.* 42c, 103-108.
- Schirmer,E.C., Glover,J.R., Singer,M.A., Lindquist,S., 1996. HSP100/Clp proteins: a common mechanism explains diverse functions. *Trends Biochem. Sci.* 21, 289-296.
- Schleiff,E., Becker,T., 2011. Common ground for protein translocation: access control for mitochondria and chloroplasts. *Nat. Rev. Mol. Cell Biol.* 12, 48-59.
- Schleiff,E., Jelic,M., Soll,J., 2003a. A GTP-driven motor moves proteins across the outer envelope of chloroplasts. *Proc. Natl. Acad. Sci. U. S. A* 100, 4604-4609.
- Schleiff,E., Soll,J., Küchler,M., Kühlbrandt,W., Harrer,R., 2003b. Characterization of the translocon of the outer envelope of chloroplasts. *J. Cell Biol.* 160, 541-551.
- Schleiff,E., Soll,J., Sveshnikova,N., Tien,R., Wright,S., Dabney-Smith,C., Subramanian,C., Bruce,B.D., 2002. Structural and guanosine triphosphate/diphosphate requirements for transit peptide recognition by the cytosolic domain of the chloroplast outer envelope receptor, Toc34. *Biochemistry* 41, 1934-1946.
- Schnell,D.J., Kessler,F., Blobel,G., 1994. Isolation of components of the chloroplast protein import machinery. *Science* 266, 1007-1012.
- Schürmann,P., Buchanan,B.B., 2008. The ferredoxin/thioredoxin system of oxygenic photosynthesis. *Antioxid. Redox. Signal.* 10, 1235-1274.
- Schürmann,P., Jacquot,J.P., 2000. Plant thioredoxin systems revisited. *Annu. Rev. Plant Physiol Plant Mol. Biol.* 51, 371-400.
- Schwenkert,S., Soll,J., Bölter,B., 2011. Protein import into chloroplasts--how chaperones feature into the game. *Biochim. Biophys. Acta* 1808, 901-911.
- Shanklin,J., DeWitt,N.D., Flanagan,J.M., 1995. The stroma of higher plant plastids contain ClpP and ClpC, functional homologs of *Escherichia coli* ClpP and ClpA: an archetypal two-component ATP-dependent protease. *Plant Cell* 7, 1713-1722.
- Shi,L.X., Theg,S.M., 2010. A stromal heat shock protein 70 system functions in protein import into chloroplasts in the moss *Physcomitrella patens*. *Plant Cell* 22, 205-220.

- Singh,H., Ashley,R.H., 2006. Redox regulation of CLIC1 by cysteine residues associated with the putative channel pore. *Biophys. J.* 90, 1628-1638.
- Sjögren,L.L., MacDonald,T.M., Sutinen,S., Clarke,A.K., 2004. Inactivation of the *clpC1* gene encoding a chloroplast Hsp100 molecular chaperone causes growth retardation, leaf chlorosis, lower photosynthetic activity, and a specific reduction in photosystem content. *Plant Physiol* 136, 4114-4126.
- Smart,O.S., Breed,J., Smith,G.R., Sansom,M.S., 1997. A novel method for structure-based prediction of ion channel conductance properties. *Biophys. J.* 72, 1109-1126.
- Sohrt,K., Soll,J., 2000. Toc64, a new component of the protein translocon of chloroplasts. *J. Cell Biol.* 148, 1213-1221.
- Stahl,T., Glockmann,C., Soll,J., Heins,L., 1999. Tic40, a new "old" subunit of the chloroplast protein import translocon. *J. Biol. Chem.* 274, 37467-37472.
- Stanne,T.M., Pojidaeva,E., Andersson,F.I., Clarke,A.K., 2007. Distinctive types of ATP-dependent Clp proteases in cyanobacteria. *J. Biol. Chem.* 282, 14394-14402.
- Stengel,A., Benz,J.P., Buchanan,B.B., Soll,J., Bölder,B., 2009. Preprotein import into chloroplasts via the Toc and Tic complexes is regulated by redox signals in *Pisum sativum*. *Mol. Plant* 2, 1181-1197.
- Stengel,A., Benz,P., Balsera,M., Soll,J., Bölder,B., 2008. TIC62 redox-regulated translocon composition and dynamics. *J. Biol. Chem.* 283, 6656-6667.
- Su,P.H., Li,H.M., 2008. *Arabidopsis* stromal 70-kD heat shock proteins are essential for plant development and important for thermotolerance of germinating seeds. *Plant Physiol* 146, 1231-1241.
- Su,P.H., Li,H.M., 2010. Stromal Hsp70 is important for protein translocation into pea and *Arabidopsis* chloroplasts. *Plant Cell* 22, 1516-1531.
- Sung,D.Y., Kaplan,F., Guy,C.L., 2001. Plant Hsp70 molecular chaperones: Protein structure, gene family, expression and function. *Physiologia Plantarum* 113, 443-451.
- Sveshnikova,N., Grimm,R., Soll,J., Schleiff,E., 2000. Topology studies of the chloroplast protein import channel Toc75. *Biol. Chem.* 381, 687-693.
- Teng,Y.S., Su,Y.S., Chen,L.J., Lee,Y.J., Hwang,I., Li,H.M., 2006. Tic21 is an essential translocon component for protein translocation across the chloroplast inner envelope membrane. *Plant Cell* 18, 2247-2257.
- Timmis,J.N., Ayliffe,M.A., Huang,C.Y., Martin,W., 2004. Endosymbiotic gene transfer: organelle genomes forge eukaryotic chromosomes. *Nat. Rev. Genet.* 5, 123-135.
- Trebitsh,T., Levitan,A., Sofer,A., Danon,A., 2000. Translation of chloroplast *psbA* mRNA is modulated in the light by counteracting oxidizing and reducing activities. *Mol. Cell Biol.* 20, 1116-1123.

- Tu,B.P., Ho-Schleyer,S.C., Travers,K.J., Weissman,J.S., 2000. Biochemical basis of oxidative protein folding in the endoplasmic reticulum. *Science* 290, 1571-1574.
- van Dooren,G.G., Tomova,C., Agrawal,S., Humbel,B.M., Striepen,B., 2008. *Toxoplasma gondii* Tic20 is essential for apicoplast protein import. *Proc. Natl. Acad. Sci. U. S. A* 105, 13574-13579.
- Vojta,L., Soll,J., Bölter,B., 2007. Requirements for a conservative protein translocation pathway in chloroplasts. *FEBS Lett.* 581, 2621-2624.
- Waegemann,K., Eichacker,S., Soll,J., 1992. Outer envelope membranes from chloroplasts are isolated as right-side-out vesicles. *Planta* 89-94.
- Waegemann,K., Soll,J., 1996. Phosphorylation of the transit sequence of chloroplast precursor proteins. *J. Biol. Chem.* 271, 6545-6554.

Acknowledgements

I thank Prof. Jürgen Soll for the possibility to work in his lab and for his continuous support (and his open door) during my PhD.

I am grateful to Bettina for always having time for me to speak about my work and for reading and improving this thesis.

I will never forget the support that I got from my colleges in the Tic lab. Thanks to Andi, Anna, Carsten, Eike, Katja, Natalie, Penny, Philipp and WaiLing for supporting me with their ideas, for bringing so much laugh to the lab and for being not only my colleagues but also friends. I cannot thank Andi enough that he was always happy to work with me, and gave me the possibility to teach a little bit during research. I am thankful to Carsten for bringing me to the secrets of electrophysiology and for always being ready to help to fight with “the machine”. I also thank Mónica that she introduced me the “world of proteins”, and showed me how to “treat them like my husband”.

I also thank to all other colleagues in the Soll lab for their advices, the nice lunchtime in the kitchen and the good working environment. I will always remember our AG Soll parties.

I thank Ulrike that she helped me with the mass spectroscopic analysis and the fluorescence measurements. Special thanks to Karl for spending his days with me during “Aufarbeitung”. I am grateful to Lars for sequencing my samples. Furthermore, I thank Gergő and Annette for showing me the “crystal-world” and Anke for her help in the evaluation of electrophysiology.

I am thankful to Hans-Jörg, Maxi and Ingrid for organizing the IMPRS program, which helped me to find this lab, to improve my skills and to find friends in the program.

I thank my husband, Ákos, who always supported me even when things went harder. And last but not least, I thank my parents who helped me all the time on my way to do what I really like and enjoy.

Curriculum Vitae

Personal data

Date of birth 1st May 1984
Place of birth Budapest, Hungary
Nationality Hungarian

Professional and educational history

Sep 2007- present **PhD**
Ludwig-Maximilians-Universität München, Germany,
Department Biology I, Plant Biochemistry
Supervisor Prof. Dr. Jürgen Soll
Thesis title Characterization of protein import channel-
 forming proteins in chloroplasts

Sep 2002- Jul 2007 **MSc** Biology and Chemistry (excellent)
Eötvös Loránd University, Budapest, Hungary
Supervisors Dr. Áron Keresztes and Dr. Péter Nyitrai
Thesis title Stimulating effect of low-concentration stressors
 in seedlings (in Hungarian)

1996- 2002 Árpád High School, Budapest, Hungary

Scientific prizes, awards and fellowships

2007-present Member of the **International Max Planck Research School** for
Molecular and Cellular Life Sciences, Martinsried, Germany

2007-2010 **Scholarship** of the Bavarian Academic Centre for
Central, Eastern and South-Eastern Europe (BAYHOST)

2006/07 **Stipendium of the Hungarian State**

2006 **Prominent Student of the Faculty**
Eötvös Loránd University, Budapest, Hungary

2006 **Achievement in Biosciences Prize**
Oxford University Press

Peer-reviewed publications

E. Kovács-Bogdán*, J. Ph. Benz*, J. Soll, B. Bölter: Tic20 forms a channel independent of Tic110 in chloroplasts. BMC Plant Biology, submitted. *these authors contributed equally.

E. Kovács-Bogdán, J. Soll, B. Bölter: Protein import into chloroplasts: The Tic complex and its regulation. Biochimica et Biophysica Acta 1803 (2010): 740-747.

E. Kovács-Bogdán, Á. Keresztes: Ultrastructural characterization of cell types in root tips of barley (*Hordeum vulgare* L.). Flora 205 (2010): 548-551.

E. Kovács-Bogdán, P. Nyitrai, Á. Keresztes: How does a little stress stimulate a plant? Plant Signaling & Behavior 5 (2010): 354 - 358.

M. Balsera, T.A. Goetze, **E. Kovács-Bogdán**, P. Schürmann, R. Wagner, B.B. Buchanan, J. Soll, B. Bölter: Characterization of Tic110, a channel-forming protein at the inner envelope membrane of chloroplasts, unveils a response to Ca^{2+} and a stromal regulatory disulfide bridge. Journal of Biological Chemistry 284 (2009): 2603-2616.

E. Kovács, P. Nyitrai, P. Czövek, M. Óvári, Á. Keresztes: Investigation into the mechanism of stimulation by low-concentration stressors in barley seedlings. Journal of Plant Physiology 166 (2009): 72-79.

P. Nyitrai, **E. Kovács**, I. Király, M. Óvári, Á. Keresztes: On the mechanism of rejuvenation of ageing detached bean leaves by low-concentration stressors. Plant Biology 11 (2009): 236-242.

E. Kovács, É. Sárvári, P. Nyitrai, J. Darók, E. Cseh, F. Láng, Á. Keresztes: Structural-functional changes in detached cucumber leaves, and modelling these by hormone-treated leaf discs. Plant Biology 9 (2007): 85-92.